

1 2



9 0

UNIVERSIDADE D COIMBRA

Sulaiman I S Abuhaiba

INTELLECTUAL DISABILITY AND EPILEPSY: MULTIMODAL BRAIN IMAGING

Tese de Doutoramento em Biologia Experimental e Biomedicina, ramo de Neurociências e Doença, orientada pelo Professor Doutor Miguel Castelo-Branco, e co-orientação do Doutor Francisco Sales, apresentada ao Instituto de Investigação Interdisciplinar da Universidade de Coimbra.

Dezembro de 2020



INSTITUTO DE
INVESTIGAÇÃO
INTERDISCIPLINAR
UNIVERSIDADE DE
COIMBRA

Sulaiman I S Abuhaiba

**INTELLECTUAL DISABILITY AND EPILEPSY: MULTIMODAL
BRAIN IMAGING
DEFICIENCIA INTELECTUAL E EPILEPSIA: IMAGEM CEREBRAL
MULTIMODAL
Dezembro de 2020**

Thesis submitted to the Institute of Interdisciplinary Research of the University of Coimbra to apply for the degree of Doctor in Experimental Biology and Biomedicine, specialization in Neuroscience and Disease under the supervision of Prof. Dr. Miguel Castelo-Branco and co-supervision of Dr. Francisco Sales

The studies presented in this thesis were carried out at the Visual Neuroscience Laboratory at IBILI (Institute for Biomedical Imaging and Life Sciences) and later at CIBIT (Coimbra Institute for biomedical Imaging and Life Sciences), EEG/tDCS Laboratory at ICNAS (Institute of Nuclear Sciences Applied to Health), and the Epilepsy Monitoring Unit at the Central Hospital of the University of Coimbra (CHUC) and were supported by the following grants: BIGDATAIMAGE (CENTRO-01-0145-FEDER-000016), INFARMED-FIS-2015-01_DIA_20150630–173, FLAD Life Sciences 2020 Prize, FP7-HEALTH-2013-INNOVATION-1-602186-BRAINTRAIN, UID/NEU/04539/2013 COMPETE POCI-01-0145-FEDER-007440, CENTRO-07-ST24-FEDER-00205, Centro 2020 FEDER, COMPETE, PAC – MEDPERSYST, POCI-01-0145-FEDER-016428. Bial 373/14, Portuguese League Against Epilepsy Award for Best Scientific Research 2017, FCT-UID/4950/2020 and FCT-UID/NEU/04539/2013–COMPETE, POCI-01-0145-FE; COMPETE FEDER.





For my Wife “Walaa”,
Whom I love for eternity and beyond,
I dedicate this thesis to you.
Without your support and encouraging words,
I would have not achieved this!

Table of Contents

Abbreviations List	7
Summary:	10
Resumo:	13
Chapter 1:	17
INTRODUCTION	18
The GABAergic System and Inhibition/Excitation Balance in Health and Disease.....	18
The GABAergic System and Physiologic High Frequency Oscillations.....	21
The Occipital Cortex as a Model to Study the GABAergic System	23
Disease Models of Impaired GABAergic System:	24
Measurement of Brain Neurotransmitters by MRS	29
Measurement of Gamma Activity by EEG:	34
Aims.....	35
Outline.....	36
References:.....	38
Chapter 2:	48
Occipital Cortex Disruption in Type 2 Diabetes Mellitus	48
Diabetic Brain or Retina? Visual Psychophysical Performance in Diabetic Patients in Relation to GABA Levels in Occipital Cortex.....	49
Occipital blood-brain barrier permeability is an independent predictor of visual outcome in type 2 diabetes, irrespective of the retinal barrier: A longitudinal study.....	67
Chapter 3:	95
Occipital Cortex Disruption in Epilepsy:	95
Cortical functional topography of high frequency gamma activity relates to perceptual decision: an Intracranial study	96
The impact of Cathodal tDCS on GABAergic-Inhibition Mediated Synchrony in epilepsy: a multimodal study on local epileptogenic and distant oscillatory patterns.....	126
Chapter 4:	151
Cortical Metabolites Disruption in Epilepsy: Future Work	151
Lovastatin as an antiepileptic: Effect of lovastatin as a physiologic challenge on the GABAergic system in drug-resistant epilepsy and TSC-Associated Epilepsy.....	152
AMT-PET for the Localization of the EZ in TSC-Associated Epilepsy and Drug Resistant Epilepsy	160
CONCLUDING REMARKS:	166
Acknowledgements:	175
CURRICULUM VITAE	177

List of Publications.....	177
----------------------------------	------------

Abbreviations List

1H-MRS	Proton magnetic resonance spectroscopy
AED	Antiepileptic drug
AMT	α -[¹¹ C]-methyl-L-tryptophan
ANOVA	Analysis of variance
ASD	Autism spectrum disorder
BBB	Blood brain barrier
BCVA	Best corrected visual acuity
BMI	Body mass index
BRB	Blood retinal barrier
Cho	Choline
Cr	Creatine
CSF	Cerebrospinal fluid
CT	Computer Tomography
DCE-MRI	Dynamic contrast-enhanced magnetic resonance imaging
ECoG	Electrocorticography
EEG	Electroencephalography
EEG-fMRI	Electroencephalography - functional magnetic resonance imaging
ERP	Evoked response potential
ERSP	Event related spectral power
ESI	Electrical source imaging
ESRD	End stage renal disease
ETDRS	Early treatment diabetic retinopathy study scale
EZ	Epileptogenic zone
FCD	Focal cortical dysplasia
FDG	fluorodeoxyglucose
FDR	false discovery rate
FLAIR	Fluid-attenuated inversion recovery
GABA	gamma-Aminobutyric acid
GABA_A	GABA receptor A
GABA_B	GABA receptor B

Glx	Glutamate/glutamine pool
GM	Grey Matter
GRE	Gradient echo
GSH	Glutathione
HbA1C	Glycosalated hemoglobin A1C
HERMES	Hadamard encoding and reconstruction of MEGA-edited spectroscopy
HFA	High frequency activity
HFOs	High frequency oscillations
IED	Interictal Epileptic Discharge
KA	quinoline acid
LMS	Longwave, medium-wave, short-wave
MA	Microaneurysm
MEG	Magnetic encephalography
MEGA-PRESS	MEshcher-GARwood Point RESolved Spectroscopy
MPRAGE	magnetization-prepared rapid acquisition with gradient echo
MRI	Magnetic resonance imaging
MRS	Magnetic resonance spectroscopy
NAA	N-acetyl aspartate
NMDA	N-Methyl-D-aspartic acid
NMR	Nuclear magnetic resonance
NPDR	Non-proliferative diabetic retinopathy
OFF_{GABA}	GABA resonance frequency off
OFF_{GSH}	Glutathione resonance frequency off
ON_{GABA}	GABA resonance frequency on
ON_{GSH}	Glutathione resonance frequency on
PCA	Posterior Cerebral Artery
PET	Positron emission tomography
RAGE	Receptor for advanced glycation end products
RLA	Retinal Leakage Analyzer
ROI	Region Of Interest
sLORETA	standardized low-resolution brain electromagnetic tomography

SOZ	Seizure Onset Zone
SPECT	Single-photon emission computed tomography
SPM8	statistical Parametric Mapping version 8
SPSS	Statistical Package for the Social Sciences
T1	longitudinal relaxation time
T2	transverse relaxation time
T2DM	Type 2 Diabetes Mellitus
TCA cycle	tricarboxylic acid cycle
TDC	Transcranial Direct Current Stimulation
TLE	Temporal Lobe Epilepsy
TSC,	Tuberous Sclerosis Complex
V1	Primary Visual Cortex
VEGF	Vascular endothelial growth factor
VNS,	Vagus Nerve Stimulation
WM	White Matter

Summary:

Excitation-inhibition (E-I) balance plays an important role in information processing, neuroplasticity and pathologic conditions. Evidence of E-I imbalance has been reported in a wide array of neuropsychiatric disorders such as autism spectrum disorder (ASD), schizophrenia, neurofibromatosis type 1, depression and attention-deficit/hyperactivity disorder. Of particular interest to us was the currently available evidence of cortical dysfunction in type 2 diabetes patients. Type 2 diabetes mellitus patients are known to have decreased cognitive ability before they develop any evidence of microvascular or macrovascular disease. This could be explained by impaired circuitry and/or E-I balance of certain networks in type 2 diabetes mellitus. It has been reported that patients with type 2 diabetes mellitus have increased levels of GABA in the occipital region in addition to evidence of blood-brain barrier disintegration in such patients. Because of this, type 2 DM was chosen as a disease model to study the possible impacts of the disease on GABAergic system in the occipital region and how that correlate with visual performance.

The study of the GABAergic system and its dysfunction in epilepsy is gaining attention for several reasons. First, while GABA is mainly an inhibitory neurotransmitter in the brain it has been shown that it can act as an excitatory neurotransmitter on immature neurons. Second, there is growing evidence of increased GABA concentration in the epileptogenic zone in patients with drug-resistant epilepsy in vivo and ex vivo. Finally, the generation of pathologic and physiologic high frequency oscillations is expected to be related to and maintained by inhibitory postsynaptic potentials that are mediated by GABA_A receptors. The second part of this thesis focuses on the study of the GABAergic system in epilepsy patients with drug-resistant disease and how it is related to physiologic or pathologic gamma activity.

We chose a cohort of type 2 diabetes mellitus patients who have early diabetic retinopathy. The goal was to assess occipital cortical GABA as a predictor of visual performance in type 2 diabetes mellitus patients. GABA was measured by proton magnetic resonance spectroscopy from the occipital region, and visual performance was assessed in three domains (chromatic, achromatic and speed

discrimination). We found for the first-time evidence of achromatic and speed discrimination abnormalities in type 2 diabetes mellitus patients as compared to healthy subjects. Moreover, we reported for the first time a positive correlation between occipital GABA and achromatic/speed discrimination thresholds (higher thresholds mean worse performance). Occipital GABA at baseline was also predictive of visual performance one year later, suggesting that modulating occipital GABA could have a long-term impact on visual performance.

The second study to be included in the scope of this thesis focused on BBB permeability in type 2 diabetic patients and its relation to visual performance. The previously mentioned cohort of type 2 DM patients who had evidence of GABAergic dysfunction were included in this subsequent study of BBB integrity. In summary, we showed a relationship between BBB leakage and blood-retinal-barrier leakage, with patients with BRB leakage having higher BBB permeability. Moreover, we showed for the first time that metabolic control is correlated with BBB permeability (poor metabolic control is associated with impaired BBB integrity). Finally, we found that BBB permeability is predictive of visual acuity at baseline, one year and two years later in type 2 diabetics with established BRB leakage.

We then moved to study the GABAergic system in a different disease model. In patients with drug resistant epilepsy, we are offered a unique opportunity where we can indirectly measure the function of the GABAergic system by measuring gamma activity with intracranial electroencephalography (EEG). The first study in this disease model focused on physiologic high frequency activity where we tested the relationship between functional topography of high gamma activity and perceptual decision-making. In summary, we found three distinct regional fingerprints of high frequency activity (HFA) in our cohort: a) Lower gamma frequency patterns dominated the anterior semantic ventral object processing, b) low gamma frequency patterns that involve dorsoventral integrating networks, and c) early sensory posterior patterns in the 60 to 250 Hz range. In summary, we show that accurate object recognition/perceptual decision-making is associated with low-gamma frequency activity that has a specific spatiotemporal signature.

The second study that belonged to the disease model of drug resistant epilepsy focused on evidence of GABAergic dysfunction in epilepsy and how the modulation of the GABAergic system in the epileptogenic zone affects epileptogenicity and the GABAergic system in other reference brain region (the occipital region). We hypothesized that c-tDCS (cathodal transcranial direct current stimulation) which has an antiepileptic effect would modulate the neurotransmitters responsible for the abnormal and complex local synchrony and abnormal rhythmic activity seen in epilepsy. This is the first study to test for the impact of c-tDCS on physiologic (evoked by visual tasks) and pathologic (epileptogenic) gamma activity and to measure GABA, glutamate and glutathione from the epileptogenic zone and occipital region simultaneously after c-tDCS in patients with drug resistant epilepsy. C-tDCS decreased the number of interictal discharges per minute. This was associated with a decrease in GABA concentration in the occipital and epileptogenic zones. We also found that cathodal tDCS stimulation of the epileptogenic zone suppressed grating evoked low gamma activity in the epileptogenic zone and increased it in the distant parieto-occipital regions. In summary, this study provided a window into the mechanism of action of c-tDCS as an antiepileptic and its effects on the GABAergic system and neural oscillatory patterning.

In summary, we show that E-I balance is maintained across the different neural networks in a given time frame and alterations in this balance is linked to cognitive impairment and visual performance in type 2 DM, and epileptogenesis in epilepsy patients. Our results also suggest that GABAergic dysfunction in the epileptogenic zone is more than a consequence of epileptogenesis, and could be epileptogenic per se.

Resumo:

O equilíbrio entre excitação e inibição tem um papel importante no processamento de informação, na neuroplasticidade e em certas condições patológicas. Um desequilíbrio entre excitação e inibição tem sido referido em várias condições neuropsiquiátricas, tais como na perturbação do espectro do autismo, esquizofrenia, neurofibromatose de tipo 1, depressão e perturbação de hiperatividade e déficit de atenção. A evidência desta disfunção cortical também em pessoas com diabetes mellitus tipo 2 revelou-se de particular interesse para nós. Sabe-se que pessoas com diabetes mellitus tipo 2 apresentam uma habilidade cognitiva diminuída antes até do aparecimento de doença micro ou macrovascular. Isto poderá ser explicado por alterações nos circuitos e/ou desequilíbrio entre excitação e inibição em certas redes neuronais. Estudos mostram que pessoas com diabetes mellitus tipo 2 têm concentrações de GABA aumentadas na região occipital, para além da evidência de disfunção da barreira hematoencefálica. Por estes motivos, a diabetes mellitus tipo 2 foi escolhida como modelo para o estudo do impacto da doença no sistema GABAérgico na região occipital e de como isso se relaciona com o desempenho em testes visuais.

O estudo do sistema GABAérgico e a sua disfunção na epilepsia tem ganho atenção por vários motivos. Primeiro, apesar do GABA funcionar como neurotransmissor inibitório, tem sido mostrado que este funciona como neurotransmissor excitatório em neurónios imaturos. Segundo, há cada vez maior evidência da concentração aumentada de GABA na zona epileptogénica em pessoas com epilepsia refratária, sugerida por estudos in vivo e ex vivo. Por último, é expectável que as oscilações de alta frequência, quer de origem patológica quer fisiológica, se formem e sejam mantidas por potenciais pós-sinápticos mediados por recetores GABA_A. A segunda parte desta tese refere-se ao estudo do sistema GABAérgico em pessoas com epilepsia refratária e como este se relaciona com a atividade fisiológica e patológica de frequências gamma. Neste trabalho foi incluído um grupo de participantes com diabetes mellitus tipo 2 e com retinopatia diabética. O objetivo era avaliar a concentração de GABA no córtex occipital como preditor do desempenho em testes visuais por estes

participantes. A concentração de GABA na região occipital foi medida usando a técnica de espectroscopia por ressonância magnética nuclear e o desempenho em testes visuais foi avaliado em três áreas (visão cromática, acromática e discriminação de velocidade). Os resultados mostraram, pela primeira vez, evidência de diferenças na visão acromática e na discriminação de velocidade em participantes com diabetes mellitus tipo 2 quando comparados com participantes saudáveis. Além disso, foi encontrada pela primeira vez uma correlação positiva entre os níveis de GABA no córtex occipital e os limiares de visão acromática e discriminação de velocidade (maiores limiares significam pior desempenho). Os valores de GABA na região occipital também foram preditivos do desempenho nos testes visuais quer na primeira avaliação, quer um ano depois, sugerindo que a modulação dos níveis de GABA no córtex occipital pode ter um impacto a longo termo no desempenho visual.

O segundo trabalho realizado no âmbito desta tese refere-se ao estudo da permeabilidade da barreira hematoencefálica em pessoas com diabetes mellitus tipo 2 e a sua relação com o desempenho nos testes visuais. Os participantes com diabetes e com evidência de disfunção GABAérgica anteriormente referidos foram incluídos no estudo seguinte acerca da integridade da barreira hematoencefálica. Em suma, os resultados mostraram uma relação entre a integridade da barreira hematoencefálica e a integridade da barreira hemato-retiniana, sendo que participantes com maior ruptura da barreira hemato-retiniana apresentavam maior permeabilidade da barreira hematoencefálica. Além disso, os resultados mostraram pela primeira vez que o controlo metabólico está correlacionado com a permeabilidade da barreira hematoencefálica (pior o controlo metabólico associado a diminuição da integridade da barreira). Por último, em participantes com diabetes tipo 2 e ruptura da barreira hemato-retiniana, os resultados mostraram que a permeabilidade da barreira hematoencefálica é preditiva da acuidade visual quer no primeiro teste quer um e dois anos mais tarde em.

Em seguida, o sistema GABAérgico foi estudado tendo outra doença como modelo. A função do sistema GABAérgico pode ser avaliada, de forma indireta, a partir da medição da atividade gamma usando eletroencefalografia intracraniana em pessoas com epilepsia refratária. No primeiro trabalho em que

usámos a epilepsia refratária como modelo, estudou-se a atividade fisiológica de alta frequência, testando a relação entre a topografia funcional da atividade gamma alta e tomada de decisão perceptual. Em suma, encontraram-se três padrões locais distintos dessa atividade de alta frequência neste grupo de participantes: a) domínio de padrões de frequência gamma baixa no processamento semântico em áreas anteriores e no processamento de objetos em áreas ventrais; b) padrões de frequência gamma baixa envolvendo redes dorsoventrais de integração de informação; c) padrões de surgimento inicial em áreas posteriores nas frequências de 60 a 250 Hz. Em suma, os resultados revelam que o reconhecimento de objetos de forma precisa e a tomada de decisão perceptual estão associados a frequências gamma baixas com determinadas características espaciotemporais.

O segundo trabalho usando a epilepsia refratária como modelo foi estudada a disfunção GABAérgica na epilepsia e como a modulação do sistema GABAérgico na zona epileptogénica afeta a epileptogenicidade e o sistema GABAérgico noutras áreas de referência (a região occipital). Considerando o efeito antiepiléptico da c-tDCS (estimulação catódica transcraniana por corrente direta), foi colocada a hipótese de que esta estimulação iria modelar os níveis de neurotransmissores responsáveis pela anormal e complexa sincronia local e pela atividade rítmica anormal comum na epilepsia. Este foi o primeiro trabalho a avaliar o impacto da c-tDCS na atividade gamma fisiológica e patológica e a medir GABA, glutamato e glutatona na zona epileptogénica e na região occipital depois da c-tDCS em participantes com epilepsia refratária. A estimulação c-tDCS diminuiu o número de descargas interictais por minuto. Esta redução revelou-se associada a uma diminuição da concentração de GABA na região occipital e na zona epileptogénica. Os resultados mostraram que a estimulação c-tDCS da zona epileptogénica cancelou a atividade gamma baixa tipicamente evocada por estímulos visuais em grelha na zona epileptogénica e aumentou essa atividade em regiões parieto-occipitais mais distantes. Em suma, este trabalho abre uma janela sobre os mecanismos de ação da estimulação c-tDCS como antiepiléptico e os seus efeitos no sistema GABAérgico e nos padrões de oscilações neuronais.

Em síntese, os trabalhos mostram que o equilíbrio entre excitação e inibição é mantido por interação de diferentes redes neuronais numa dada janela temporal e as alterações desse equilíbrio estão associadas a dificuldades cognitivas e ao desempenho em testes visuais em pessoas com diabetes tipo 2 e à epileptogênese em pessoas com epilepsia. Os nossos resultados também sugerem que a disfunção GABAérgica na zona epileptogénica é mais do que uma consequência da epileptogénese, e poderá ser epileptogénica por si.

Chapter 1:
Introduction

INTRODUCTION

It has been hypothesized that the excitation/inhibition balance is associated with the pathophysiology of different neuropsychiatric conditions including autism spectrum disorder and epilepsy (Sohal & Rubenstein, 2019). For instance, the reduced inhibition in the cortex and hippocampus due to GABAergic interneuron defects may lead to abnormal neuronal circuits and nonoptimal processing of information which could be correlated with an increased risk of epileptogenesis. Several studies have pointed to the role of E-I balance in neuronal homeostasis and synaptic autoregulatory feedback (Bourgeron, 2015; Canitano & Pallagrosi, 2017; Geschwind & Levitt, 2007; C. Mullins et al., 2016; Nelson & Valakh, 2015; Ramocki & Zoghbi, 2008; John L.R. Rubenstein, 2010; Sohal & Rubenstein, 2019; Toro et al., 2010; Wondolowski & Dickman, 2013).

The GABAergic System and Inhibition/Excitation Balance in Health and Disease

It is important to emphasize that the E-I balance does not necessarily mean an equal amount of excitatory and inhibitory signals in the neuronal circuitry. At the single neuron level, the numbers of excitatory and inhibitory synapses are highly regulated with a constant E-I ratio. However, at the large scale of cortical circuits, things get complicated easily and the E-I ratio will remain tightly regulated, but it will vary between different circuits and on the dynamic timescales (Hengen et al., 2013). For instance, in an animal model of neurofibromatosis type 1 it has been reported that GABAergic imbalance with pre- and postsynaptic changes are region-specific (Gonçalves et al., 2017).

As we will see later in my work related to epilepsy, the oversimplified idea that excitation and inhibition are singular entities could be simply seen as wrong. One cannot simply assume that if the level of excitation in a circuit exceeds that of inhibition, that the activity of that circuit will increase forever. This would only occur in the absence of any homeostatic mechanism. In fact, what we see is that the ability of the circuit to generate activity will increase in that scenario until it is maximized or until marginal increases in activity begin to recruit more inhibitory circuits. In that sense, a new state of E-I balance will be reached that is specific for that circuit at that timescale.

The activity of the different neuronal circuits, whether increased or decreased by the effect of the E-I balance, occurs on fast timescales (Litwin-Kumar & Doiron,

2012). Another important role of the GABAergic inhibitory system in the cortex is to shape the flow of activity through microcircuits “fine-tuning of the signal to decrease noisy circuits” (A. T. Lee et al., 2014; S. H. Lee et al., 2014).

The maintenance of a regularized E-I balance depends on intrinsic neuronal excitability, synaptic transmission and synaptic plasticity at the cellular level; and on the complex interplay between excitatory glutamatergic neurons and inhibitory GABAergic interneurons at the circuit level (Bourgeron, 2015; Gao & Penzes, 2015; Geschwind & Levitt, 2007; E. Lee et al., 2017).

The evaluation of the E-I balance at the global circuitry level can be performed by a proxy measure (electroencephalography (EEG) or magnetoencephalography (MEG)) or by directly measuring the levels of GABA and glutamate by magnetic resonance spectroscopy (MRS) (Edgar et al., 2013; Port et al., 2016). In EEG, gamma-band oscillations are considered to be a functional measurement of E-I balance within local neural circuits (M. A. Whittington, Traub, et al., 2000).

Autism spectrum disorder (ASD) has been extensively studied as a neuropsychiatric disorder with pathophysiological basis related to E-I balance (Bozzi et al., 2018; Carvalho Pereira et al., 2018; Gonçalves et al., 2017; Howell & Smith, 2019; Oliveira et al., 2018; Port et al., 2019; J. L.R. Rubenstein & Merzenich, 2003). ASD is a neurodevelopmental disorder, and it has been shown that E-I balance plays an important role in the normal development and function of the brain and that E-I balance is maintained from the single cell level up to large-scale neuronal circuits (Sohal & Rubenstein, 2019). In ASD, alterations of neurotransmitter levels within different cortical regions have been previously reported (Brown et al., 2013; Horder et al., 2018; Kubas et al., 2012; Mescher et al., 1998) and disruptions in E-I balance are correlated with the severity of the main ASD symptoms (Horder et al., 2018). In an monogenetic animal model of ASD (NF1), cortical and striatal GABA/glutamate ratios were reported to be increased with very high GABA_A receptor expression in the hippocampus (Gonçalves et al., 2017)

Neurofibromatosis type 1 (NF1) is a disease that has been well studied in the light of the E-I balance hypothesis. NF1 is an autosomal dominant developmental disorder with an estimated prevalence of 1 in 3500 (Kayl & Moore, 2000). The disease is caused by mutations in the NF1 gene (Ballester et al., 1990). It has

been found that patients with NF1 have a significantly lower GABA levels in the visual cortex as compared to healthy controls (Maria J. Ribeiro et al., 2015; Violante et al., 2013).

The occipital visual cortex is considered a model area to study the GABAergic system and its integrity in healthy and diseased people (Maria José Ribeiro et al., 2012; Violante et al., 2012). GABAergic system activity in the visual cortex is related to performance levels in visual perceptual tasks assessing orientation-specific surround suppression (Yoon et al., 2010) and orientation discrimination performance (Edden et al., 2009). Inhibitory mechanisms related to contrast sensitivity are relatively well understood in the visual cortex. Therefore, as we will see in my work and others' the occipital visual cortex is usually chosen as a reference region to study the GABAergic system activity at baseline and after an intervention.

The GABAergic System and Physiologic High Frequency Oscillations

The study of high frequency oscillations (HFOs) is gaining increased attention by neuroscientists and epileptologists.

When neurophysiologists started recording brain activity from the scalp and directly from within the brain, it was clear that various oscillations are produced that are important for the different cognitive tasks. These oscillations were classified in a series of frequency bands which were designated by Greek letters such as mu, theta, alpha, beta and gamma oscillations (Jefferys et al., 2012).

In the last three decades, the study of brain activity in frequency bands above 30 Hz with electroencephalography became possible because of the rise of broad-band digital EEG which allowed for the recording of signals that can reach 500 Hz or above. Moreover, animal studies showed that gamma oscillations in the 38 to 100 Hz in several cortical and subcortical brain areas to play an important role (Bressler & Freeman, 1980).

Currently, the gamma frequency range is defined as frequency components between 30 and 100 Hz and HFOs refer to frequencies beyond 100 Hz (Buzsáki et al., 2012). However, it is crucial to discuss gamma oscillations whenever we talk about HFOs because of the shared mechanisms of generation. Sullivan et al 2011 showed that HFOs and gamma oscillations exist together in the hippocampus and they share overlapping mechanisms and physiologic conditions (Sullivan et al., 2011).

Of particular interest is the fact that gamma oscillations around 40 Hz in the visual cortex may be associated with visual perception (Singer & Gray, 1995). It has been suggested that gamma oscillations in this range contribute to how the visual cortex bind different visual scene features into a percept “the binding hypothesis”. It has also been shown that gamma oscillations act as a general mechanism to bind together local neurons and by phase synchronization and may synchronize neural activities of spatially separate cortical areas (Roelfsema et al., 1997). Gamma oscillations therefore play an important role in the integration of neural networks within and across brain structures.

For example, in schizophrenia, gamma band abnormalities have been reported in a variety of contexts. An abnormal gamma oscillatory activity in this disease has been linked to first episode of psychosis (Symond et al., 2005). Gamma

oscillations are also seen to be disturbed in untreated schizophrenic patients (Gallinat et al., 2004) and in unaffected relatives (Leicht et al., 2010, 2011).

At the local circuit level, gamma activity is generated through feedback inhibition on pyramidal neurons by the action of inhibitory fast-acting interneurons (Tamás et al., 2000). The activation of these fast-acting interneurons by optogenetics is sufficient to generate gamma oscillations in the mammalian cortex (Cardin et al., 2009; Sohal et al., 2009). In other words, gamma activity can be modulated by directly or indirectly altering the GABAergic system (M. A. Whittington, Faulkner, et al., 2000).

Clearly, it is now evident that GABAergic inhibition plays a crucial role in the rhythmic pacing of neuronal activity in health and disease states (Uhlhaas et al., 2009). Accordingly, dysfunctions in GABAergic interneurons result in changes in neural synchrony and gamma activity (Lewis et al., 2005).

The Occipital Cortex as a Model to Study the GABAergic System

GABAergic inhibition plays an important role in neural processing by maintaining network oscillations, synaptic plasticity and response gain. Moreover, the disruption of the GABAergic system is associated with different neurological disorders such as epilepsy, schizophrenia, anxiety, Alzheimer's disease and ASD (Moult, 2009)

Sensory processing in the primary visual cortex (V1) is a well-researched topic in systems neuroscience. The importance of inhibition in V1 stems from different features of the primary visual cortex that are needed to process sensory information appropriately. Firstly, surround suppression is needed to sharpen the neuronal orientation selectivity (Okamoto et al., 2009). Hubel and Wiesel were the first to propose a simple model in which excitatory feed forward connections give rise to orientation-selective cortical receptive fields in V1 (Hubel & Wiesel, 1959). Information processing in the visual cortex is likely to be influenced by the network state in addition to the action of individual neurons (Fiser et al., 2004; Han et al., 2008; Ringach, 2009) and this gives even more importance to E-I balance in the visual cortex.

For instance, in an attentive and aroused subject, one notices that low-amplitude gamma activity is predominant, whereas when the subject is inactive or sleepy, we see a dominance of high-amplitude low-frequency oscillations (Niedermeyer & Silva, 2005). GABAergic neurons have been long proposed to play an important role in the generation of gamma oscillations (Freund, 2003; Mann et al., 2005). Given the fact that the V1 and occipital region were extensively studied by researchers across many species, which allowed for the characterization of the GABAergic system and inhibitory inputs in this region to an extent that future researchers prefer to use this region as a reference or a model region to study E-I in health and disease (Isaacson & Scanziani, 2011)

Disease Models of Impaired GABAergic System:

Type 2 Diabetes Mellitus

Diabetes mellitus type 2 (DM) is a multisystemic endocrinological disorder that is known to influence the eyes, kidneys, and central nervous system in addition to other body organs (Olokoba et al., 2012; Strachan et al., 2009). Early in the disease, visual performance is poorly correlated with the grade of non-proliferative diabetic retinopathy (Yau et al., 2012). Moreover, metabolic biomarkers cannot predict visual performance in the early stages of type 2 DM (Hove et al., 2006).

(Buzsáki et al., 2007; Logothetis et al., 2001; Lyoo et al., 2009; van Bussel et al., 2016) showed that patients with type 2 DM who had a decreased resting-state brain activity developed poorer memory performance and executive functioning. GABA and glutamate concentrations in different brain regions have been linked to normal brain functioning and cognitive impairment in type 2 DM (Buzsáki et al., 2007; Logothetis et al., 2001; Lyoo et al., 2009; van Bussel et al., 2016). In an animal model of type 2 DM, there was evidence of impaired GABA and glutamate homeostasis in the brain “disrupted E-I balance” (Sickmann et al., 2010). More evidence has emerged on the hypothesis of impaired GABAergic system in brain regions specific to cognitive deficits in type 2 DM (Thielen et al., 2019). Again, increased GABA concentration was the culprit. (van Bussel et al., 2016) have also showed a higher GABA concentration in different brain regions in type 2 diabetes mellitus patients when compared to healthy individuals. Moreover, the E-I balance in such patients was in favor of more GABA than glutamate. A recent study showed that poor metabolic control in T2DM is associated with higher GABA/Glx ratio, however when taken individually, GABA and Glx were reported to be lower in T2DM patients as compared to controls (d’Almeida et al., 2020). These results are consistent with the notion that abnormal neurotransmission and E-I balance is correlated with metabolic control in particular in T2DM (d’Almeida et al., 2020).

Interestingly, color contrast detection has been reported to be impaired very early in type 2 DM patients, before there is any evidence of retinopathy (Reis et al., 2014). Another important thing to note is that there is strong evidence of altered cortical neurochemistry in type 2 DM that is associated with mild cognitive

impairment (Kalmijn et al., 1995) with increased concentration of GABA in the occipital lobe compared to non-diabetics (van Bussel et al., 2016). van Bussel also showed a positive correlation between occipital GABA, HbA1C and severity of cognitive impairment.

Disruption of GABAergic inhibitory circuits in the occipital region has been associated with impaired visual function in schizophrenia, neurofibromatosis type 1, major depressive disorder (Norton et al., 2016; Maria J. Ribeiro et al., 2015; Violante et al., 2013; Yoon et al., 2010). However, the association between occipital GABA and visual performance in type 2 DM was still to be explored.

Drug Resistant Epilepsy:

Epilepsy is the most common serious neurological disorder, and it accounts for 1% of global disease burden according to the WHO (World Health Organization, 2005). Approximately, up to 30% of patients with epilepsy will not be seizure-free despite taking adequate antiepileptic drugs in maximum dose (Berg, 2009; Berg et al., 2010). Such cases are referred as drug-resistant epilepsy. Patients with possible localization of their drug-resistant epilepsy can benefit from resection surgery (Chandra et al., 2010). The localization of the onset of seizures in such patients is made possible with the utilization of EEG, Video-EEG, MRI, SPECT and MEG. Electrocorticography (ECoG) and MEG also provide valuable information for the purposes of localization (Chandra et al., 2010). Unfortunately, the identification of a localized focus even in seizures that seem focal in onset may fail in one third of patients (Chandra et al., 2010). Because of that, the identification of molecular and cellular biomarkers is needed in drug-resistant epilepsy patients which can provide localization information, further expand our understanding of epileptogenesis, and explain how certain antiepileptics work.

GABA, the principal inhibitory neurotransmitter in the brain, has long been thought to be related to epileptogenesis (Isokawa-Akesson et al., 1989; Miller & Ferrendelli, 1990; Telfeian & Connors, 1998). While some studies show that GABA transmission is decreased in patients with epilepsy, it is also worth mentioning that some studies show immature GABAergic inhibitory system may contribute to epileptogenesis (Galanopoulou, 2007). For instance, (Cepeda et al., 2007; Cherubini et al., 1991), show that predominant GABAergic synaptic transmission in an immature neuronal network may lead to depolarization and

excessive cell firing, where GABA acts as an excitatory neurotransmitter. Patients with drug resistant epilepsy are reported to have a higher frequency of spontaneous inhibitory postsynaptic currents which are related to the generation of pathologic high frequency oscillations (Cepeda et al., 2006). Moreover, there is current evidence of increased GABA receptor activity relative to glutamate receptor activity in severe cases of cortical dysplasia (André et al., 2008). (André et al., 2008) has also suggested that the pattern of GABAergic system disruption might be specific to the type of epilepsy syndrome the patient has.

Interestingly, the use of antiepileptic medications in patients with idiopathic generalized epilepsy is correlated with an increase in GABA concentration in the occipital region (Simister et al., 2003a) but no change in GABA concentration in the frontal region (Simister et al., 2003b) when measured by H-MRS PRESS. Therefore, it is sensible to choose the occipital region as a reference region to study the effects of different antiepileptics on the E-I balance in drug-resistant epilepsy.

Focal cortical dysplasia and tuberous sclerosis are possible etiologies of drug-resistant epilepsy. It has been reported that GABA concentration is found to be markedly elevated in the epileptogenic zone in seizure disorders that are characterized by an abnormal cortex (Taki et al., 2009). There is also an almost consensus now on increased levels of GABA in *ex vivo* spectroscopy experiments of brain biopsies from patients with drug-resistant epilepsy (Aasly et al., 1999; Petroff, Pleban, et al., 1995; Petroff, Rothman, et al., 1995).

A very recent study showed clearly that pathological high frequency oscillations are associated with increased GABAergic synaptic activity in the epileptic focus, further emphasizing the role of GABAergic interneurons in the generation of pathological HFOs (Cepeda et al., 2020). The current evidence points towards the idea that pathologic HFOs are epileptogenic, rather than a mere consequence of epileptogenesis. Interestingly, pacemaker GABA activity is also associated with pathologic HFOs, further confirming that GABA is not purely an inhibitory neurotransmitter when it comes to the epileptogenic zone (Cepeda et al., 2020). Figure 1.1 shows the cellular mechanisms of generation of different oscillations in epilepsy.

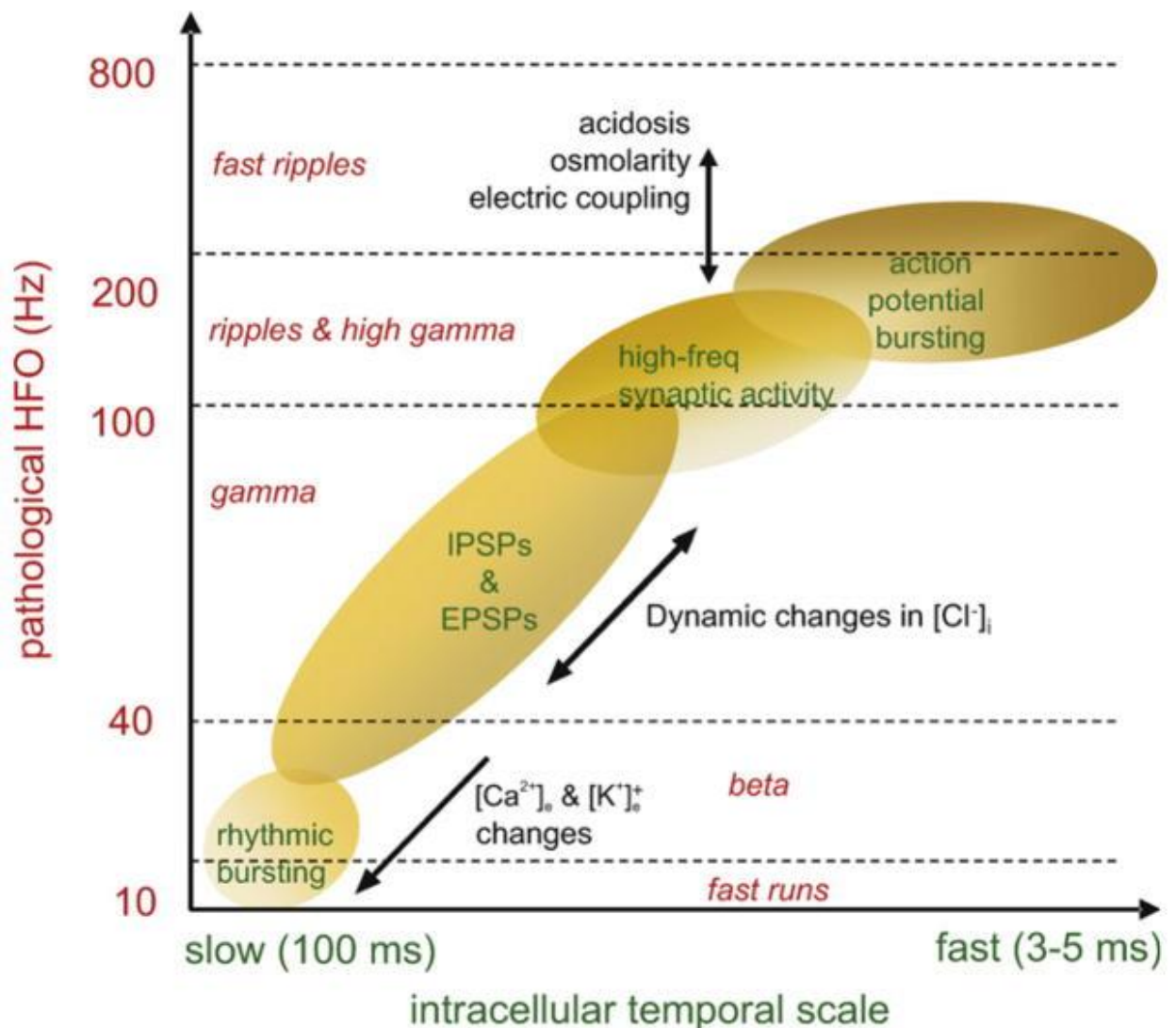


Figure 1.1: The cellular mechanisms of generation of pathologic gamma and high frequency oscillations. Source: (Jefferys et al., 2012). Permission to use was obtained.

A seizure can be seen as a result of hypersynchronous neuronal discharges during which summation of nearly synchronously occurring action potentials and postsynaptic currents give rise to large amplitude epileptic EEG patterns. The first clear evidence of GABAergic inhibition as a causative mechanism of epileptogenesis emerges from the work of (Khazipov & Holmes, 2003) where they showed epileptic spiking in a kainic acid model of epilepsy from the hippocampus in rats in the gamma frequency range to be caused by inhibitory GABA neuronal synchronization and little to no role of glutamatergic excitatory currents. The work of (Gulyás et al., 2010; Mann & Paulsen, 2007; Miles A. Whittington et al., 2011)

also contributes to the hypothesis that the generation of pathologic gamma oscillations in epilepsy shares the same mechanism of physiologic gamma oscillations, i.e. by the virtue of synchronous GABAergic inhibition mediated via GABA_A receptors.

Interestingly, epileptic syndromes that are characterized by slow rhythmic activity such as absence seizures have also been linked to increased activity of the GABAergic system. Activation of GABA_B receptor-mediated inhibitory postsynaptic potentials in the thalamocortical circuits result in slow responses that are in the 3 Hz frequency range (von Krosigk et al., 1993)

Modulation of The GABAergic System in Epilepsy by Cathodal Direct Current Stimulation (Fregni et al., 2006) showed that c-tDCS stimulation of the EZ in patients with drug-resistant epilepsy decreased cortical excitability in the epileptogenic focus. (Auvichayapat et al., 2013) also studied the antiepileptic efficacy of c-tDCS in 36 children with drug-resistant epilepsy. C-tDCS was efficient in decreasing epileptiform discharges for 48 hours. (Yook et al., 2011) reported dramatic results when they used c-tDCS on an 11-year-old girl with drug resistant epilepsy due to focal cortical dysplasia.

The antiepileptic effects of c-tDCS are expected to come into play by decreasing cortical excitability and altering synaptic efficacy (Nitsche et al., 2003). Cathodal tDCS is shown to decrease the number of epileptic spikes, the firing rate of pyramidal cells and suppressed GABAergic interneurons in a simulation model (Denoyer et al., 2020). In this explicit model, they used an epileptogenic network that is capable of producing spike-like events involving more GABAergic neurons which is in agreement with other experimental studies (Lévesque et al., 2016).

Measurement of Brain Neurotransmitters by MRS

Magnetic resonance imaging (MRI) is an imaging technique that allows the direct visualization of soft tissues in addition to giving information about functional states. MRI takes advantage of the atomic nuclei found in different molecules which can absorb and emit energy when placed in an external magnetic field. Because hydrogen atoms exist in abundance in the human body, they are often used to generate radio frequency signals that can be detected by the MRI signals. Hydrogen nuclei possess an intrinsic property called nuclear spin. In simple words, the nuclei of hydrogen can rotate in a magnetic field. When hydrogen nuclei are placed in a magnetic field, they tend to align themselves parallel with the field.

Spinning protons precess or wobble around the axis of the external magnetic field. The frequency of this precession is known as resonance frequency or Larmor frequency and is proportional to the strength of the magnetic field.

Protons have a specific resonance frequency at which they absorb energy to move to a higher energy state. The net magnetization is then brought away from equilibrium and the nuclei will spin around the field's axis with a frequency of 42.58 MHz/T (In Vivo NMR Spectroscopy: Principles and Techniques, 3rd Edition | Wiley). Radio waves at this frequency are emitted from the body which can be measured and analyzed by the MRI system to produce images or spectra. The energy is then retransmitted when the radio frequency is turned off (RF pulse). Images obtained here are known as T1 recovery to thermal equilibrium. The recovery rate is different for each tissue which allows for the differentiation between the different tissues in a T1 image.

Proton magnetic resonance spectroscopy (^1H -MRS) is a form of MRI used to detect and measure the concentration of different tissue metabolites in vivo (Harris et al., 2017). This technique exploits the fact that each metabolite produces a unique MRS signal because of the different spin frequencies or resonance frequencies of protons within a molecule (In Vivo NMR Spectroscopy: Principles and Techniques, 3rd Edition | Wiley). The hydrogen nucleus which is found in most biologic metabolites exhibit a resonance behavior in a magnetic field. The resonance frequency of the hydrogen nucleus in each molecule is

dependent upon the chemical environment of the molecule and this can be taken advantage of to separate the signal of different metabolites in a tissue with MRS. The first factor to affect the resonance frequency of protons in a molecule is known as chemical shift. The nucleus is shielded from the external magnetic field by surrounding electrons and the configuration of the electron cloud surrounding the hydrogen nucleus will affect the resonance frequency.

The signals are separated along the chemical shift axis to reveal a spectrum with a different distinct peak that include N-acetyl aspartate (NAA), creatine (Cr), myoinositol (ml) and choline (Cho) in the brain. However, many other metabolites are also found in the brain such as neurotransmitters which have a weaker signal that is difficult to separate from the signals of other larger molecules. The easiest way to identify the signal of the smaller molecules is to reduce the information content of the one-dimensional spectrum “editing the spectrum”. The most commonly used approach is known as J-coupling editing (Near et al., 2013; Puts & Edden, 2012; Rothman et al., 1993). Molecules that can be identified with this approach include ascorbic acid, GABA, lactate, aspartate, N-acetyl aspartyl glutamate, 2-hydroxygutarate, glutathione (GSH), glutamate, glycine and serine. Because water is the most abundant proton containing metabolite in the brain, it will contribute the most to the detected signal by MRS. Therefore, water suppression pulses are used to suppress the water peak and allow the visualization of the spectra of other less abundant brain metabolites. Water is suppressed by exciting protons in water by applying a resonance frequency that is the same as the frequency of water.

The common approach when using MRS is to select a specified region of interest within the brain. This is known as single voxel MRS and is the approach used in this thesis. The measured signal is plotted onto a spectrum where the x axis is the resonance frequency whereas the y axis represents the amplitude of the measured signal. Figure 1.1 shows an example of an MRS spectrum.

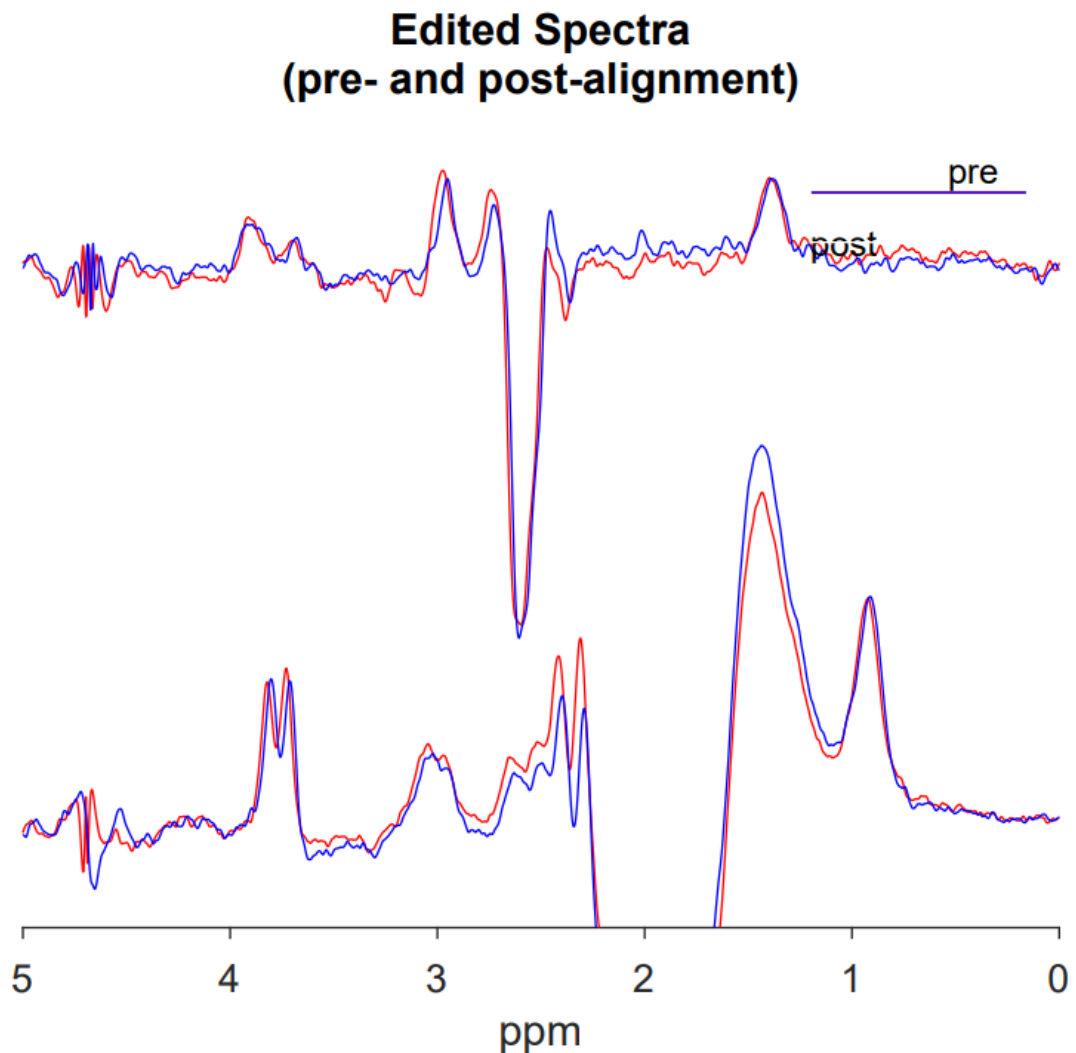


Figure 1.1: Edited Spectra obtained from a single voxel in the occipital region in a patient with drug resistant epilepsy. Spectral registration with post-hoc choline-creatine alignment (pre-included in Gannet toolbox) was used to obtain the post-alignment edited spectra (Mikkelsen et al., 2018). Ppm stands for parts per million.

GABA MRS:

γ -aminobutyric acid (GABA) is the main inhibitory neurotransmitter in the human brain and GABAergic inhibition plays an important role in shaping the patterns of neuronal activity, information processing and synaptic plasticity. GABA is present in the brain at relatively small millimolar (1 mM) concentrations (Govindaraju et al., 2000; Rae, 2014). They can be detected in vivo by ^1H magnetic resonance spectroscopy (^1H -MRS). This technique suffers from incomplete resolution of

metabolite signals. This limitation results in overlapping of the signal of low-concentration metabolites by the signal of large-concentration metabolites. Spectral editing techniques such as MEscher-Garwood Point RESolved Spectroscopy (MEGA-PRESS) (Mescher et al., 1998) can simplify the results to focus on metabolites of low-concentration such as GABA (Rothman et al., 1993) and GSH (Terpstra et al., 2003).

To quantify GABA, J-editing is used (P. G. Mullins et al., 2014). GABA signal can be separated into sub-peaks because it has a weakly coupled spin system. Because GABA has three methylene groups that contain a hydrogen nucleus, we get three distinct signals in the GABA signal at 1.9, 2.3 and 3.0 ppm. In MEGA-PRESS approach, the GABA signal at 3.0 ppm is coupled to a signal at 1.9 ppm. A frequency-selective pulse is applied at 1.9 ppm which will have an effect at both 1.9 and 3.0 ppm, and this will leave other uncoupled resonances unaffected. This is known as an “ON” scan. The scan is then repeated without the editing pulse and it will be known as an “OFF” scan. Finally, a difference between the spectra obtained during repeated ON and OFF scans result in a spectrum only containing the signals of the molecule of interest, in this case GABA. This method is explained in detail in (P. G. Mullins et al., 2014). GABA is finally quantified by measuring the area under the peak which is modelled as a Gaussian.

MEGA-PRESS can edit only one metabolite at a time from a single brain region, making it a very time-consuming method to measure brain metabolites. Because of this limitation, long acquisition times are needed, and you notice that most studies that utilize MEGA-PRESS have a limited number of studied metabolites and brain regions. Accordingly, most studies that utilize MEGA-PRESS to measure GABA usually do not include other brain metabolites that are of importance such as GSH (P. G. Mullins et al., 2014).

Recently, the Hadamard Encoding and Reconstruction of MEGA-Edited Spectroscopy (HERMES) approach (Chan et al., 2016) allowed the editing of more than one metabolite with overlapping signals within a single acquisition.

In HERMES approach, the editing pulses can be separately applied to GABA spins at 1.9 ppm and GSH spins at 4.56 ppm. Four sub-experiments labeled A, B, C and D are performed to apply editing to the signals of GABA and GSH (ON_{GABA} , ON_{GSH}), (ON_{GABA} , OFF_{GSH}), (OFF_{GABA} , ON_{GSH}) and (OFF_{GABA} , OFF_{GSH}).

The editing scheme is shown in Figure 1.3. The GABA-edited difference spectrum is calculated by subtracting the two OFF_{GABA} scans from the sum of the two ON_{GABA} scans. Similarly, one can get the GSH-edited difference spectrum (Saleh et al., 2016).

Both MEGA-PRESS and HERMES approaches were used in this thesis in two different works.

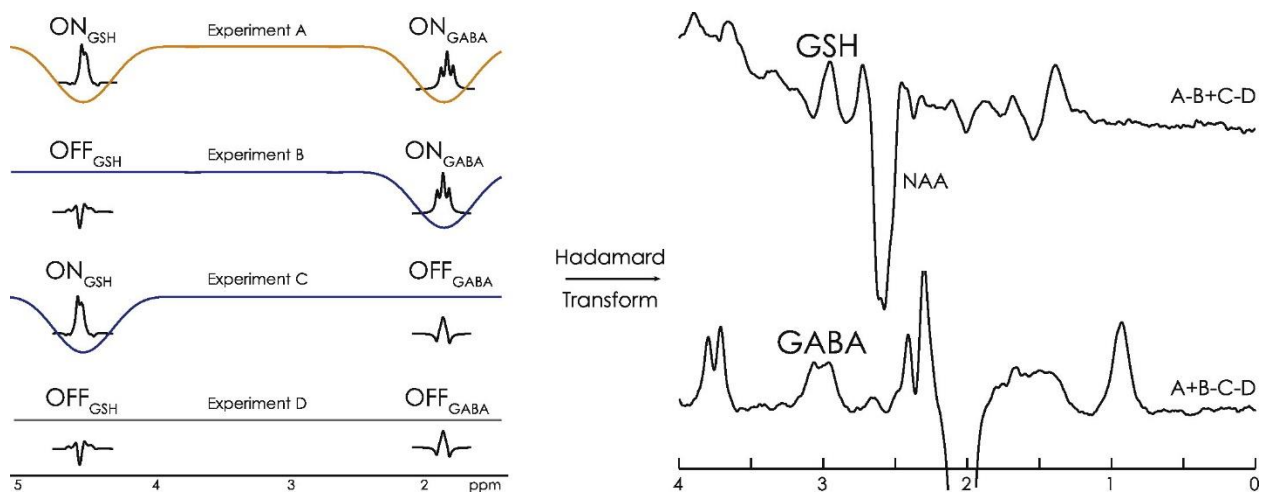


Figure 1.3: HERMES approach to separate GABA and GSH signals. Source: (Saleh et al., 2016). Permission to use was obtained.

Measurement of Gamma Activity by EEG:

Evoked oscillatory responses are phase-locked to the stimulus onset and usually have an average latency of 100 msec following the stimulus onset (Tallon-Baudry & Bertrand, 1999). On the other hand, induced oscillatory activity is not phase-locked to the stimulus onset and averaging will cancel them (Tallon-Baudry & Bertrand, 1999). It has been previously suggested that induced gamma activity reflect micro saccadic eye movement rather than neuronal processing during cognitive paradigms (Yuval-Greenberg et al., 2008), therefore the approach chosen for this thesis was to analyze evoked gamma activity.

Another possible artifact that is known to impact the measured gamma activity by scalp EEG is the muscular artifact (Shackman, 2010). Since this type of activity is characterized by irregular spikes and waves, they can be significantly reduced by preprocessing steps and by averaging many trials when doing evoked response potential experiments (Barr & Daskalakis, 2010). In the second part of this thesis where the disease model is that of drug resistant epilepsy, we measured gamma activity using scalp and intracranial EEG electrodes. The EEG signal acquisition and processing are described in the subsequent chapters as they were different for each work.

Aims

The rationale of this thesis is to understand the role of the GABAergic system in physiologic and pathologic conditions, using two distinct disease models.

The GABAergic system's integrity is crucial for normal brain development, synaptic plasticity, rhythmic brain activity, and local or distant synchronization. The importance of GABAergic inhibition in normal physiologic conditions is evident from our understanding of the pathway of information processing in the primary visual cortex. Disruptions of the GABAergic system are reported in a wide array of neuropsychiatric diseases including ASD, schizophrenia, Alzheimer's disease, and epilepsy. The literature also points to possible GABAergic disruptions in endocrinological diseases such as type 2 diabetes mellitus.

By utilizing a comprehensive array of techniques (MRS, EEG, visual tasks) and defined cohorts we aim to analyze the impact of different disease models on the E-I balance in general and the GABAergic system and gamma activity in particular. We aim to study how visual performance in type 2 diabetes mellitus (T2DM) patients correlate with the degree of GABAergic disruption in the occipital region, and the relationship between blood brain barrier integrity and visual performance in T2DM.

We also aim to understand the physiological value of cortical gamma activity in perceptual decision processing. Finally, we aim to study how GABAergic system disruption is epileptogenic and not a mere consequence in drug resistant epilepsy and how the modulation of this system by the means of noninvasive stimulation could relate with less epileptogenicity.

Outline

It is clear now that the excitation-inhibition balance hypothesis plays an integral role in explaining a large range of physiologic and pathologic conditions. In the scope of E-I balance hypothesis, one may now be able to explain how individual neurons and up to neural networks in the brain work and how the state of such a system may be correlated with a certain disease.

The GABAergic inhibitory system is critical for optimum processing of sensory information in the primary visual cortex. This system is also responsible for rhythmic brain activity “oscillations”. It appears that fast oscillations are related to GABA_A receptor activity, whereas the generation of slow frequency oscillations is mediated by GABA_B receptors. In this work we studied different pathologies that we hypothesized to have an impact on the E-I balance.

In **Chapter 1** a general introduction is presented that explains the main concepts and current literature related to the thesis. We also provide a brief description of the methodologies used in this work focusing mainly on MRS and EEG.

Chapter 2 is subdivided into two sections. The main model of disease in this chapter is “type 2 diabetes mellitus” (T2DM). **Chapter 2.1** focuses on the effect of T2DM on the E-I balance and the GABAergic system in the occipital region. It correlated visual performance in a cohort of T2DM patients with the concentration of GABA measured by MRS in the occipital region. **Chapter 2.2** discusses the impact of T2DM on blood-brain-barrier (BBB) integrity and how it correlates with visual performance. This can be seen as a continuation of the previous work where we try to focus on the principle of neurovascular coupling in the occipital region.

In **Chapter 3** there are two sections. In **Chapter 3.1** we focus on physiologic high frequency gamma activity and how it relates to perceptual decision from an intracranial study. In this work, I was a second author where I contributed with methods development, data acquisition, analysis, and manuscript writing. In **Chapter 3.2** we dig deeper into pathologic high frequency oscillations and how they relate to epileptogenesis and the disruption of the GABAergic system. In here, we present a work-in-progress about cathodal tDCS as an antiepileptic. In this work, we study how cathodal tDCS impacts the GABAergic system in the

epileptogenic zone as compared to a reference area in the occipital region. This work has been submitted to a journal awaiting publication.

Chapter 4 focuses on how certain cortical metabolites are disrupted in drug-resistant epilepsy. Again, we have two sections in here. In **Chapter 4.1** we present our work on how lovastatin impacts the E-I balance in epileptic patients and how this correlates with changes in physiologic gamma oscillations. This is a work-in-progress where we are still recruiting patients. In **Chapter 4.2** we present the proposal and protocol of a new project that will commence in November 2020 to study the value of AMT-PET for the localization of the epileptogenic zone in tuberous sclerosis associated epilepsy and drug resistant epilepsy.

Finally, in **Chapter 5** “Concluding remarks” we provide an integrative analysis of the different diseases studied and summarize our results and approaches.

References:

- Aasly, J., Silfvenius, H., Aas, T. C., Sonnewald, U., Olivecrona, M., Juul, R., & White, L. R. (1999). Proton magnetic resonance spectroscopy of brain biopsies from patients with intractable epilepsy. *Epilepsy Research*, 35(3), 211–217. [https://doi.org/10.1016/S0920-1211\(99\)00011-X](https://doi.org/10.1016/S0920-1211(99)00011-X)
- André, V. M., Cepeda, C., Vinters, H. v., Huynh, M., Mathern, G. W., & Levine, M. S. (2008). Pyramidal cell responses to γ -aminobutyric acid differ in type I and Type II cortical dysplasia. *Journal of Neuroscience Research*, 86(14), 3151–3162. <https://doi.org/10.1002/jnr.21752>
- Auvichayapat, N., Rotenberg, A., Gersner, R., Ngodklang, S., Tiamkao, S., Tassaneeyakul, W., & Auvichayapat, P. (2013). Transcranial direct current stimulation for treatment of refractory childhood focal epilepsy. *Brain Stimulation*, 6(4), 696–700. <https://doi.org/10.1016/j.brs.2013.01.009>
- Ballester, R., Marchuk, D., Boguski, M., Saulino, A., Letcher, R., Wigler, M., & Collins, F. (1990). The NF1 locus encodes a protein functionally related to mammalian GAP and yeast IRA proteins. *Cell*, 63(4), 851–859. [https://doi.org/10.1016/0092-8674\(90\)90151-4](https://doi.org/10.1016/0092-8674(90)90151-4)
- Barr, M. S., & Daskalakis, Z. J. (2010). The potentially deleterious impact of muscle activity on gamma band inferences. In *Neuropsychopharmacology* (Vol. 35, Issue 3, pp. 848–849). Nature Publishing Group. <https://doi.org/10.1038/npp.2009.174>
- Berg, A. T. (2009). Identification of Pharmacoresistant Epilepsy. In *Neurologic Clinics* (Vol. 27, Issue 4, pp. 1003–1013). Elsevier. <https://doi.org/10.1016/j.ncl.2009.06.001>
- Berg, A. T., Berkovic, S. F., Brodie, M. J., Buchhalter, J., Cross, J. H., van Emde Boas, W., Engel, J., French, J., Glauser, T. A., Mathern, G. W., Moshé, S. L., Nordli, D., Plouin, P., & Scheffer, I. E. (2010). Revised terminology and concepts for organization of seizures and epilepsies: Report of the ILAE Commission on Classification and Terminology, 2005-2009. *Epilepsia*, 51(4), 676–685. <https://doi.org/10.1111/j.1528-1167.2010.02522.x>
- Bourgeron, T. (2015). From the genetic architecture to synaptic plasticity in autism spectrum disorder. In *Nature Reviews Neuroscience* (Vol. 16, Issue 9, pp. 551–563). Nature Publishing Group. <https://doi.org/10.1038/nrn3992>
- Bozzi, Y., Provenzano, G., & Casarosa, S. (2018). Neurobiological bases of autism–epilepsy comorbidity: a focus on excitation/inhibition imbalance. *European Journal of Neuroscience*, 47(6), 534–548. <https://doi.org/10.1111/ejn.13595>
- Bressler, S. L., & Freeman, W. J. (1980). Analyse de fréquence de l'EEG du système olfactif chez le chat, le lapin et le rat. *Electroencephalography and Clinical Neurophysiology*, 50(1–2), 19–24. [https://doi.org/10.1016/0013-4694\(80\)90319-3](https://doi.org/10.1016/0013-4694(80)90319-3)
- Brown, M. S., Singel, D., Hepburn, S., & Rojas, D. C. (2013). Increased glutamate concentration in the auditory cortex of persons with autism and first-degree relatives: A $^1\text{H-MRS}$ study. *Autism Research*, 6(1), 1–10. <https://doi.org/10.1002/aur.1260>
- Buzsáki, G., Kaila, K., & Raichle, M. (2007). Inhibition and Brain Work. In *Neuron* (Vol. 56, Issue 5, pp. 771–783). Neuron. <https://doi.org/10.1016/j.neuron.2007.11.008>
- Canitano, R., & Pallagrosi, M. (2017). Autism spectrum disorders and schizophrenia spectrum disorders: Excitation/inhibition imbalance and developmental trajectories. *Frontiers in Psychiatry*, 8(MAY). <https://doi.org/10.3389/fpsy.2017.00069>

- Cardin, J. A., Carlén, M., Meletis, K., Knoblich, U., Zhang, F., Deisseroth, K., Tsai, L. H., & Moore, C. I. (2009). Driving fast-spiking cells induces gamma rhythm and controls sensory responses. *Nature*, 459(7247), 663–667. <https://doi.org/10.1038/nature08002>
- Carvalho Pereira, A., Violante, I. R., Mougá, S., Oliveira, G., & Castelo-Branco, M. (2018). Medial Frontal Lobe Neurochemistry in Autism Spectrum Disorder is Marked by Reduced N-Acetylaspartate and Unchanged Gamma-Aminobutyric Acid and Glutamate + Glutamine Levels. *Journal of Autism and Developmental Disorders*, 48(5), 1467–1482. <https://doi.org/10.1007/s10803-017-3406-8>
- Cepeda, C., André, V. M., Levine, M. S., Salamon, N., Miyata, H., Vinters, H. v., & Mathern, G. W. (2006). Epileptogenesis in pediatric cortical dysplasia: The dysmature cerebral developmental hypothesis. In *Epilepsy and Behavior* (Vol. 9, Issue 2, pp. 219–235). Academic Press. <https://doi.org/10.1016/j.yebeh.2006.05.012>
- Cepeda, C., André, V. M., Wu, N., Yamazaki, I., Uzgil, B., Vinters, H. v., Levine, M. S., & Mathern, G. W. (2007). Immature neurons and GABA networks may contribute to epileptogenesis in pediatric cortical dysplasia. *Epilepsia*, 48(SUPPL. 5), 79–85. <https://doi.org/10.1111/j.1528-1167.2007.01293.x>
- Cepeda, C., Levinson, S., Nariai, H., Yazon, V. W., Tran, C., Barry, J., Oikonomou, K. D., Vinters, H. v., Fallah, A., Mathern, G. W., & Wu, J. Y. (2020). Pathological high frequency oscillations associate with increased GABA synaptic activity in pediatric epilepsy surgery patients. *Neurobiology of Disease*, 134, 104618. <https://doi.org/10.1016/j.nbd.2019.104618>
- Chan, K. L., Puts, N. A. J., Schär, M., Barker, P. B., & Edden, R. A. E. (2016). HERMES: Hadamard encoding and reconstruction of MEGA-edited spectroscopy. *Magnetic Resonance in Medicine*, 76(1), 11–19. <https://doi.org/10.1002/mrm.26233>
- Chandra, P., Neurology, M. T.-A. of I. A. of, & 2010, undefined. (n.d.). Epilepsy surgery: recommendations for India. Ncbi.Nlm.Nih.Gov. Retrieved October 24, 2020, from <https://www.ncbi.nlm.nih.gov/pmc/articles/pmc2924525/>
- Cherubini, E., Gaiarsa, J. L., & Ben-Ari, Y. (1991). GABA: an excitatory transmitter in early postnatal life. *Trends in Neurosciences*, 14(12), 515–519. [https://doi.org/10.1016/0166-2236\(91\)90003-D](https://doi.org/10.1016/0166-2236(91)90003-D)
- d’Almeida, O. C., Violante, I. R., Quendera, B., Moreno, C., Gomes, L., & Castelo-Branco, M. (2020). The neurometabolic profiles of GABA and Glutamate as revealed by proton magnetic resonance spectroscopy in type 1 and type 2 diabetes. *PLOS ONE*, 15(10), e0240907. <https://doi.org/10.1371/journal.pone.0240907>
- Denoyer, Y., Merlet, I., Wendling, F., & Benquet, P. (2020). Modelling acute and lasting effects of tDCS on epileptic activity. *Journal of Computational Neuroscience*, 48(2), 161–176. <https://doi.org/10.1007/s10827-020-00745-6>
- Edden, R. A. E., Muthukumaraswamy, S. D., Freeman, T. C. A., & Singh, K. D. (2009). Orientation discrimination performance is predicted by GABA concentration and gamma oscillation frequency in human primary visual cortex. *Journal of Neuroscience*, 29(50), 15721–15726. <https://doi.org/10.1523/JNEUROSCI.4426-09.2009>
- Edgar, J. C., Khan, S. Y., Blaskey, L., Chow, V. Y., Rey, M., Gaetz, W., Cannon, K. M., Monroe, J. F., Cornew, L., Qasmieh, S., Liu, S., Welsh, J. P., Levy, S. E., & Roberts, T. P. L. (2013). Neuromagnetic Oscillations Predict Evoked-Response

- Latency Delays and Core Language Deficits in Autism Spectrum Disorders. *Journal of Autism and Developmental Disorders*, 45(2), 395–405. <https://doi.org/10.1007/s10803-013-1904-x>
- Fiser, J., Chiu, C., & Weliky, M. (2004). Small modulation of ongoing cortical dynamics by sensory input during natural vision. *Nature*, 431(7008), 573–578. <https://doi.org/10.1038/nature02907>
- Fregni, F., Thome-Souza, S., Nitsche, M. A., Freedman, S. D., Valente, K. D., & Pascual-Leone, A. (2006). A controlled clinical trial of cathodal DC polarization in patients with refractory epilepsy. *Epilepsia*, 47(2), 335–342. <https://doi.org/10.1111/j.1528-1167.2006.00426.x>
- Freund, T. F. (2003). Interneuron Diversity series: Rhythm and mood in perisomatic inhibition. In *Trends in Neurosciences* (Vol. 26, Issue 9, pp. 489–495). Elsevier Ltd. [https://doi.org/10.1016/S0166-2236\(03\)00227-3](https://doi.org/10.1016/S0166-2236(03)00227-3)
- Galanopoulou, A. S. (2007). Developmental patterns in the regulation of chloride homeostasis and GABAA receptor signaling by seizures. *Epilepsia*, 48(SUPPL. 5), 14–18. <https://doi.org/10.1111/j.1528-1167.2007.01284.x>
- Gallinat, J., Winterer, G., Herrmann, C. S., & Senkowski, D. (2004). Reduced oscillatory gamma-band responses in unmedicated schizophrenic patients indicate impaired frontal network processing. *Clinical Neurophysiology*, 115(8), 1863–1874. <https://doi.org/10.1016/j.clinph.2004.03.013>
- Gao, R., & Penzes, P. (2015). Common Mechanisms of Excitatory and Inhibitory Imbalance in Schizophrenia and Autism Spectrum Disorders. *Current Molecular Medicine*, 15(2), 146–167. <https://doi.org/10.2174/1566524015666150303003028>
- Geschwind, D. H., & Levitt, P. (2007). Autism spectrum disorders: developmental disconnection syndromes. In *Current Opinion in Neurobiology* (Vol. 17, Issue 1, pp. 103–111). *Curr Opin Neurobiol.* <https://doi.org/10.1016/j.conb.2007.01.009>
- Gonçalves, J., Violante, I. R., Sereno, J., Leitão, R. A., Cai, Y., Abrunhosa, A., Silva, A. P., Silva, A. J., & Castelo-Branco, M. (2017). Testing the excitation/inhibition imbalance hypothesis in a mouse model of the autism spectrum disorder: In vivo neurospectroscopy and molecular evidence for regional phenotypes. *Molecular Autism*, 8(1), 47. <https://doi.org/10.1186/s13229-017-0166-4>
- Govindaraju, V., Young, K., & Maudsley, A. A. (2000). Proton NMR chemical shifts and coupling constants for brain metabolites. *NMR in Biomedicine*, 13(3), 129–153. [https://doi.org/10.1002/1099-1492\(200005\)13:3<129::AID-NBM619>3.0.CO;2-V](https://doi.org/10.1002/1099-1492(200005)13:3<129::AID-NBM619>3.0.CO;2-V)
- Gulyás, A. I., Szabó, G. G., Ulbert, I., Holderith, N., Monyer, H., Erdélyi, F., Szabó, G., Freund, T. F., & Hájos, N. (2010). Parvalbumin-containing fast-spiking basket cells generate the field potential oscillations induced by cholinergic receptor activation in the hippocampus. *Journal of Neuroscience*, 30(45), 15134–15145. <https://doi.org/10.1523/JNEUROSCI.4104-10.2010>
- Han, F., Caporale, N., & Dan, Y. (2008). Reverberation of Recent Visual Experience in Spontaneous Cortical Waves. *Neuron*, 60(2), 321–327. <https://doi.org/10.1016/j.neuron.2008.08.026>
- Harris, A. D., Saleh, M. G., & Edden, R. A. E. (2017). Edited 1H magnetic resonance spectroscopy in vivo: Methods and metabolites. In *Magnetic Resonance in Medicine* (Vol. 77, Issue 4, pp. 1377–1389). John Wiley and Sons Inc. <https://doi.org/10.1002/mrm.26619>

- Hengen, K. B., Lambo, M. E., VanHooser, S. D., Katz, D. B., & Turrigiano, G. G. (2013). Firing rate homeostasis in visual cortex of freely behaving rodents. *Neuron*, 80(2), 335–342. <https://doi.org/10.1016/j.neuron.2013.08.038>
- Horder, J., Petrinovic, M. M., Mendez, M. A., Bruns, A., Takumi, T., Spooren, W., Barker, G. J., Kunnecke, B., & Murphy, D. G. (2018). Glutamate and GABA in autism spectrum disorder—a translational magnetic resonance spectroscopy study in man and rodent models. *Translational Psychiatry*, 8(1). <https://doi.org/10.1038/s41398-018-0155-1>
- Hove, M. N., Kristensen, J. K., Lauritzen, T., & Bek, T. (2006). The relationships between risk factors and the distribution of retinopathy lesions in type 2 diabetes. *Acta Ophthalmologica Scandinavica*, 84(5), 619–623. <https://doi.org/10.1111/j.1600-0420.2006.00710.x>
- Howell, B. W., & Smith, K. M. (2019). Synaptic structural protein dysfunction leads to altered excitation inhibition ratios in models of autism spectrum disorder. In *Pharmacological Research* (Vol. 139, pp. 207–214). Academic Press. <https://doi.org/10.1016/j.phrs.2018.11.019>
- Hubel, D. H., & Wiesel, T. N. (1959). Receptive fields of single neurones in the cat's striate cortex. *The Journal of Physiology*, 148(3), 574–591. <https://doi.org/10.1113/jphysiol.1959.sp006308>
- In Vivo NMR Spectroscopy: Principles and Techniques, 3rd Edition | Wiley. (n.d.). Retrieved October 24, 2020, from <https://www.wiley.com/en-us/In+Vivo+NMR+Spectroscopy%3A+Principles+and+Techniques%2C+3rd+Edition-p-9781119382515>
- Isaacson, J. S., & Scanziani, M. (2011). How inhibition shapes cortical activity. In *Neuron* (Vol. 72, Issue 2, pp. 231–243). NIH Public Access. <https://doi.org/10.1016/j.neuron.2011.09.027>
- Isokawa-Akesson, M., Wilson, C. L., & Babb, T. L. (1989). Inhibition in synchronously firing human hippocampal neurons. *Epilepsy Research*, 3(3), 236–247. [https://doi.org/10.1016/0920-1211\(89\)90030-2](https://doi.org/10.1016/0920-1211(89)90030-2)
- Jefferys, J. G. R., Menendez de la Prida, L., Wendling, F., Bragin, A., Avoli, M., Timofeev, I., & Lopes da Silva, F. H. (2012). Mechanisms of physiological and epileptic HFO generation. In *Progress in Neurobiology* (Vol. 98, Issue 3, pp. 250–264). PMC Canada manuscript submission. <https://doi.org/10.1016/j.pneurobio.2012.02.005>
- Kalmijn, S., Feskens, E. J., Launer, L. J., Stijnen, T., & Kromhout, D. (1995). Glucose intolerance, hyperinsulinaemia and cognitive function in a general population of elderly men. *Diabetologia*, 38(9), 1096–1102.
- Kayl, A. E., & Moore, B. D. (2000). Behavioral phenotype of neurofibromatosis, type 1. In *Mental Retardation and Developmental Disabilities Research Reviews* (Vol. 6, Issue 2, pp. 117–124). Ment Retard Dev Disabil Res Rev. [https://doi.org/10.1002/1098-2779\(2000\)6:2<117::AID-MRDD5>3.0.CO;2-X](https://doi.org/10.1002/1098-2779(2000)6:2<117::AID-MRDD5>3.0.CO;2-X)
- Khazipov, R., & Holmes, G. L. (2003). Synchronization of kainate-induced epileptic activity via GABAergic inhibition in the superfused rat hippocampus in vivo. *Journal of Neuroscience*, 23(12), 5337–5341. <https://doi.org/10.1523/jneurosci.23-12-05337.2003>
- Kubas, B., Kułak, W., Sobaniec, W., Tarasow, E., Łebkowska, U., & Walecki, J. (2012). Metabolite alterations in autistic children: A ¹H MR spectroscopy study. *Advances in Medical Sciences*, 57(1), 152–156. <https://doi.org/10.2478/v10039-012-0014-x>

- Lee, A. T., Gee, S. M., Vogt, D., Patel, T., Rubenstein, J. L., & Sohal, V. S. (2014). Pyramidal neurons in prefrontal cortex receive subtype-specific forms of excitation and inhibition. *Neuron*, 81(1), 61–68. <https://doi.org/10.1016/j.neuron.2013.10.031>
- Lee, E., Lee, J., & Kim, E. (2017). Excitation/Inhibition Imbalance in Animal Models of Autism Spectrum Disorders. In *Biological Psychiatry* (Vol. 81, Issue 10, pp. 838–847). Elsevier USA. <https://doi.org/10.1016/j.biopsych.2016.05.011>
- Lee, S. H., Marchionni, I., Bezaire, M., Varga, C., Danielson, N., Lovett-Barron, M., Losonczy, A., & Soltesz, I. (2014). Parvalbumin-positive basket cells differentiate among hippocampal pyramidal cells. *Neuron*, 82(5), 1129–1144. <https://doi.org/10.1016/j.neuron.2014.03.034>
- Leicht, G., Karch, S., Karamatskos, E., Giegling, I., Möller, H. J., Hegerl, U., Pogarell, O., Rujescu, D., & Mulert, C. (2011). Alterations of the early auditory evoked gamma-band response in first-degree relatives of patients with schizophrenia: Hints to a new intermediate phenotype. *Journal of Psychiatric Research*, 45(5), 699–705. <https://doi.org/10.1016/j.jpsychires.2010.10.002>
- Leicht, G., Kirsch, V., Giegling, I., Karch, S., Hantschk, I., Möller, H. J., Pogarell, O., Hegerl, U., Rujescu, D., & Mulert, C. (2010). Reduced Early Auditory Evoked Gamma-Band Response in Patients with Schizophrenia. *Biological Psychiatry*, 67(3), 224–231. <https://doi.org/10.1016/j.biopsych.2009.07.033>
- Lévesque, M., Herrington, R., Hamidi, S., & Avoli, M. (2016). Interneurons spark seizure-like activity in the entorhinal cortex. *Neurobiology of Disease*, 87, 91–101. <https://doi.org/10.1016/j.nbd.2015.12.011>
- Lewis, D. A., Hashimoto, T., & Volk, D. W. (2005). Cortical inhibitory neurons and schizophrenia. In *Nature Reviews Neuroscience* (Vol. 6, Issue 4, pp. 312–324). Nature Publishing Group. <https://doi.org/10.1038/nrn1648>
- Litwin-Kumar, A., & Doiron, B. (2012). Slow dynamics and high variability in balanced cortical networks with clustered connections. *Nature Neuroscience*, 15(11), 1498–1505. <https://doi.org/10.1038/nn.3220>
- Logothetis, N. K., Pauls, J., Augath, M., Trinath, T., & Oeltermann, A. (2001). Neurophysiological investigation of the basis of the fMRI signal. *Nature*, 412(6843), 150–157. <https://doi.org/10.1038/35084005>
- Lyoo, I. K., Yoon, S. J., Musen, G., Simonson, D. C., Weinger, K., Bolo, N., Ryan, C. M., Kim, J. E., Renshaw, P. F., & Jacobson, A. M. (2009). Altered prefrontal glutamate-glutamine- γ -aminobutyric acid levels and relation to low cognitive performance and depressive symptoms in type 1 diabetes mellitus. *Archives of General Psychiatry*, 66(8), 878–887. <https://doi.org/10.1001/archgenpsychiatry.2009.86>
- Mann, E. O., & Paulsen, O. (2007). Role of GABAergic inhibition in hippocampal network oscillations. In *Trends in Neurosciences* (Vol. 30, Issue 7, pp. 343–349). Trends Neurosci. <https://doi.org/10.1016/j.tins.2007.05.003>
- Mann, E. O., Suckling, J. M., Hajos, N., Greenfield, S. A., & Paulsen, O. (2005). Perisomatic feedback inhibition underlies cholinergically induced fast network oscillations in the rat hippocampus in vitro. *Neuron*, 45(1), 105–117. <https://doi.org/10.1016/j.neuron.2004.12.016>
- Mescher, M., Merkle, H., Kirsch, J., Garwood, M., & Gruetter, R. (1998). Simultaneous in vivo spectral editing and water suppression. *NMR in Biomedicine*, 11(6), 266–272. [https://doi.org/10.1002/\(SICI\)1099-1492\(199810\)11:6<266::AID-NBM530>3.0.CO;2-J](https://doi.org/10.1002/(SICI)1099-1492(199810)11:6<266::AID-NBM530>3.0.CO;2-J)

- Mikkelsen, M., Saleh, M. G., Near, J., Chan, K. L., Gong, T., Harris, A. D., Oeltzschner, G., Puts, N. A. J., Cecil, K. M., Wilkinson, I. D., & Edden, R. A. E. (2018). Frequency and phase correction for multiplexed edited MRS of GABA and glutathione. *Magnetic Resonance in Medicine*, 80(1), 21–28. <https://doi.org/10.1002/mrm.27027>
- Miller, J. W., & Ferrendelli, J. A. (1990). Characterization of gabaergic seizure regulation in the midline thalamus. *Neuropharmacology*, 29(7), 649–655. [https://doi.org/10.1016/0028-3908\(90\)90026-N](https://doi.org/10.1016/0028-3908(90)90026-N)
- Moult, P. R. (2009). Neuronal glutamate and GABAA receptor function in health and disease. In *Biochemical Society Transactions* (Vol. 37, Issue 6, pp. 1317–1322). *Biochem Soc Trans.* <https://doi.org/10.1042/BST0371317>
- Mullins, C., Fishell, G., & Tsien, R. W. (2016). Unifying Views of Autism Spectrum Disorders: A Consideration of Autoregulatory Feedback Loops. In *Neuron* (Vol. 89, Issue 6, pp. 1131–1156). Cell Press. <https://doi.org/10.1016/j.neuron.2016.02.017>
- Mullins, P. G., McGonigle, D. J., O’Gorman, R. L., Puts, N. A. J., Vidyasagar, R., Evans, C. J., & Edden, R. A. E. (2014). Current practice in the use of MEGA-PRESS spectroscopy for the detection of GABA. *Neuroimage*, 86, 43–52. <https://doi.org/10.1016/j.neuroimage.2012.12.004>
- Murray, C., Lopez, A., & Organization, W. H. (1994). Global comparative assessments in the health sector: disease burden, expenditures and intervention packages. https://apps.who.int/iris/bitstream/handle/10665/41177/9241561750_en_HR.pdf
- Near, J., Evans, C. J., Puts, N. A. J., Barker, P. B., & Edden, R. A. E. (2013). J-difference editing of gamma-aminobutyric acid (GABA): Simulated and experimental multiplet patterns. *Magnetic Resonance in Medicine*, 70(5), 1183–1191. <https://doi.org/10.1002/mrm.24572>
- Nelson, S. B., & Valakh, V. (2015). Excitatory/Inhibitory Balance and Circuit Homeostasis in Autism Spectrum Disorders. In *Neuron* (Vol. 87, Issue 4, pp. 684–698). Cell Press. <https://doi.org/10.1016/j.neuron.2015.07.033>
- Niedermeyer, E., & Silva, F. da. (2005). *Electroencephalography: basic principles, clinical applications, and related fields.* https://books.google.com/books?hl=en&lr=&id=tndqYGPHQdEC&oi=fnd&pg=PR11&ots=GP5l4575ns&sig=rsUay_Xc_G9UDa4e0uQiwBSZPM
- Nitsche, M. A., Fricke, K., Henschke, U., Schlitterlau, A., Liebetanz, D., Lang, N., Henning, S., Tergau, F., & Paulus, W. (2003). Pharmacological modulation of cortical excitability shifts induced by transcranial direct current stimulation in humans. *Journal of Physiology*, 553(1), 293–301. <https://doi.org/10.1113/jphysiol.2003.049916>
- Norton, D. J., McBain, R. K., Pizzagalli, D. A., Cronin-Golomb, A., & Chen, Y. (2016). Dysregulation of visual motion inhibition in major depression. *Psychiatry Research*, 240, 214–221. <https://doi.org/10.1016/j.psychres.2016.04.028>
- Okamoto, M., Naito, T., Sadakane, O., Osaki, H., & Sato, H. (2009). Surround suppression sharpens orientation tuning in the cat primary visual cortex. *European Journal of Neuroscience*, 29(5), 1035–1046. <https://doi.org/10.1111/j.1460-9568.2009.06645.x>
- Oliveira, B., Mitjans, M., Nitsche, M. A., Kuo, M. F., & Ehrenreich, H. (2018). Excitation-inhibition dysbalance as predictor of autistic phenotypes. *Journal of Psychiatric Research*, 104, 96–99. <https://doi.org/10.1016/j.jpsychires.2018.06.004>

- Olokoba, A. B., Obateru, O. A., & Olokoba, L. B. (2012). Type 2 diabetes mellitus: A review of current trends. In *Oman Medical Journal* (Vol. 27, Issue 4, pp. 269–273). Oman Medical Specialty Board. <https://doi.org/10.5001/omj.2012.68>
- Petroff, O. A. C., Pleban, L. A., & Spencer, D. D. (1995). Symbiosis between in vivo and in vitro NMR spectroscopy: The creatine, N-acetylaspartate, glutamate, and GABA content of the epileptic human brain. *Magnetic Resonance Imaging*, 13(8), 1197–1211. [https://doi.org/10.1016/0730-725X\(95\)02033-P](https://doi.org/10.1016/0730-725X(95)02033-P)
- Petroff, O. A. C., Rothman, D. L., Behar, K. L., & Mattson, R. H. (1995). Initial Observations on Effect of Vigabatrin on In Vivo ¹H Spectroscopic Measurements of γ -Aminobutyric Acid, Glutamate, and Glutamine in Human Brain. *Epilepsia*, 36(5), 457–464. <https://doi.org/10.1111/j.1528-1157.1995.tb00486.x>
- Port, R. G., Edgar, J. C., Ku, M., Bloy, L., Murray, R., Blaskey, L., Levy, S. E., & Roberts, T. P. L. (2016). Maturation of auditory neural processes in autism spectrum disorder - A longitudinal MEG study. *NeuroImage: Clinical*, 11, 566–577. <https://doi.org/10.1016/j.nicl.2016.03.021>
- Port, R. G., Oberman, L. M., & Roberts, T. P. L. (2019). Revisiting the excitation/inhibition imbalance hypothesis of ASD through a clinical lens. In *British Journal of Radiology* (Vol. 92, Issue 1101). British Institute of Radiology. <https://doi.org/10.1259/bjr.20180944>
- Puts, N. A. J., & Edden, R. A. E. (2012). In vivo magnetic resonance spectroscopy of GABA: A methodological review. In *Progress in Nuclear Magnetic Resonance Spectroscopy* (Vol. 60, pp. 29–41). *Prog Nucl Magn Reson Spectrosc*. <https://doi.org/10.1016/j.pnmrs.2011.06.001>
- Rae, C. D. (2014). A guide to the metabolic pathways and function of metabolites observed in human brain ¹H magnetic resonance spectra. In *Neurochemical Research* (Vol. 39, Issue 1, pp. 1–36). <https://doi.org/10.1007/s11064-013-1199-5>
- Ramocki, M. B., & Zoghbi, H. Y. (2008). Failure of neuronal homeostasis results in common neuropsychiatric phenotypes. In *Nature* (Vol. 455, Issue 7215, pp. 912–918). Nature Publishing Group. <https://doi.org/10.1038/nature07457>
- Reis, A., Mateus, C., Melo, P., Figueira, J., Cunha-Vaz, J., & Castelo-Branco, M. (2014). Neuroretinal dysfunction with intact blood-retinal barrier and absent vasculopathy in type 1 diabetes. *Diabetes*, 63(11), 3926–3937. <https://doi.org/10.2337/db13-1673>
- Ribeiro, Maria J., Violante, I. R., Bernardino, I., Edden, R. A. E., & Castelo-Branco, M. (2015). Abnormal relationship between GABA, neurophysiology and impulsive behavior in neurofibromatosis type 1. *Cortex*, 64, 194–208. <https://doi.org/10.1016/j.cortex.2014.10.019>
- Ribeiro, Maria José, Violante, I. R., Ribeiro, I., Bernardino, I., Ramos, F., Saraiva, J., Reviriego, P., Upadhyaya, M., Silva, E. D., & Castelo-Branco, M. (2012). Abnormal achromatic and chromatic contrast sensitivity in neurofibromatosis type 1. *Investigative Ophthalmology and Visual Science*, 53(1), 287–293. <https://doi.org/10.1167/iovs.11-8225>
- Ringach, D. L. (2009). Spontaneous and driven cortical activity: implications for computation. In *Current Opinion in Neurobiology* (Vol. 19, Issue 4, pp. 439–444). *Curr Opin Neurobiol*. <https://doi.org/10.1016/j.conb.2009.07.005>
- Roelfsema, P. R., Engel, A. K., König, P., & Singer, W. (1997). Visuomotor integration is associated with zero time-lag synchronization among cortical areas. *Nature*, 385(6612), 157–161. <https://doi.org/10.1038/385157a0>

- Rothman, D. L., Petroff, O. A. C., Behar, K. L., & Mattson, R. H. (1993). Localized ^1H NMR measurements of γ -aminobutyric acid in human brain in vivo. *Proceedings of the National Academy of Sciences of the United States of America*, 90(12), 5662–5666. <https://doi.org/10.1073/pnas.90.12.5662>
- Rubenstein, J. L.R., & Merzenich, M. M. (2003). Model of autism: Increased ratio of excitation/inhibition in key neural systems. In *Genes, Brain and Behavior* (Vol. 2, Issue 5, pp. 255–267). *Genes Brain Behav.* <https://doi.org/10.1034/j.1601-183X.2003.00037.x>
- Rubenstein, John L.R. (2010). Three hypotheses for developmental defects that may underlie some forms of autism spectrum disorder. In *Current Opinion in Neurology* (Vol. 23, Issue 2, pp. 118–123). *Curr Opin Neurol.* <https://doi.org/10.1097/WCO.0b013e328336eb13>
- Saleh, M. G., Oeltzschner, G., Chan, K. L., Puts, N. A. J., Mikkelsen, M., Schär, M., Harris, A. D., & Edden, R. A. E. (2016). Simultaneous edited MRS of GABA and glutathione. *NeuroImage*, 142, 576–582. <https://doi.org/10.1016/j.neuroimage.2016.07.056>
- Shackman, A. J. (2010). The potentially deleterious impact of muscle activity on gamma band inferences. In *Neuropsychopharmacology* (Vol. 35, Issue 3, p. 847). Nature Publishing Group. <https://doi.org/10.1038/npp.2009.173>
- Sickmann, H. M., Waagepetersen, H. S., Schousboe, A., Benie, A. J., & Bouman, S. D. (2010). Obesity and type 2 diabetes in rats are associated with altered brain glycogen and amino-acid homeostasis. *Journal of Cerebral Blood Flow and Metabolism*, 30(8), 1527–1537. <https://doi.org/10.1038/jcbfm.2010.61>
- Simister, R. J., McLean, M. A., Barker, G. J., & Duncan, J. S. (2003a). A proton magnetic resonance spectroscopy study of metabolites in the occipital lobes in epilepsy. *Epilepsia*, 44(4), 550–558. <https://doi.org/10.1046/j.1528-1157.2003.19102.x>
- Simister, R. J., McLean, M. A., Barker, G. J., & Duncan, J. S. (2003b). Proton MRS reveals frontal lobe metabolite abnormalities in idiopathic generalized epilepsy. *Neurology*, 61(7), 897–902. <https://doi.org/10.1212/01.WNL.0000086903.69738.DC>
- Singer, W., & Gray, C. M. (1995). Visual feature integration and the temporal correlation hypothesis. In *Annual Review of Neuroscience* (Vol. 18, pp. 555–586). Annual Reviews Inc. <https://doi.org/10.1146/annurev.ne.18.030195.003011>
- Sohal, V. S., & Rubenstein, J. L. R. (2019). Excitation-inhibition balance as a framework for investigating mechanisms in neuropsychiatric disorders. *Molecular Psychiatry*, 24(9), 1248–1257. <https://doi.org/10.1038/s41380-019-0426-0>
- Sohal, V. S., Zhang, F., Yizhar, O., & Deisseroth, K. (2009). Parvalbumin neurons and gamma rhythms enhance cortical circuit performance. *Nature*, 459(7247), 698–702. <https://doi.org/10.1038/nature07991>
- Strachan, M. W. J., Reynolds, R. M., Frier, B. M., Mitchell, R. J., & Price, J. F. (2009). The role of metabolic derangements and glucocorticoid excess in the aetiology of cognitive impairment in type 2 diabetes. Implications for future therapeutic strategies. In *Diabetes, Obesity and Metabolism* (Vol. 11, Issue 5, pp. 407–414). Blackwell Publishing Ltd. <https://doi.org/10.1111/j.1463-1326.2008.00963.x>
- Sullivan, D., Csicsvari, J., Mizuseki, K., Montgomery, S., Diba, K., & Buzsáki, G. (2011). Relationships between hippocampal sharp waves, ripples, and fast gamma oscillation: Influence of dentate and entorhinal cortical activity. *Journal of*

- Neuroscience, 31(23), 8605–8616. <https://doi.org/10.1523/JNEUROSCI.0294-11.2011>
- Symond, M. B., Harris, A. W. F., Gordon, E., & Williams, L. M. (2005). “Gamma synchrony” in first-episode schizophrenia: A disorder of temporal connectivity? *American Journal of Psychiatry*, 162(3), 459–465. <https://doi.org/10.1176/appi.ajp.162.3.459>
- Taki, M. M., Harada, M., Mori, K., Kubo, H., Nose, A., Matsuda, T., & Nishitani, H. (2009). High gamma-aminobutyric acid level in cortical tubers in epileptic infants with tuberous sclerosis complex measured with the MEGA-editing J-difference method and a three-Tesla clinical MRI Instrument. *NeuroImage*, 47(4), 1207–1214. <https://doi.org/10.1016/j.neuroimage.2009.05.060>
- Tallon-Baudry, C., & Bertrand, O. (1999). Oscillatory gamma activity in humans and its role in object representation. In *Trends in Cognitive Sciences* (Vol. 3, Issue 4, pp. 151–162). Trends Cogn Sci. [https://doi.org/10.1016/S1364-6613\(99\)01299-1](https://doi.org/10.1016/S1364-6613(99)01299-1)
- Tamás, G., Buhl, E. H., Lörincz, A., & Somogyi, P. (2000). Proximally targeted GABAergic synapses and gap junctions synchronize cortical interneurons. *Nature Neuroscience*, 3(4), 366–371. <https://doi.org/10.1038/73936>
- Telfeian, A. E., & Connors, B. W. (1998). Layer-specific pathways for the horizontal propagation of epileptiform discharges in neocortex. *Epilepsia*, 39(7), 700–708. <https://doi.org/10.1111/j.1528-1157.1998.tb01154.x>
- Terpstra, M., Henry, P. G., & Gruetter, R. (2003). Measurement of reduced glutathione (GSH) in human brain using LCModel analysis of difference-edited spectra. *Magnetic Resonance in Medicine*, 50(1), 19–23. <https://doi.org/10.1002/mrm.10499>
- Thielen, J. W., Gancheva, S., Hong, D., Rohani Rankouhi, S., Chen, B., Apostolopoulou, M., Anadol-Schmitz, E., Roden, M., Norris, D. G., & Tendolkar, I. (2019). Higher GABA concentration in the medial prefrontal cortex of Type 2 diabetes patients is associated with episodic memory dysfunction. *Human Brain Mapping*, 40(14), 4287–4295. <https://doi.org/10.1002/hbm.24702>
- Toro, R., Konyukh, M., Delorme, R., Leblond, C., Chaste, P., Fauchereau, F., Coleman, M., Leboyer, M., Gillberg, C., & Bourgeron, T. (2010). Key role for gene dosage and synaptic homeostasis in autism spectrum disorders. In *Trends in Genetics* (Vol. 26, Issue 8, pp. 363–372). Trends Genet. <https://doi.org/10.1016/j.tig.2010.05.007>
- Uhlhaas, P. J., Pipa, G., Lima, B., Melloni, L., Neuenschwander, S., Nikolić, D., & Singer, W. (2009). Neural synchrony in cortical networks: History, concept and current status. *Frontiers in Integrative Neuroscience*, 3(JUL), 17. <https://doi.org/10.3389/neuro.07.017.2009>
- van Bussel, F. C. G., Backes, W. H., Hofman, P. A. M., Puts, N. A. J., Edden, R. A. E., van Boxtel, M. P. J., Schram, M. T., Stehouwer, C. D. A., Wildberger, J. E., & Jansen, J. F. A. (2016). Increased GABA concentrations in type 2 diabetes mellitus are related to lower cognitive functioning. *Medicine (United States)*, 95(36). <https://doi.org/10.1097/MD.0000000000004803>
- Violante, I. R., Ribeiro, M. J., Cunha, G., Bernardino, I., Duarte, J. v., Ramos, F., Saraiva, J., Silva, E., & Castelo-Branco, M. (2012). Abnormal brain activation in Neurofibromatosis type 1: A link between visual processing and the default mode network. *PLoS ONE*, 7(6). <https://doi.org/10.1371/journal.pone.0038785>
- Violante, I. R., Ribeiro, M. J., Edden, R. A. E., Guimarães, P., Bernardino, I., Rebola, J., Cunha, G., Silva, E., & Castelo-Branco, M. (2013). GABA deficit in the visual

- cortex of patients with neurofibromatosis type 1: Genotype-phenotype correlations and functional impact. *Brain*, 136(3), 918–925. <https://doi.org/10.1093/brain/aws368>
- von Krosigk, M., Bal, T., & McCormick, D. A. (1993). Cellular mechanisms of a synchronized oscillation in the thalamus. *Science*, 261(5119), 361–364. <https://doi.org/10.1126/science.8392750>
- Whittington, M. A., Faulkner, H. J., Doheny, H. C., & Traub, R. D. (2000). Neuronal fast oscillations as a target site for psychoactive drugs. In *Pharmacology and Therapeutics* (Vol. 86, Issue 2, pp. 171–190). *Pharmacol Ther.* [https://doi.org/10.1016/S0163-7258\(00\)00038-3](https://doi.org/10.1016/S0163-7258(00)00038-3)
- Whittington, M. A., Traub, R. D., Kopell, N., Ermentrout, B., & Buhl, E. H. (2000). Inhibition-based rhythms: Experimental and mathematical observations on network dynamics. *International Journal of Psychophysiology*, 38(3), 315–336. [https://doi.org/10.1016/S0167-8760\(00\)00173-2](https://doi.org/10.1016/S0167-8760(00)00173-2)
- Whittington, Miles A., Cunningham, M. O., LeBeau, F. E. N., Racca, C., & Traub, R. D. (2011). Multiple origins of the cortical gamma rhythm. *Developmental Neurobiology*, 71(1), 92–106. <https://doi.org/10.1002/dneu.20814>
- Wondolowski, J., & Dickman, D. (2013). Emerging links between homeostatic synaptic plasticity and neurological disease. In *Frontiers in Cellular Neuroscience* (Vol. 7, Issue NOV). *Front Cell Neurosci.* <https://doi.org/10.3389/fncel.2013.00223>
- Yau, J. W. Y., Rogers, S. L., Kawasaki, R., Lamoureux, E. L., Kowalski, J. W., Bek, T., Chen, S. J., Dekker, J. M., Fletcher, A., Grauslund, J., Haffner, S., Hamman, R. F., Ikram, M. K., Kayama, T., Klein, B. E. K., Klein, R., Krishnaiah, S., Mayurasakorn, K., O'Hare, J. P., ... Wong, T. Y. (2012). Global prevalence and major risk factors of diabetic retinopathy. *Diabetes Care*, 35(3), 556–564. <https://doi.org/10.2337/dc11-1909>
- Yook, S.-W., Park, S.-H., Seo, J.-H., Kim, S.-J., & Ko, M.-H. (2011). Suppression of Seizure by Cathodal Transcranial Direct Current Stimulation in an Epileptic Patient - A Case Report -. *Annals of Rehabilitation Medicine*, 35(4), 579. <https://doi.org/10.5535/arm.2011.35.4.579>
- Yoon, J. H., Maddock, R. J., Rokem, A., Silver, M. A., Minzenberg, M. J., Ragland, J. D., & Carter, C. S. (2010). GABA concentration is reduced in visual cortex in schizophrenia and correlates with orientation-specific surround suppression. *Journal of Neuroscience*, 30(10), 3777–3781. <https://doi.org/10.1523/JNEUROSCI.6158-09.2010>
- Yuval-Greenberg, S., Tomer, O., Keren, A. S., Nelken, I., & Deouell, L. Y. (2008). Transient Induced Gamma-Band Response in EEG as a Manifestation of Miniature Saccades. *Neuron*, 58(3), 429–441. <https://doi.org/10.1016/j.neuron.2008.03.027>

Chapter 2:

Occipital Cortex Disruption in Type 2 Diabetes Mellitus

Occipital GABA Dysfunction and Visual Performance in Type 2 DM:

Diabetic Brain or Retina? Visual Psychophysical Performance in Diabetic Patients in Relation to GABA Levels in Occipital Cortex (Published original article)

Occipital BBB Disruption and Visual Performance in Type 2 DM:

Occipital blood-brain barrier permeability is an independent predictor of visual outcome in type 2 diabetes, irrespective of the retinal barrier: A longitudinal study (Published original article)

Diabetic Brain or Retina? Visual Psychophysical Performance in Diabetic Patients in Relation to GABA Levels in Occipital Cortex

Sulaiman I Abuhaiba^{1,2, 3, 4*}, *Mafalda Sanches*^{1,2*}, *Otília C. d'Almeida*^{1,2,5}, Bruno Quendera^{2,5}, Leonor Gomes⁶, Carolina Moreno⁶, Daniela Guelho⁶, Miguel Castelo-Branco^{1,2,5}

ABSTRACT

Visual impairment is one of the most feared complications of Type 2 Diabetes Mellitus. Here, we aimed to investigate the role of occipital cortex γ -aminobutyric acid (GABA) as a predictor of visual performance in type 2 diabetes. 18 type 2 diabetes patients were included in a longitudinal prospective one-year study, as well as 22 healthy age-matched controls. We collected demographic data, HbA1C and used a novel set of visual psychophysical tests addressing color, achromatic luminance, and speed discrimination in both groups. Psychophysical tests underwent dimension reduction with principal component analysis into three synthetic variables: speed, achromatic luminance, and color discrimination. A MEGA-PRESS magnetic resonance brain spectroscopy sequence was used to measure occipital GABA levels in the type 2 diabetes group. Retinopathy grading and retinal microaneurysms counting were performed in the type 2 diabetes group for single-armed correlations.

Speed discrimination thresholds were significantly higher in the type 2 diabetes group in both visits: mean difference (95% confidence interval), [0.86 (0.32 – 1.40) in the first visit, 0.74 (0.04 – 1.44) in the second visit]. GABA from the occipital cortex predicted speed and achromatic luminance discrimination thresholds within the same visit ($r = 0.54$ and 0.52 ; $p = 0.02$ and 0.03 , respectively) in type 2 diabetes group. GABA from the occipital cortex also predicted speed discrimination thresholds one year later ($r = 0.52$; $p = 0.03$) in the type 2 diabetes group. Our results suggest that speed discrimination is impaired in type 2 diabetes and that occipital cortical GABA is a novel predictor of visual psychophysical performance independently from retinopathy grade, metabolic control, or disease duration in the early stages of the disease.

KEYWORDS

Brain and Retina; Diabetes; Psychophysics and Visual Performance; GABA; Occipital Cortex; Brain Spectroscopy

INTRODUCTION

Type 2 diabetes mellitus is a chronic metabolic disorder in which the effects of insulin resistance impact on multiple organs in the body, including the eyes, kidneys and the cardiovascular and central nervous systems (Strachan et al. 2009; Zhang et al. 2010). The worldwide prevalence of the disease has been increasing exponentially in the last few years, with the most recent estimates reporting that 382 million adults had diabetes in 2013 (Guariguata et al. 2014). One of the most feared complications of people with diabetes is the progressive visual impairment which is in general attributed to diabetic retinopathy and consequent vision loss (Coyne et al. 2004; Luckie et al. 2007). Severe visual impairment occurs 2 to 3 times more frequently in people with diabetes compared to the general population (Hayward et al. 2002).

Early in the disease, there is little association between the degree of non-proliferative diabetic retinopathy and visual performance (Yau et al. 2012). The relationship between retinopathy and visual impairment only becomes apparent in later stages of the disease such as in proliferative diabetic retinopathy, diabetic macular edema and vision threatening diabetic retinopathy (Moss et al. 1988; Miki et al. 2001; Yau et al. 2012). On the other hand, metabolic biomarkers have not been found to predict visual performance in the early stages of type 2 diabetes (Hove et al. 2006). Despite this, evidence has emerged that color contrast detection impairment may happen early in the disease (Bears Jr. et al. 2006; Reis et al. 2014).

There is increasing evidence of mild cognitive impairment early in type 2 diabetes (Kalmijn et al. 1995) that could be related to an altered cortical neurochemistry. For instance, it had been shown that type 2 diabetes patients have a higher γ -aminobutyric acid (GABA) concentration in the occipital lobe compared to non-diabetics (van Bussel et al. 2016).

Additionally, type 2 diabetes patients with higher HbA1C levels and lower cognitive functioning had a higher occipital GABA concentration as well (van Bussel et al. 2016).

Several studies reported a correlation between GABA in the occipital cortex with altered visual function and/or inhibition in other diseases such as schizophrenia (Yoon et al. 2010), neurofibromatosis type 1 (Violante et al. 2013; Ribeiro et al. 2015), major depressive disorder (Norton et al. 2016) and in healthy subjects (Edden et al. 2009). The association between occipital GABA and visual performance is still to be explored in type 2 diabetes.

The current study aimed to investigate visual impairment through visual psychophysical testing in a longitudinal setting to identify possible predictors of visual psychophysical performance and their reliability over one-year period, with a particular focus on occipital GABA. Our hypothesis is that changes in GABA, secondary to metabolic derangement in diabetes, might also impact visual function in relation to putatively affected physiological mechanisms related to cortical processing of visual psychophysical tasks.

EXPERIMENTAL PROCEDURES

The collected data are part of an observational and prospective study over one year of a cohort of type 2 diabetes patients with evidence only for early retinal complications (mild non-proliferative diabetic retinopathy).

Participants

Patients enrolled in this study met the following inclusion criteria: diagnosed with type 2 diabetes according to current WHO criteria, age 40 – 75 years, mild to moderate non-proliferative diabetic retinopathy (Early Treatment Diabetic Retinopathy Study (ETDRS) level \leq 35) and disease activity shown by microaneurysms. Exclusion criteria included the presence of cataract disease, glaucoma, any other retinal disease, any eye surgery or treatment within a period of 6-months, pregnancy or breastfeeding, being on psychotropic medication or having any mood, anxiety or thought disorders as assessed by their treating physicians based on the clinical history. Patients with cardiac pacemaker or presence of metal implants on the body were also excluded. All participants gave a written informed consent. Tenets of the Declaration of Helsinki were followed and approval from the institutional board was obtained. Medical history and

demographic data were recorded and fundus photography imaging for ETDRS grading was performed. Metabolic control assessed by HbA1C, ophthalmological examination, visual psychophysical testing and multimodal imaging were performed. We included 11 males and 7 females in our type 2 diabetes group.

The control group included 22 healthy subjects, age 49 – 71 years who underwent HbA1C assessment, ophthalmological examination and visual psychophysical testing.

Visual acuity assessment

Best Corrected Visual Acuity (BCVA) score was determined by letter counting using different charts for both left and right eyes. Subjects were instructed to read each line in sequence from left to right and top to bottom starting from the top-leftmost letters of each chart. The eyes with higher BCVA were used for the correlation studies.

Color fundus photography

Color fundus photographs of both eyes were taken according to the Early Treatment Diabetic Retinopathy Study (ETDRS) protocol. The 7-field photographs at 30° were obtained with a Zeiss FF450 camera (Carl Zeiss Meditec, Dublin, CA) after pupil dilatation. The photographs were used for DR classification according to ETDRS grading. Images of the macula field were used for automatic microaneurysm (MA) counting.

Computerized psychophysical tests

Set-up

Psychophysical testing software was programmed in MATLAB (MATLAB 2011a, The Mathworks Inc., Natick, MA) and previously tested in glaucoma patients (Mateus et al. 2015) using The Psychophysics Toolbox (PTB-3). Stimuli were presented on a 24-inch LCD-IPS monitor with a screen resolution of 1920x1200 pixels and a refresh rate of 60 Hz.

General characteristics of the test features

The psychophysical tests included three main novel features and featured a 2 alternative forced choice paradigm. This required the participant to compare and discriminate a certain visual feature (speed, achromatic luminance, and color discrimination) between two distinct moving dots (a reference and a target dot presented in opposite hemifields). The two dots only differed in the visual feature

currently being tested.

The two squared dots measured 0.3x0.3 degrees for the speed discrimination task and 0.6x0.6 degrees for both the achromatic luminance and color discrimination tasks. Participants were instructed to fixate on a central black cross that had the size of 1 visual degree in the center of the screen. The stimuli and the fixation point were presented on a grey background. The background had a luminance of 25 cd/m². The duration of the trial was 400ms and the reference and target dots were presented at the same time to the participant while randomly alternating between the visual hemifields. The dots were moving back and forth along a 2-degree random trajectory. Since dots were presented at the same time with random vectorial direction, the task could not be performed on the basis of estimating the final position of each dot.

The participant was positioned 50 cm away, after correction for refraction, from the display system in a darkened room. The experiments were executed monocularly where the eye with the highest BCVA was selected. The tests were repeated 4 times corresponding to the four different meridians assessed (the horizontal meridian at 0 degrees and the vertical meridian at 90 degrees, and two oblique meridians at 45 and 135 degrees). The number of trials per each meridian was determined by a nonlinear logarithmic staircase procedure which is explained in detail in (Mateus et al. 2015).

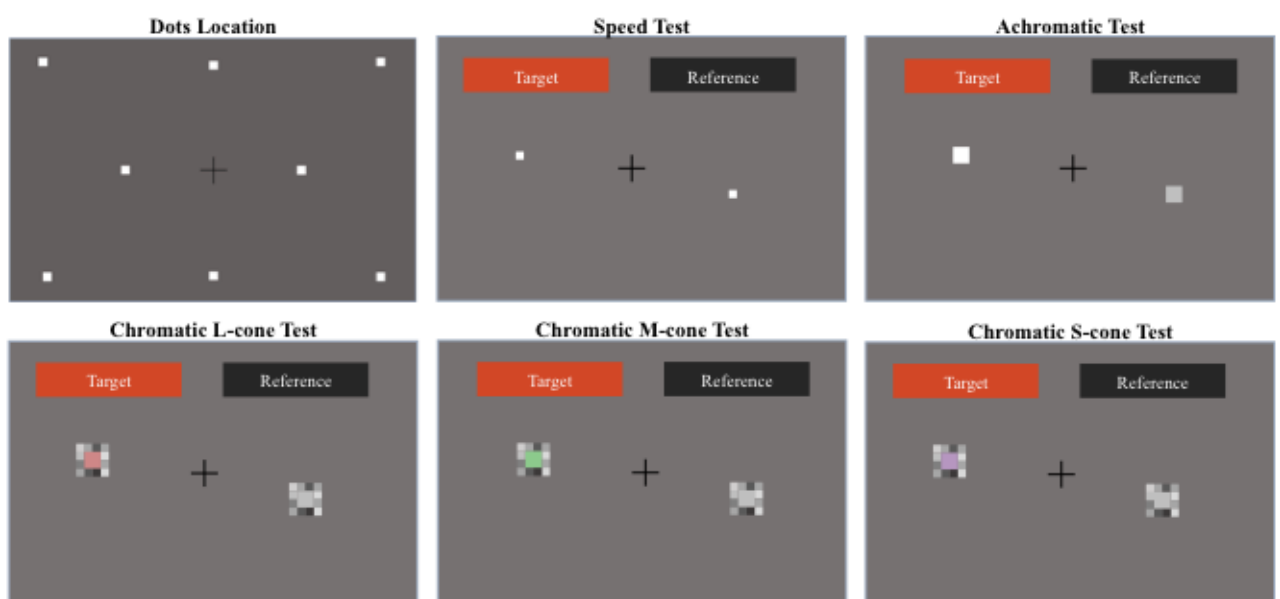


Figure 1: An illustration of the different visual psychophysical feature contrast

discrimination tests used. The top-left corner image shows the possible positions of the reference and target dots. The remainder images show the different discrimination tasks in which the target dot represents the visual feature (speed, achromatic or chromatic contrast) which the subject is supposed to discriminate from the reference one.

Speed discrimination test

In this test, the reference and target dots had the same color, white, and same luminance, 30 cd/m^2 . The only different feature was the velocity of the target dot. The reference dot had a fixed velocity of 5 degrees/s whereas the target dot had an initial velocity of 24 degrees/s . The participant had to indicate which dot was moving faster and depending on their response the logarithmic staircase procedure would decrease the velocity of the target dot in subsequent trials until it reaches the reference velocity. The discrimination threshold is given by the algorithm when the participant is no longer able to discriminate the difference in velocity between the two dots.

Achromatic luminance discrimination test

In this test, both the reference and target dots were moving at the same velocity of 5 degrees/s and had an equal gray appearance where $R = G = B$. The only visual feature that was different between the target and reference dots was luminance. While the reference dot had a luminance of 30 cd/m^2 , the target dot had an initial luminance of 70 cd/m^2 . Similar to the speed discrimination test, the luminance of the target dot was gradually brought near to the reference dot according to the participant's responses per the logarithmic staircase procedure. The discrimination threshold was given by the algorithm once the participant is no longer able to discriminate the difference in luminance between the two dots.

Color Discrimination Test

In this test, both the reference and target dots shared the same velocity of 5 degrees/s and the same luminance of 30 cd/m^2 . The noise luminance strategy was used to minimize the residual luminance cues. The addition of luminance noise ensures that the participant is only discriminating the chrominance cues (Castelo-Branco et al. 2004; Mateus et al., 2015). This was achieved by placing

a matrix of luminance noise around each dot which was composed of 0.3-degree squared dots with 6 different luminance levels (30, 34, 38, 42, 46, or 48 cd/m²). The luminance of each dot of this matrix randomly changed in each trial.

The reference dot had a LMS (long-wave, medium-wave, short-wave) coordinate of ($l = 0.4106$, $m = 0.4108$, and $s = 0.4241$) which gave the appearance of a gray-color dot. The target dot had different colors depending on which cone population is being tested. For example, while testing the L-cone feature, the m and s values were fixed at the reference level. L-cone test started at an $l = 0.4732$ (a pale red dot), the m -cone test started at an $m = 0.5158$ (a green dot) and the s -cone test started at an $s = 0.9$ (a purple dot). Similar to the achromatic luminance and speed discrimination tests, the target dot distinct feature, whether L, M or S cone stimulation, was brought down near the reference dot LMS coordinates according to the participant responses.

Dimension Reduction of the Psychophysical Thresholds

The tests were repeated in four different meridian (0, 45, 90, and 135) and the thresholds for each meridian for a single feature were highly correlated. Therefore, principle component analysis was performed in SPSS to provide three representative variables for speed, achromatic luminance and color discrimination thresholds.

For speed discrimination thresholds, the values of the four meridians for the type 2 diabetes and the controls were included in the principal component analysis and a single factor was extracted which explains most of the variance (> 85%) from the four different meridians for that feature. Factor extraction for the achromatic luminance discrimination thresholds was performed in the same way as we did for speed discrimination thresholds.

Color discrimination tests included three different features depending on which main cone population was being stimulated and four different meridians for each feature, hence 12 different highly correlated variables. We chose to put all of the 12 repeated measures to our principal component analysis algorithm and extracted a single component that explained the variance in most of the different cone tests and was correlated with L, M and S cone thresholds from the different meridians.

The extracted factors had a mean of 0 and a standard deviation of 1, hence

standardized variables.

Brain structural Magnetic Resonance Imaging (MRI) and Spectroscopy (MRS)

Data were acquired on a 3T Siemens Scanner (Siemens Magnetom 3T TimTrio, Erlangen, Germany). T1-weighted structural images of the brain were acquired with a MPRAGE sequence with: 1 mm³ isotropic voxel, repetition time 2.53 s, echo time 3.42 ms, inversion time 1100 ms, flip angle 7°, field of view 256x256 mm², 256x256 matrix, 176 slices and GRAPPA acceleration factor = 2. T2-weighted brain images were acquired from a FLAIR sequence with: 1 mm³ isotropic voxel, repetition time 5 s, echo time 2.98 ms, inversion time 1.8 s, 256x256 matrix, 160 slices, GRAPPA acceleration factor = 2. A GABA-edited magnetic resonance spectra was collected using the MEGA-PRESS method (Edden et al. 2014) from a 27 cm³ isotropic voxel, with echo time 68 ms, repetition time 1.5 s, 392 averages and 1024 data points. The T1 and T2-weighted images were analyzed for structural abnormalities and bright objects detection. The MRS voxel was positioned medially in the Occipital Cortex (Figure 2 A). Grey matter (GM), white matter (WM) and cerebrospinal fluid (CSF) fractions of the voxel were determined for each participant after tissue segmentation of the T1-weighted images using an in-house Matlab (R2012a, The MathWorks, USA) script based on the SPM8 (Wellcome Trust Centre for Neuroimaging, Institute of Neurology, UCL, London, UK, <http://www.fil.ion.ucl.ac.uk/spm/>) and VBM8 (<http://dbm.neuro.uni-jena.de/vbm8/>) toolboxes. The MEGA-PRESS data were processed with Gannet software (Edden et al. 2014). GABA and total Creatine signals were obtained from the difference edited spectra. GABA and total Creatine peaks were fitted to a simple Gaussian and to a double Lorentzian models, respectively, and integrated for quantification (Figure 2 B). Results are expressed as levels of GABA/Cr. Normalization to Creatine was used in order to reduce intersubject variance from both different signal-to-noise levels and CSF fraction within the voxel (Bogner et al. 2010).

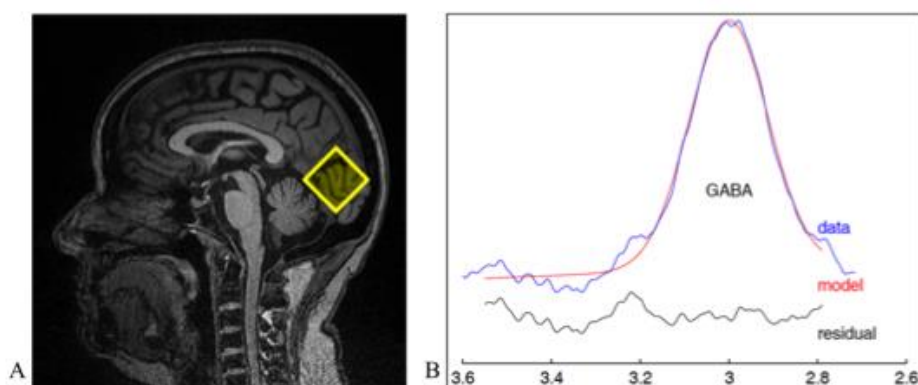


Figure 2: A – Anatomical structural MRI showing MEGA-PRESS voxel placement from a type 2 diabetes subject at the occipital cortex. B - Example of the output spectra acquired from the same participant with Gannet Software which shows GABA peak integration and model fit.

Statistical analysis

Statistical analyses were performed with IBM SPSS Statistics version 20 software. Paired-sample t-student tests were used to investigate if there were differences between means of the main outcome variables within the period of one year. Pearson's correlations were used to search for associations between the different variables in our study. Of particular interest was to assess the GABA/Cr predictive role of visual psychophysical thresholds as measured by correlating GABA/Cr from the first visit with psychophysical synthetic thresholds from the second visit one year later. Our statistical significance threshold was set at a p-value < 0.05.

RESULTS

Demographic and Clinical Data

A summary of the patients' and controls' demographic, metabolic and systemic features is presented in Table 1.

Table 1: General characteristics of type 2 diabetes and control groups. Continuous scales are presented in mean (95% confidence interval).

	Control (N=22)	Type 2 Diabetes (N=18)	p-value
Demographic Characteristics			
Age (years)	55.63 (52.63 – 58.63)	58.72 (54.84 – 62.60)	0.217

Gender	9 M 13 F	11 M 7 F	0.341 ⁺
Disease duration (years)	N.A.*	14.94 (12.28 – 17.60)	N.A.
Metabolic and Systemic Characteristics			
HbA1C (%)	5.30 (5.09 – 5.51) (m.c. = 11)	7.99 (7.40 – 8.58)	< 0.001
Systolic blood pressure (mm Hg)	125.62 (116.17 – 135.07) (m.c. = 9)	148.17 (144.10 – 152.24)	< 0.001
Diastolic blood pressure (mm Hg)	73.38 (67.84 – 78.92) (m.c. = 9)	74.11 (69.77 – 78.45)	0.838
BMI ^d (kg/m ²)	25.12 (23.65 – 26.59) (m.c. = 5)	30.52 (28.63 – 32.41)	< 0.001
Ocular and Visual Characteristics			
BCVA ^a score	98.06 (91.59 – 104.53) (m.c. = 4)	85.22 (83.49 – 86.95)	< 0.001
ETDRS ^b level	N.A.	30.83 (27.64 – 34.02)	N.A.
MA ^c number	N.A.	5.89 (3.13 – 8.65)	N.A.

^aBCVA: Best Correct Visual Acuity

^bETDRS: Early Treatment Diabetic Retinopathy Study

^cMA: Microaneurysms

^dBMI: Body Mass Index

* N.A.: Not Applicable

- m.c.: missing cases

+ Fisher's exact test was used

Changes in systemic and ocular parameters over one year

Paired t-tests were used to compare variables changes between the two visits. BCVA and systolic blood pressure improved significantly over the period of one year and were accompanied by a significant decrease in the number of retinal MA. Table 2 summarizes these findings.

Table 2: Changes in systemic, metabolic and visual parameters over one year in the T2DM group (N = 18). Continuous scales are presented in mean (95% confidence interval).

	First Visit	Second Visit	p-value*
BMI	30.52 (28.63 – 32.41)	30.55 (28.61 – 32.49)	0.739
HbA1C	7.99 (7.40 – 8.58)	7.87 (7.17 – 8.57)	0.530
Visual Acuity	85.22 (83.49 – 86.95)	87.50 (85.84 – 89.16)	0.004

Retinal Microaneurysms	5.89 (3.13 – 8.65)	4.06 (1.65 – 6.47)	0.020
Systolic Blood Pressure	148.17 (141.32 – 155.02)	138.28 (134.21 – 142.35)	0.010
Diastolic Blood Pressure	74.11 (69.78 – 78.45)	73.28 (70.37 – 76.19)	0.724
Psychophysics (variables are standardized and derived from PCA):			
Speed	0.41 (- 0.06 – 0.88)	0.29 (- 0.34 – 0.92)	0.680
Achromatic Luminance	0.29 (- 0.34 – 0.92)	0.14 (- 0.25 – 0.53)	0.663
Color Discrimination	0.08 (- 0.29 – 0.45)	0.33 (- 0.33 – 0.99)	0.415

* Paired-sample t-test was used

Visual impairment in type 2 diabetes and systemic biomarkers

Additionally, using our novel set of visual psychophysical thresholds we found that speed discrimination thresholds were statistically different between type 2 diabetes and controls in both visits as is depicted in Table 3.

Table 3: Differences in psychophysical thresholds between the type 2 diabetes and control groups.

	Control (N=22)	Type 2 Diabetes (N=18)			
		First Visit	p	Second Visit	p
Speed	- 0.45 (- 0.60 – - 0.30)	0.41 (- 0.06 – 0.88)	0.003	0.29 (- 0.34 – 0.92)	0.040
Achromatic Luminance	- 0.19 (- 0.59 – 0.21)	0.29 (- 0.34 – 0.92)	0.183	0.14 (- 0.25 – 0.53)	0.271
Color Discrimination	- 0.17 (- 0.52 – 0.18)	0.08 (- 0.29 – 0.45)	0.347	0.33 (- 0.33 – 0.99)	0.204

These are standardized variables, hence the negative sign in the controls, meaning better performance. Controls had a single visit for their visual psychophysical assessment.

P-values represent the statistical significance of the difference in mean between Type 2 Diabetes and Control groups.

BCVA was found to be negatively correlated with age in both visits and can also be predicted by age as is demonstrated in Table 4. BCVA was also correlated with disease duration and Body Mass Index (BMI) was predictive of BCVA one year later.

Table 4: BCVA within-visit correlations and BCVA prediction one year later by demographic, metabolic and ocular parameters in T2DM. (N=18).

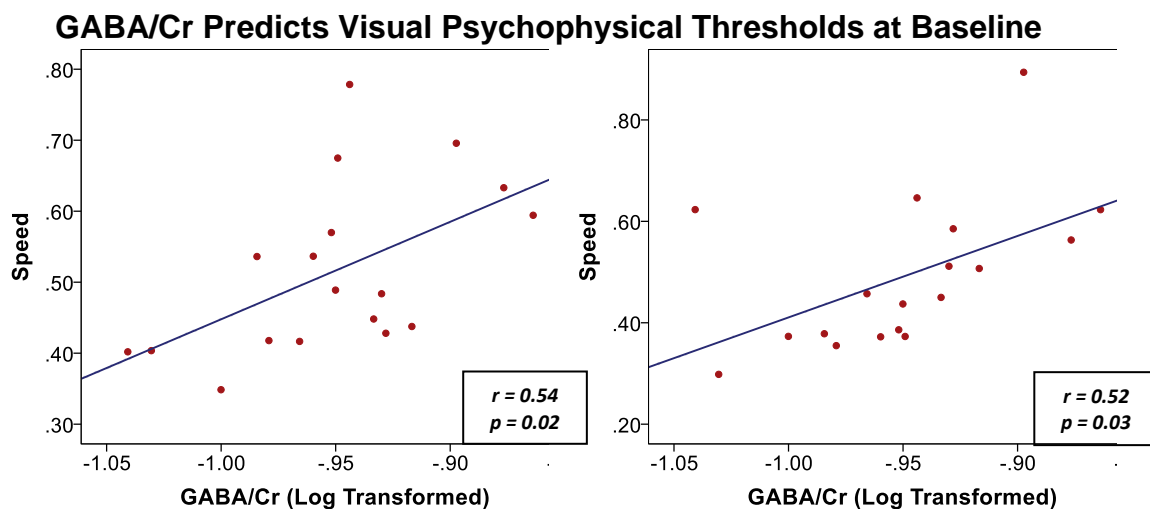
	r	p-value
Within-visit Correlations for the first visit		
Disease Duration	- 0.43	0.078

Age	- 0.54	0.022
HbA1C	- 0.20	0.421
ETDRS Level	- 0.34	0.172
Number of MA	0.09	0.721
BMI	- 0.32	0.203
Within-visit Correlations for the second visit		
HbA1C	- 0.17	0.505
Number of MA	0.28	0.258
BMI	- 0.50	0.033
Prediction One Year Later		
Disease Duration	- 0.25	0.315
Age	- 0.46	0.055
HbA1C	- 0.10	0.696
ETDRS Level	- 0.23	0.356
Number of MA	0.08	0.761
BMI	- 0.50	0.036

Speed discrimination thresholds also showed a positive correlation with ETDRS level ($r = 0.44$, $p = 0.071$). In the second visit, HbA1C positively correlated with achromatic luminance discrimination thresholds ($r = 0.60$, $p = 0.009$).

Occipital cortex GABA as a predictor of visual performance

GABA/Cr was not influenced by grey matter content in the analyzed occipital cortical voxels ($r = 0.20$, $p = 0.430$). GABA/Cr significantly predicted speed and achromatic luminance discrimination thresholds within the first visit and one year later as is illustrated in Figure 3. GABA/Cr showed no significant pattern of correlation when correlating with color discrimination (small negative trend, but non-significant). GABA/Cr was not related to age, disease duration, HbA1C, BMI, number of MA or ETDRS level.



GABA/Cr Predicts Visual Psychophysical Thresholds One-Year Later

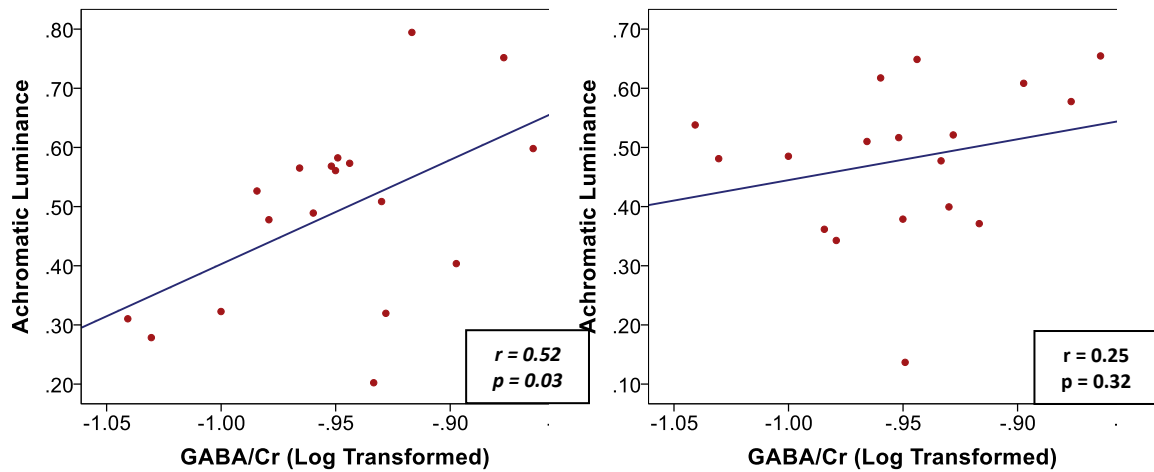


Figure 3: GABA/Cr predicts speed and achromatic luminance discrimination thresholds at baseline. GABA/Cr also predicts speed discrimination thresholds *one year later*. r in the boxes represents Pearson's correlation coefficient and p is the p-value of that correlation. All variables were log transformed.

DISCUSSION

In this study, we have three main novel findings related to type 2 diabetes visual performance in early diabetic retinopathy. Our cohort of type 2 diabetes patients scored worse in a novel speed discrimination task compared to healthy controls, and their lower visual acuity was predicted by systemic and retinal biomarkers whereas their speed and achromatic luminance discrimination thresholds were mainly explained by cortical processing.

Visual acuity was mildly impaired in the type 2 diabetes group which can be related to glycemic control (HbA1C level above 7.0%) (Mahmood and Aamir 2005) and elevated systolic blood pressure at baseline. Systolic blood pressure was previously reported to be negatively correlated with visual acuity (Ernest-Nwoke et al. 2014; Taura et al. 2015), and our findings are consistent with this notion, since visual acuity seemed to improve in the second visit while systolic blood pressure was also lower compared to the first visit. The difference in the number of MA in the type 2 diabetes group can be related to its high turnover rate (appearance and disappearance rate) (Ribeiro et al. 2013).

Our novel set of visual psychophysical testing is partially dependent on speed contrast detection of moving dots and several studies have shown that contrast-dependent visual tasks could be impaired in early type 2 diabetes (Krásný et al. 2006; Reis et al. 2014; Tsai et al. 2016). Indeed, we report for the first time that speed discrimination is impaired in type 2 diabetes patients as their thresholds

were significantly higher than the control group in both visits. The notion that patients may perform differently and in relation to GABA levels depending on the type of visual task involved has been previously reported in major depressive disorder (Norton et al. 2016).

Visual acuity was negatively correlated with disease duration and age at baseline, and was predicted by the patient's age one year later which agrees with the current literature (de Fine Olivarius et al. 2011; Trento et al. 2016). Similar to Misra et al findings, we show that speed and achromatic luminance discrimination thresholds are correlated with retinopathy grade and HbA1C respectively (Misra et al. 2010).

Occipital cortical GABA/Cr was of interest to us because it is known to be altered in type 2 diabetes (van Bussel et al. 2016) and to be higher in diabetes patients with cognitive impairment. As motion detection tasks were shown previously to be related to cortical processing and occipital GABA (Edden et al. 2009), we hypothesized that psychophysical tests with visual features of speed, achromatic luminance and color discrimination of moving dots will also be at least partly dependent on cortical processing.

A novel finding of our study is the observation that GABA/Cr not only predicts speed and achromatic luminance discrimination thresholds at baseline, but also one-year later. Higher GABA/Cr seems to be associated with higher speed and achromatic luminance discrimination thresholds which can be clinically translated into worse performance. The fact that GABA/Cr is positively correlated with worse psychophysical performance or contrast detection within and across time suggests that high levels of this neurotransmitter have a deleterious role. This is consistent with the observation that higher occipital GABA was found to be correlated with type 2 diabetes and cognitive impairment (van Bussel et al. 2016), and higher brain GABA concentration was also reported in Zucker Diabetic Fatty rat models (Sickmann et al. 2012). Additionally, it seems that contrast detection is dependent on occipital GABA/Cr but the direction of this relationship is different according to the task involved (speed and achromatic luminance versus color discrimination), see also Norton et al. 2016.

One limitation of this study is that GABA/Cr values were not available for correlation with visual psychophysical thresholds within the control group.

In conclusion, we show that type 2 diabetes patients have visual impairment early in the disease even with early retinopathy by a novel speed discrimination task. We also show that occipital cortical GABA/Cr, seems to be a novel predictor of speed and achromatic discrimination thresholds at baseline and one year later, irrespective of level changes, in type 2 diabetes.

CONFLICT OF INTEREST

All authors declare that they have no conflicts of interest.

REFERENCES

- Bearse Jr. MA, Adams AJ, Han Y, et al (2006) A multifocal electroretinogram model predicting the development of diabetic retinopathy. *Prog Retin Eye Res* 25:425–448. doi: 10.1016/j.preteyeres.2006.07.001
- Bogner W, Gruber S, Doelken M, et al (2010) In vivo quantification of intracerebral GABA by single-voxel (1)H-MRS-How reproducible are the results? *Eur J Radiol* 73:526–531. doi: 10.1016/j.ejrad.2009.01.014
- Castelo-Branco M, Faria P, Forjaz V, et al (2004) Simultaneous Comparison of Relative Damage to Chromatic Pathways in Ocular Hypertension and Glaucoma: Correlation with Clinical Measures. *Investig Ophthalmology Vis Sci* 45:499. doi: 10.1167/iovs.03-0815
- Coyne KS, Margolis MK, Kennedy-Martin T, et al (2004) The impact of diabetic retinopathy: perspectives from patient focus groups. *Fam Pr* 21:447–453. doi: 10.1093/fampra/cmh417
- de Fine Olivarius N, Siersma V, Almind GJ, et al (2011) Prevalence and progression of visual impairment in patients newly diagnosed with clinical type 2 diabetes: a 6-year follow up study. *BMC Public Health* 11:80. doi: 10.1186/1471-2458-11-80
- Edden RAE, Muthukumaraswamy SD, Freeman TCA, Singh KD (2009) Orientation discrimination performance is predicted by GABA concentration and gamma oscillation frequency in human primary visual cortex. *J Neurosci* 29:15721–6. doi: 10.1523/JNEUROSCI.4426-09.2009
- Edden RAE, Puts NAJ, Harris AD, et al (2014) Gannet: A batch-processing tool for the quantitative analysis of gamma-aminobutyric acid–edited MR

spectroscopy spectra. *J Magn Reson Imaging* 40:1445–1452. doi: 10.1002/jmri.24478

Ernest-Nwoke IO, Ozor MO, Akpamu U, et al (2014) Relationship between Body Mass Index, Blood Pressure, and Visual Acuity in Residents of Esan West Local Government Area of Edo State, Nigeria. *Physiol J* 2014:1–5. doi: 10.1155/2014/510460

Guariguata L, Whiting DR, Hambleton I, et al (2014) Global estimates of diabetes prevalence for 2013 and projections for 2035. *Diabetes Res Clin Pr* 103:137–149. doi: 10.1016/j.diabres.2013.11.002

Hayward LM, Burden ML, Burden AC, et al (2002) What is the prevalence of visual impairment in the general and diabetic populations: are there ethnic and gender differences? *Diabet Med* 19:27–34.

Hove MN, Kristensen JK, Lauritzen T, Bek T (2006) The relationships between risk factors and the distribution of retinopathy lesions in type 2 diabetes. *Acta Ophthalmol Scand* 84:619–623. doi: 10.1111/j.1600-0420.2006.00710.x

Kalmijn S, Feskens EJ, Launer LJ, et al (1995) Glucose intolerance, hyperinsulinaemia and cognitive function in a general population of elderly men. *Diabetologia* 38:1096–1102.

Krásný J, Brunnerová R, Průhová S, et al (2006) [The contrast sensitivity test in early detection of ocular changes in children, teenagers, and young adults with diabetes mellitus type I]. *Ces a Slov Oftalmol Cas Ces Oftalmol Spol a Slov Oftalmol Spol* 62:381–94.

Luckie R, Leese G, McAlpine R, et al (2007) Fear of visual loss in patients with diabetes: results of the prevalence of diabetic eye disease in Tayside, Scotland (P-DETS) study. *Diabet Med* 24:1086–1092. doi: 10.1111/j.1464-5491.2007.02180.x

Mahmood K, Aamir AH (2005) Glycemic control status in patients with type-2 diabetes. *J Coll Physicians Surg Pak* 15:323–5. doi: 10.3923/jcpsp.2005.15032325

- Mateus C, Raimundo M, Oliveiros B, et al (2015) A New Approach to Assess Early Progressive Loss Across Multiple Visual Channels In the Natural History of Glaucoma. *J Glaucoma*. doi: 10.1097/IJG.0000000000000226
- Miki E, Lu M, Lee ET, et al (2001) The incidence of visual impairment and its determinants in the WHO Multinational Study of Vascular Disease in Diabetes. *Diabetologia* 44 Suppl 2:S31-6.
- Misra S, Saxena S, Kishore P, et al (2010) Association of contrast sensitivity with LogMAR visual acuity and glycosylated hemoglobin in non-insulin dependent diabetes mellitus. *J Ocul Biol Dis Infor* 3:60. doi: 10.1007/s12177-010-9056-0
- Moss SE, Klein R, Klein BE (1988) The incidence of vision loss in a diabetic population. *Ophthalmology* 95:1340–1348.
- Norton DJ, McBain RK, Pizzagalli DA, et al (2016) Dysregulation of visual motion inhibition in major depression. *Psychiatry Res* 240:214–221. doi: 10.1016/j.psychres.2016.04.028
- Reis A, Mateus C, Melo P, et al (2014) Neuroretinal dysfunction with intact blood-retinal barrier and absent vasculopathy in type 1 diabetes. *Diabetes* 63:3926–37. doi: 10.2337/db13-1673
- Ribeiro MJ, Violante IR, Bernardino I, et al (2015) Abnormal relationship between GABA, neurophysiology and impulsive behavior in neurofibromatosis type 1. *Cortex* 64:194–208. doi: 10.1016/j.cortex.2014.10.019
- Ribeiro ML, Nunes SG, Cunha-Vaz JG (2013) Microaneurysm turnover at the macula predicts risk of development of clinically significant macular edema in persons with mild nonproliferative diabetic retinopathy. *Diabetes Care* 36:1254–9. doi: 10.2337/dc12-1491
- Sickmann HM, Waagepetersen HS, Schousboe A, et al (2012) Brain glycogen and its role in supporting glutamate and GABA homeostasis in a type 2 diabetes rat model. *Neurochem Int* 60:267–275. doi: 10.1016/j.neuint.2011.12.019

- Strachan MW, Reynolds RM, Frier BM, et al (2009) The role of metabolic derangements and glucocorticoid excess in the aetiology of cognitive impairment in type 2 diabetes. Implications for future therapeutic strategies. *Diabetes Obes Metab* 11:407–414. doi: 10.1111/j.1463-1326.2008.00963.x
- Taura MD, Adamu L, Modibbo M (2015) Study of Relationship between Blood Pressure and Visual Acuity among Nigerians. *FASEB J* 29:555.4-.
- Trento M, Durando O, Lavecchia S, et al (2016) Vision related quality of life in patients with type 2 diabetes in the EUROCONDOR trial. *Endocrine*. doi: 10.1007/s12020-016-1097-0
- Tsai L-T, Liao K-M, Jang Y, et al (2016) Detecting Visual Function Abnormality with a Contrast-Dependent Visual Test in Patients with Type 2 Diabetes. *PLoS One* 11:e0162383. doi: 10.1371/journal.pone.0162383
- van Bussel FCG, Backes WH, Hofman PAM, et al (2016) Increased GABA concentrations in type 2 diabetes mellitus are related to lower cognitive functioning. *Medicine (Baltimore)* 95:e4803. doi: 10.1097/MD.0000000000004803
- Violante IR, Ribeiro MJ, Edden RAE, et al (2013) GABA deficit in the visual cortex of patients with neurofibromatosis type 1: genotype-phenotype correlations and functional impact. *Brain* 136:918–25. doi: 10.1093/brain/aws368
- Yau JW, Rogers SL, Kawasaki R, et al (2012) Global prevalence and major risk factors of diabetic retinopathy. *Diabetes Care* 35:556–564. doi: 10.2337/dc11-1909
- Yoon JH, Maddock RJ, Rokem A, et al (2010) GABA concentration is reduced in visual cortex in schizophrenia and correlates with orientation-specific surround suppression. *J Neurosci* 30:3777–81. doi: 10.1523/JNEUROSCI.6158-09.2010
- Zhang X, Saaddine JB, Chou CF, et al (2010) Prevalence of diabetic retinopathy in the United States, 2005-2008. *Jama* 304:649–656. doi: 10.1001/jama.2010.1111

Occipital blood-brain barrier permeability is an independent predictor of visual outcome in type 2 diabetes, irrespective of the retinal barrier: A longitudinal study

S. I. Abuhaiba^{1,2,3,4} | M. Cordeiro^{2,5} | A. Amorim^{1,6,7} | Â. Cruz¹ | B. Quendera⁷ | C. Ferreira^{1,7} | L. Ribeiro⁸ | R. Bernardes^{1,7} | M. Castelo-Branco^{1,7}

Abstract

Blood brain barrier permeability in type 2 diabetic patients has been previously shown to be altered in certain brain regions such as the basal ganglia and the hippocampus. Because of the histological and functional similarities between the blood-brain-barrier (BBB) and the blood-retinal-barrier (BRB) we aimed to investigate how the permeability of both barriers predicts visual outcome. We included two control groups (Acute unilateral stroke patients $n=9$, and type 2 diabetics without BRB leakage $n=10$) and a case study group of type 2 diabetics with established BRB leakage ($n=17$). We evaluated gender, age, disease duration, metabolic impairment, retinopathy grade, and BBB permeability as predictors of visual acuity at baseline, 12 months and 24 months in the type 2 diabetics without BRB leakage group and the case study group. We have also explored the differences in BBB permeability in the occipital lobe and frontal lobe in the three different groups. K^{trans} (volume transfer coefficient) and V_p (fractional plasma volume) were estimated. The BBB permeability parameter V_p was higher in the case study group compared to the unaffected hemisphere of stroke patients control group, suggesting changed vascular dynamics in the occipital lobe of type 2 diabetics with established BRB leakage. These patients showed significant correlation between glycated hemoglobin (HbA1C) levels and occipital and frontal K^{trans} . We report for the first time that occipital BBB permeability is an independent predictor of visual acuity at baseline, 12 months and 24 months in type 2 diabetics with established BRB leakage. Our results suggest that occipital BBB permeability might be an independent biomarker for visual impairment in patients with established BRB leakage.

KEYWORDS

diabetes, blood-brain barrier, retinal-blood barrier, MRI, brain imaging

INTRODUCTION

Diabetes Mellitus is one of the most devastating diseases of the 21st century, affecting about 382 million people and estimated to affect 471 million by 2035 (1). It is a metabolic disorder characterized by chronic hyperglycemia and disturbances of carbohydrate, fat and protein metabolism, resulting from defects in insulin secretion, insulin action, or both (2).

Diabetic retinopathy is a very common comorbidity in diabetes and is present in about 60% of Type 2 Diabetes patients with more than 10 years of established disease and in almost every Type 1 Diabetes patient older than 20 (2,3). It is a microvascular complication, with prevalence strongly related to the duration of the disease, and is the most frequent cause of new cases of blindness among adults aged between 20 and 74 years (4). It is estimated to take at least five years for the development of the first signs of retinopathy after the onset of diabetes. Type 2 diabetes patients generally have many years of undiagnosed disease, hence they have a significant risk of diabetic retinopathy at the time of diagnosis (5,6).

Visual loss results primarily from increased permeability of retinal existing vessels (7) (leading to edema) and growth of new abnormal retinal vessels (proliferative retinopathy) that occurs as a consequence of abnormal blood flow, abnormal permeability, and defective perfusion of capillaries. As a result, retinal ischemia stimulates a pathologic neovascularization mediated by angiogenic factors, such as vascular endothelial growth factor (VEGF), which results in proliferative diabetic retinopathy (4).

At the brain level, the early consequences of diabetes are less evident and more difficult to assess, as the brain is not as optically accessible for direct observation as the retina. However, there is evidence of cognitive impairment related to metabolic disturbances in type 2 diabetes patients (8) and blood-brain-barrier

(BBB) permeability dysfunction in diabetic rats (9). BBB permeability has been shown to increase in specific brain regions in rats with Streptozotocin-induced diabetes, namely the hippocampus. (10–12). Hyperglycemia has been associated with altered BBB transport functions (e.g., glucose, insulin, choline, amino acids, etc.), integrity (tight junction disruption), and oxidative stress in central nervous system (CNS) microcapillaries (13). These have a potential causal role for upregulation and activation of the receptor for advanced glycation end-products (RAGE). Difficulty in detecting vascular impairments in the large and heterogeneous brain microvascular bed in vivo has led to controversial findings, especially regarding the effects of diabetes on the BBB. It was previously reported that type 2 diabetics have an increased signal on magnetic resonance brain imaging with intravenous gadolinium (Gd) diethylenetriamine pentaacetic acid (Gd-DTPA) compared to healthy controls in the basal ganglia, a finding that is suggestive of increased blood-brain barrier permeability in type 2 diabetics (14).

The retina is an external prolongation of the brain, from the embryological point of view and, from this perspective, the blood-retinal-barrier (BRB) shares histological and functional similarities with the BBB. In the early stages of diabetic macular edema, breakdown of BRB may occur, resulting in accumulation of extracellular fluid in the macula (15). Functional retinal changes and psychophysical visual impairment have been previously described in type 2 diabetes patients with retinopathy (16,17), but a possible correlation with BBB leakage has not been explored yet. A recent study by our group has shown evidence for neurophysiological and psychophysical changes even prior to BRB leakage (18), which suggests that neurophysiological and vascular phenotypes may be separable at least during a part of the natural history of the disease.

In this study, we aim to elucidate the possible interplay between BBB permeability and BRB permeability. We are also interested in studying possible relationships between the BBB permeability within the occipital lobe and visual performance in type 2 diabetic patients.

MATERIALS AND METHODS

Participants

In this study, we recruited 17 type 2 diabetic patients with established blood-retinal-barrier leakage - “Case Study Group”. We also recruited two control groups for comparative analysis: 9 non-diabetic patients with acute unilateral stroke and 10 type 2 diabetic patients without blood-retinal-barrier leakage.

The participants were recruited from the Institute for Biomedical Imaging and Life Sciences (IBILI) and the Central Hospital of University of Coimbra (CHUC). All participants were provided with a formal written consent which explained the study protocol, the required investigations and any other information needed by the participant to make a sound decision to join the study.

The inclusion criteria for the case study group and the type 2 diabetic patients without BRB leakage group included any patient with type 2 diabetes who is aged 75 years or younger, and who have non-proliferative diabetic retinopathy (NPDR). Participants with cataracts or other eye diseases that could interfere with fundus examinations, eye surgery or treatment within the previous 6-months, pregnancy, lactation, renal failure (acute or chronic), severe cardiovascular disease (brain stroke, myocardial infarction, limb injury), known allergic or hypersensitivity reactions to Gadobutrol, used in dynamic contrast enhanced – magnetic resonance imaging (DCE-MRI), or known contraindications to MRI (cardiac pacemaker, claustrophobia, cochlear implants) were excluded from these two groups. The classification of the type 2 diabetic patients into a case study participant or a control participant was made possible by the evaluation of the retinal-barrier-status by retinal leakage analyzer (RLA) at the baseline visit. Participants from these two groups underwent routine clinical history and physical examination assessment, HbA1C level assessment, and color fundus photography. Best corrected visual acuity (BCVA) was assessed at the baseline visit, 12-month time-point and 24-month time point and is presented as decimal visual acuity. The blood-brain-barrier permeability was assessed by DCE-MRI.

The inclusion criteria for the acute unilateral stroke patients group included any non-diabetic patient with a unilateral hemispheric vascular lesion, i.e. blood-brain-

barrier permeability parameters were obtained from the healthy hemisphere, who is aged 75 years or younger. We excluded any participant who is pregnant, lactating, with renal failure (acute or chronic), with known allergic or hypersensitivity reactions to Gadobutrol, used in DCE-MRI, or known contraindications to MRI (cardiac pacemaker, claustrophobia, cochlear implants). Participants from this group also underwent clinical history and physical examination assessment in addition to the measurement of blood-brain-barrier permeability by DCE-MRI.

The presence or absence of deep white matter lesions indicative of silent ischemia was assessed by an experienced neuroradiologist in the three groups.

Ethics

This study was performed per the ethical principles of the Declaration of Helsinki. Eligible patients only participated in the study after providing written informed consent. This study was approved by the Ethics Committee of the Faculty of Medicine of the University of Coimbra.

Study Protocol

Type 2 diabetics were contacted by our institution for participation and an informed consent was provided. The participants underwent RLA assessment to classify them between type 2 diabetics with established BRB leakage (case study group) or type 2 diabetics without BRB leakage (a control group). During the same visit, the participants also underwent colored fundoscopic photography, best corrected visual acuity assessment, and history and physical examination including the presence or absence of other co-morbidities such as hypercholesterolemia or hypertension. Additionally, the participants underwent structural MRI and DCE-MRI for the assessment of the blood-brain-barrier permeability and the presence or absence of deep white matter lesions at the same baseline visit. BRB assessment by RLA and BBB assessment by DCE-MRI were performed on the same day.

At the second visit, 12 months later, the type 2 diabetics were contacted again, and the best corrected visual acuity test was redone. Finally, at 24 months, the two groups had their best corrected visual acuity reassessed.

Retinal leakage analysis

The retinal leakage analyzer (RLA) quantifies localized fluorescein leakage from the retina into the vitreous across the BRB in humans, at multiple spatial locations. If the BRB is intact, there should be virtually no leakage, where the amount of leakage is proportional to BRB damage. RLA was used in the type 2 diabetic participants to classify the patients between type 2 diabetics with established BRB leakage (case study group) and type 2 diabetics without BRB leakage (a control group).

Retinal and vitreous fluorescence were measured within the first 10 and 15 minutes after intravenous injection of 14mg/ Kg of 20% sodium fluorescein using the Heidelberg Retina Angiograph. The system was run using the default setup for leakage analysis. Fluorescein measurements obtained from the vitreous were then converted into leakage maps describing the distribution of the BRB permeability indices.

Two types of information were obtained simultaneously: one for optical imaging of the retina, and the other representing fluorescence measurements from the areas being scanned. To compute the BRB permeability, a simplex index of permeability was determined. The measurement of the permeability index assumes 1-dimensional diffusion of fluorescein across the retinal plane and includes measurements of fluorescence near the retina.

Type 2 diabetics with unilateral or bilateral BRB leakage were classified as the case study group (n = 17) while those without BRB leakage in both eyes were classified as the control group (n = 10). Figure-1 shows the differences between an abnormal RLA versus a normal RLA.

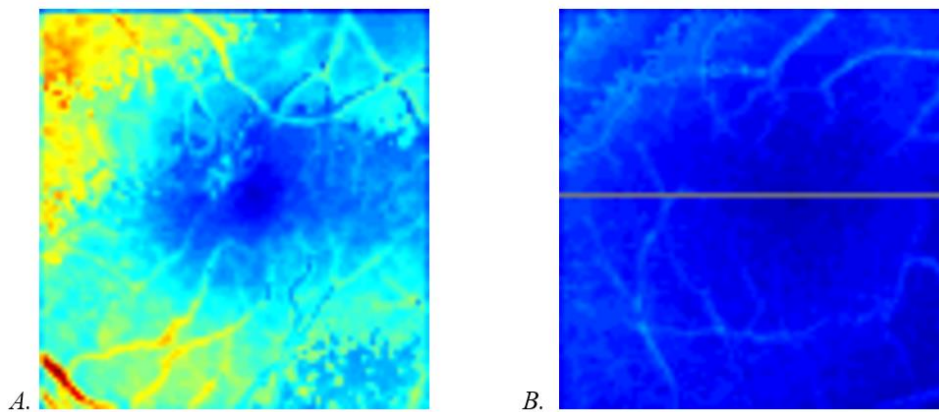


Figure-1: A. An RLA map that shows increased fluorescence due to retinal blood vessels' leakage in a type 2 diabetic patient compared to B. who is a type 2 diabetic without retinal leakage. For an RLA map to be considered normal, there should be no leakage at all.

Structural MRI and DCE-MRI

DCE-MRI typically consists of a T1-weighted sequence repeated several times over the course of several minutes following a contrast bolus injection. The main advantage of DCE-MRI over qualitative post-contrast T1-weighted imaging or visual evidence of gadolinium enhancement is that it is more sensitive to BBB damage (19). It also allows to quantitatively measure the extent of contrast accumulation as a function of time, by applying an appropriate pharmacokinetic model, and ultimately to produce estimates of BBB permeability in the volume of plasma cleared for the tracer per unit of time and per unit of tissue volume.

We asked the patients to fast for 4 hours before imaging. MRI was performed using a 3.0 Tesla scanner (3T MAGNETOM Trio, A Tim System, Siemens Medical Solutions, Erlangen, Germany) with a standard phased array 12-channel head matrix coil. The subjects were positioned on the scanner table with the head at the center of the head-coil, and provided with headphones and paddings to minimize head movements during the scan. Structural and functional sequences were acquired, namely, MPRAGE_p2_1mm-iso, 1H-Spectroscopy sv_s529, t1_tse_rs_tra. Then, a paramagnetic contrast agent - Gadobutrol (Gadovist 1,0 mmol/ml, Bayer Pharma AG, Berlin, Germany) - was injected after the third sequence, using a previously applied intravenous catheter into the antecubital

vein, with a power-injector (Optistar™ MR Contrast Delivery System, Mallinckrodt Pharmaceuticals, St. Louis, United States) with programmed flow rate and volume (constant rate of 3.5 mL/s). The dose was 0.1mmol/kg body-weight (i.e., most of the times approximately 7 mL to 9 mL). The rate and volume of saline-flush injection was 3.5 mL/s and 20 mL, respectively.

In order to estimate the baseline T_1 map, we obtained 3 variable flip-angle gradient echo (GRE) sequences (TR 5.9 ms; TE 2.11 ms; FA 2°, 5°, or 10°; 128 × 128 matrix, 1.875 × 1.845-mm in-plane pixel size, 240 × 240-mm field of view, resulting in 5-mm slice thickness and 1950 Hz/pixel bandwidth). On the other hand, the perfusion sequence was the same with a flip-angle of 20° and 20 continuous measurements.

The 3D GRE sequence had the following settings: TR/TE 5.9/1.5 ms, FOV 240 mm, matrix 128×128, slice thickness 5 mm, 32 slices, flip-angle 20°, for 20 times with a temporal resolution of about 11s.

BBB permeability estimation

The evaluation of blood-brain-barrier permeability (BBBp) was performed by a trained biomedical engineer (author AM) and supervised (for region of interest (ROI) selection) by an experienced neuroradiologist using an in-house custom software developed in Matlab by AM. The ROIs were bilateral in the case study group and in type 2 diabetics without BRB leakage (a control group), and contralateral to the stroke side in the second control group of acute unilateral stroke patients.

After motion correction and registration, we manually drew a region of interest that included the occipital lobe (Grey and White Matter) and a control region that included the frontal lobe, see Figure-2. Pharmacokinetic modeling was performed using the Patlak Model, which is considered superior to the conventional Tofts and extended Tofts models in estimating low BBB permeability changes (20,21), in order to obtain the volume transfer coefficient (K^{trans}), and fractional plasma volume (V_p) which are considered as reliable parameters of BBBp. The arterial

input function (AIF) used was the Parker modeled AIF (22). The process concluded with the computation of the mean values of K^{trans} and V_p for each ROI.

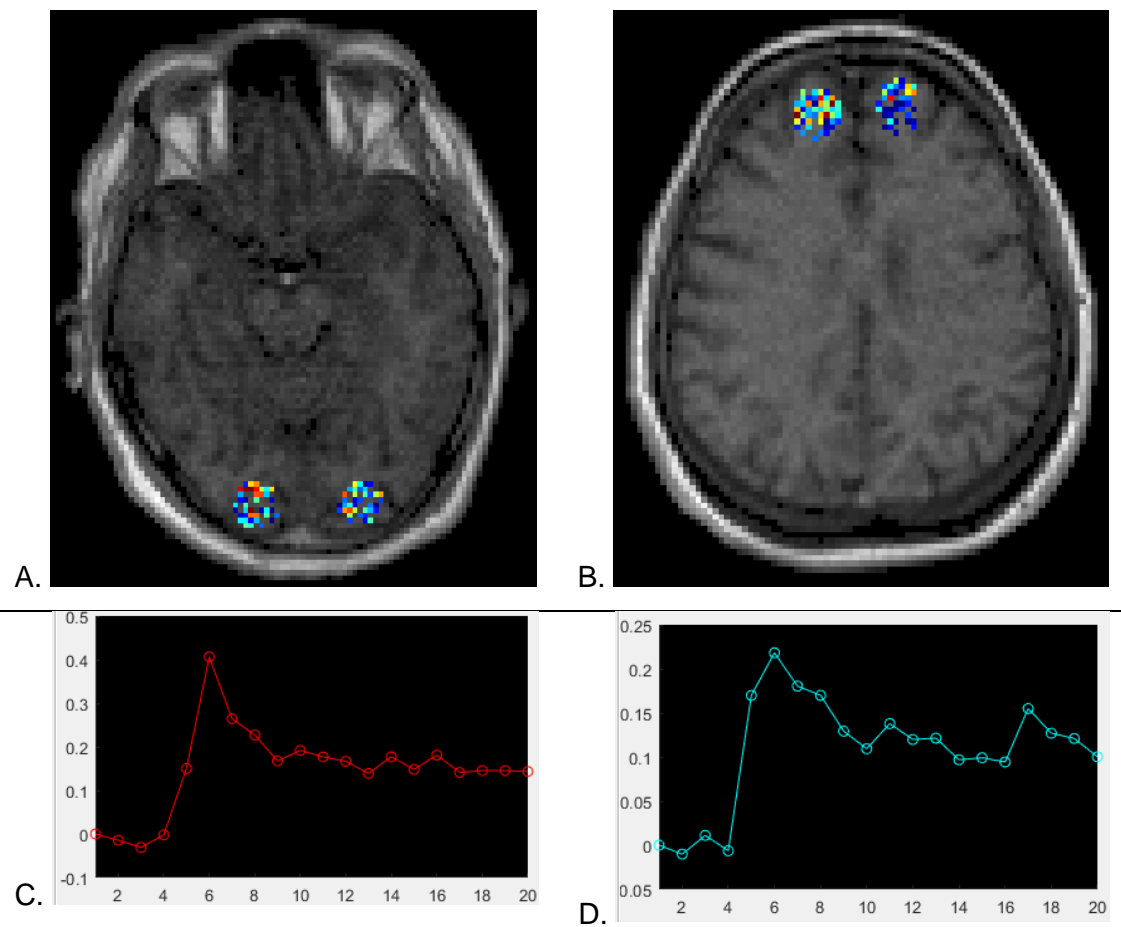


Figure-2: A. Shows the placement of the occipital lobe ROI with a parametric map of K^{trans} . The ROI included multiple slices to include 1000 voxels in average. B. Shows the placement of the frontal lobe ROI with a parametric map of K^{trans} . The ROI included multiple slices to include 1000 voxels in average. C. and D. depict the relative contrast enhancement over time measured from the occipital and frontal ROIs respectively.

The placement of the ROIs was bilateral in type 2 diabetic patients and contralateral to the vascular lesion, i.e. stroke, in the acute unilateral stroke patients.

Statistical analysis

Statistical analysis was performed using IBM SPSS Statistics 23.0. ANOVA test was used to compare the continuous variables between the three groups. Chi-square test was used to compare proportional variables between the three

groups, i.e. gender, comorbidities, and the presence of deep white matter lesions. Independent samples student t-test was used to compare BBBp and visual acuity parameters between participants with or without comorbidities within the case study group. Pearson's correlation was used to study the relationship between BBBp at baseline and the body mass index, disease duration, or HbA1C within the case study group and the control group of type 2 diabetics without BRB leakage. Pearson's correlation was also used to evaluate the predictive relationship of BBBp and visual acuity at baseline, 12 months and 24 months within the case study group and the control group of type 2 diabetics without BRB leakage. Bonferroni correction for multiple comparisons was used.

RESULTS

Patient characteristics

Table-1 summarizes the demographic, clinical, radiological, ocular, and retinal characteristics of the three groups included in this study. Our case study group "Type 2 Diabetics with Established BRB Leakage" was not statistically different from the control group of type 2 diabetics without BRB leakage or the control group of non-diabetics with acute unilateral stroke patients. Despite the absence of statistically significant differences, we noticed certain trends in our case study group. Type 2 diabetics with established BRB leakage tend to have a slightly increased frequency of hypertension, hypercholesterolemia, and deep white matter lesions compared to the control group of type 2 diabetics without BRB leakage. Additionally, type 2 diabetics with established BRB leakage were more likely to have advanced retinopathy grade and a slightly lower decimal visual acuity at baseline.

Table-1: General characteristics of the different study groups.

Parameter	Case Study Group* (n = 17)	Type 2 Diabetics Without BRB Leakage (n = 10)	Acute Unilateral Stroke Patients (n = 9)	p-value

Age [years]	61.12 (8.19)	61.7 (8.46)	64.77 (6.82)	> 0.05
BMI [kg/m ²]	30.38 (4.51)	30.33 (3.07)	27.05 (3.30)	> 0.05
Gender (M:F)	8:9	7:3	6:3	> 0.05
Comorbidities				
Hypertension	88.2%	80%	44.4%	> 0.05
Hypercholesterolemia	52.9%	30%	77.8%	> 0.05
Deep White Matter Lesions				
None	53%	66.7%	22.2%	> 0.05
Yes	47%	33.3%	77.8%	
General Characteristics of Type 2 Diabetic Groups				
Duration of Type 2 Diabetes Diagnosis	15.65 (6.06)	16.7 (4.17)		> 0.05
HbA1C [%]	7.93 (1.32)	8.00 (1.24)		> 0.05
Ocular and Retinal Characteristics				
Right Eye				
Diabetic Retinopathy Grade				
Early	35.3%	50%		> 0.05
C, D or F	64.7%	50%		
Visual Acuity	0.85 (0.05)	0.87 (0.04)		> 0.05
Left Eye				
Diabetic Retinopathy Grade				
Early	47.1%	50%		> 0.05
C, D or F	52.9%	50%		
Visual Acuity	0.85 (0.04)	0.87 (0.02)		> 0.05

None of the tested parameters showed a statistically significant difference between the three groups. Hypertension, hypercholesterolemia and deep white matter lesions were slightly more reported in the case study group compared to the negative control group. The diabetic retinopathy grade was more advanced in the case study group and visual acuity showed a trend to be slightly lower in

the same group. Continuous variables are presented as mean (standard deviation).

* Case Study Group: Type 2 Diabetics with Established BRB Leakage

The BBB status in the Three Groups

Table-2 summarizes the main differences in the BBB permeability parameters, between the three groups. The case study group had a statistically significant (survived correction for multiple comparisons) higher mean of occipital V_p compared to the control group of acute unilateral stroke patients (the contralateral hemisphere in stroke patients).

Table-2: Blood-brain-barrier permeability differences between the three study groups.

	Case Study Group* (n = 17)	Type 2 Diabetics Without BRB Leakage (n = 10)	Contralateral Hemisphere in Acute Unilateral Stroke Patients (n = 9)	ANOVA p-value
Occipital				
K^{trans} [min^{-1}]	0.006 (0.001)	0.006 (0.001)	0.007 (0.003)	N.S.
V_p	0.006 (0.002)	0.007 (0.003)	0.003 (0.002)	0.001
Frontal				
K^{trans} [min^{-1}]	0.005 (0.001)	0.005 (0.001)	0.006 (0.001)	N.S.
V_p	0.004 (0.001)	0.004 (0.001)	0.003 (0.001)	0.007

Variables are presented in the format: Mean (Standard Deviation). The difference in mean of occipital lobe V_p survived correction for multicomparisons when comparing the **case study group** to the **control group of acute unilateral stroke patients**.

K^{trans} : volume transfer coefficient reflecting vascular permeability.

V_p : fractional plasma volume

* Case Study Group: Type 2 Diabetics with Established BRB Leakage

Relationship Between BBBp and the Disease Duration, BMI, and HbA1C in the Case Study Group versus the Control Group of Type 2 Diabetics Without BRB Leakage

Table-3 summarizes the correlations between BBBp parameters from the occipital and frontal lobes, and disease duration, body mass index and HbA1C.

Type 2 diabetics with established BRB leakage had a statistically significant correlation between their HbA1C and occipital and frontal K^{trans} . This correlation was absent in the control group of type 2 diabetics without BRB leakage.

Table-3: Correlation between blood-brain-barrier permeability and the general characteristics within the case study and the control group of type 2 diabetics without BRB leakage.

	Disease Duration	p	BMI	p	HbA1C	p
Case Study Group*						
Occipital						
K^{trans} [min^{-1}]	-0.018	N.S.	0.418	N.S.	0.612	0.013
V_p	0.079	N.S.	0.104	N.S.	0.011	N.S.
Frontal						
K^{trans} [min^{-1}]	0.096	N.S.	0.121	N.S.	0.579	0.019
V_p	0.074	N.S.	0.143	N.S.	-0.163	N.S.
Type 2 Diabetics Without BRB Leakage						
Occipital						
K^{trans} [min^{-1}]	-0.211	N.S.	-0.092	N.S.	-0.367	N.S.
V_p	-0.177	N.S.	-0.714	N.S.	-0.251	N.S.
Frontal						

K^{trans} [min^{-1}]	0.279	N.S.	-0.143	N.S.	-0.116	N.S.
V_p	-0.118	N.S.	-0.086	N.S.	-0.351	N.S.

Diabetics with established BRB leakage showed a positive correlation between occipital blood-brain-barrier permeability presented in K^{trans} and HbA1C. These correlations cannot be found in the negative control group.

Shaded values are statistically significant correlations.

K^{trans} : volume transfer coefficient reflecting vascular permeability.

V_p : fractional plasma volume

* Case Study Group: Type 2 Diabetics with Established blood-retinal-barrier Leakage

Prediction of Visual Acuity from the Systemic and Demographic Features within the Case Study Group and the Control Group of Type 2 Diabetics Without BRB Leakage

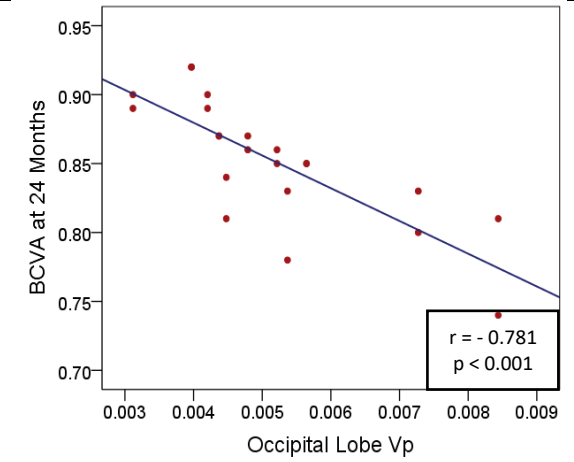
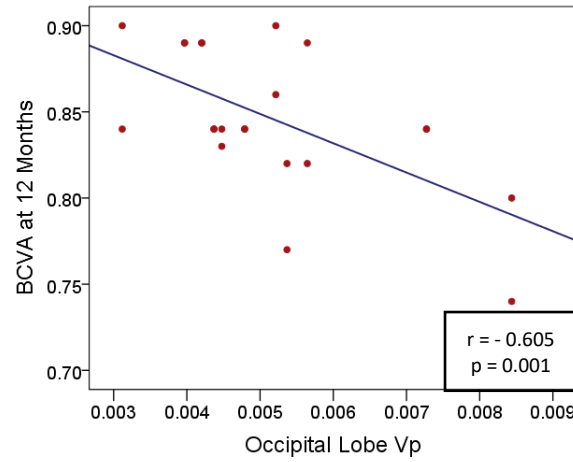
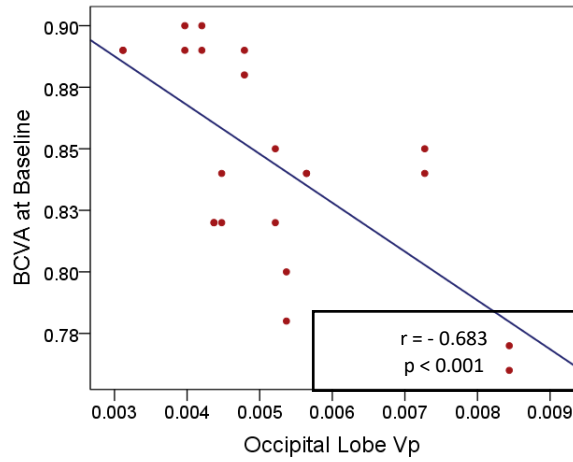
Neither the disease duration, nor the baseline HbA1C levels within the case study group were predictive of visual acuity at baseline, 12 months or 24 months. BMI predicted visual acuity at 12 months and 24 months ($r = -0.451$ and $r = -0.393$, $p < 0.05$ respectively) in the case study group. Disease duration, baseline HbA1C and BMI were not predictive of visual acuity at baseline, 12 months or 24 months in the control group of type 2 diabetics without BRB leakage.

Relationship Between BBBp and Visual Acuity in the Case Study Group versus the Control Group of Type 2 Diabetics Without BRB Leakage

Occipital V_p was predictive of visual acuity at baseline, 12 months and 24 months later in the case study group after correction for multiple comparisons. These correlations are presented in Figure-3. These correlations were absent in the control group of type 2 diabetics without BRB leakage.

Prediction of Best Corrected Visual Acuity by the Occipital Lobe Vp

Type 2 Diabetics with Established BRB Leakage



Type 2 Diabetics without BRB Leakage

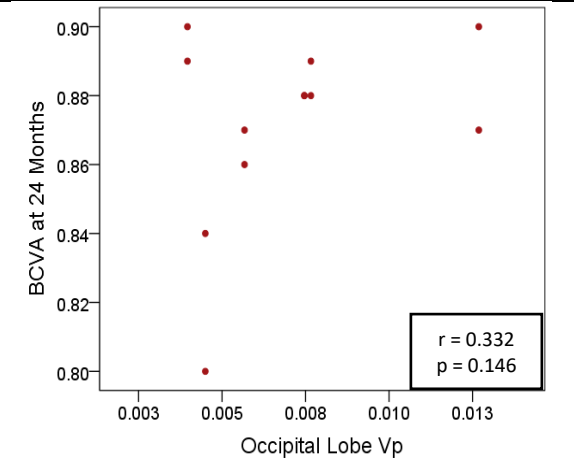
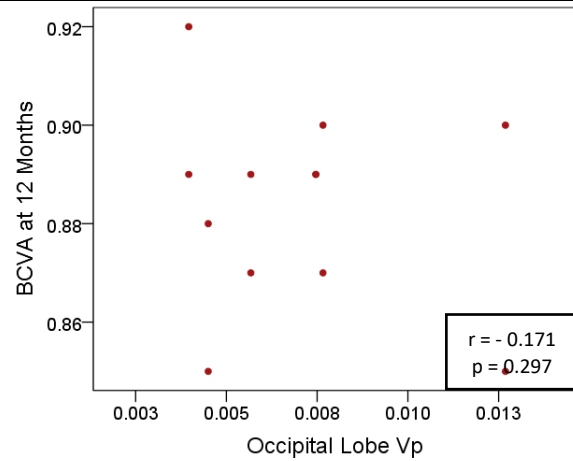
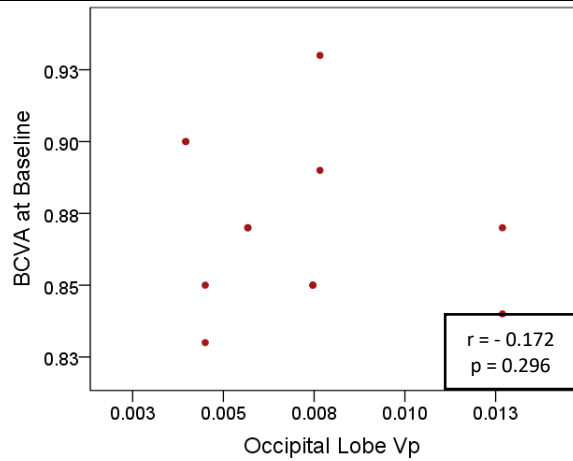


Figure-3: Occipital lobe Vp was negatively correlated with visual acuity in the type 2 diabetics with established BRB leakage at baseline, 12 months and 24 months. These predictive correlations were not found in type 2 diabetics without BRB leakage. The red dots represent number of eyes not subjects. Bonferroni corrected significance level $p = 0.004$. BRB: blood-retinal-barrier. Vp: fractional plasma volume. BCVA: best corrected visual acuity.

BBBp and Comorbidities in Type 2 Diabetics with Established BRB Leakage

Type 2 diabetics with established BRB leakage and hypertension had a higher occipital lobe K^{trans} and V_p when compared to those without hypertension. Table-4 summarizes the differences between patients with other comorbidities and those without comorbidities within the case study group.

Table-4: Blood-brain-barrier permeability in relation to hypertension, hypercholesterolemia and deep white matter lesions within the case study group (Type 2 Diabetics with Established blood-retinal-barrier Leakage).

	With Hypercholesterolemia	Without Hypercholesterolemia	p-value
Occipital			
K^{trans} [min^{-1}]	0.005 (0.001)	0.006 (0.002)	N.S.
V_p	0.004 (0.001)	0.007 (0.003)	N.S.
Frontal			
K^{trans} [min^{-1}]	0.005 (0.001)	0.005 (0.001)	N.S.
V_p	0.004 (0.001)	0.004 (0.001)	N.S.
With Hypertension			
	With Hypertension	Without Hypertension	
Occipital			
K^{trans} [min^{-1}]	0.006 (0.001)	0.005 (0.0004)	0.023
V_p	0.006 (0.002)	0.004 (0.0002)	0.004
Frontal			
K^{trans} [min^{-1}]	0.005 (0.001)	0.005 (0.01)	N.S.
V_p	0.004 (0.001)	0.003 (0.001)	0.013
With any DWM Lesions			
	With any DWM Lesions	Without DWM Lesions	p-value
Occipital			
K^{trans} [min^{-1}]	0.006 (0.001)	0.005 (0.001)	N.S.
V_p	0.007 (0.003)	0.005 (0.002)	N.S.
Frontal			

K^{trans} [min^{-1}]	0.005 (0.001)	0.005 (0.001)	N.S.
V_p	0.004 (0.001)	0.004 (0.001)	N.S.
	Diabetic Retinopathy Grades (C, D or F)	Early Diabetic Retinopathy	p-value
Occipital			
K^{trans} [min^{-1}]	0.006 (0.002)	0.005 (0.001)	N.S.
V_p	0.007 (0.003)	0.005 (0.002)	N.S.
Frontal			
K^{trans} [min^{-1}]	0.005 (0.001)	0.005 (0.001)	N.S.
V_p	0.004 (0.001)	0.004 (0.001)	N.S.

Variables are presented in the format: Mean (Standard Deviation). Type 2 diabetics with established blood-retinal-barrier leakage and hypertension had a higher occipital lobe K^{trans} and V_p when compared to those without hypertension. K^{trans} : volume transfer coefficient reflecting vascular permeability.

V_p : fractional plasma volume

Visual Acuity in Relation to the Baseline Status of Deep White Matter Lesions and Diabetic Retinopathy Grade within the Case Study Group

Finally, we compared visual acuity at baseline, 12 months and 24 months in relationship to the presence of deep white matter lesions or diabetic retinopathy grade, see Table-5. Patients who have deep white matter lesions at baseline are more likely to have a lower visual acuity 24 months later. This same group, as depicted in Table-4, had a higher occipital blood-brain-barrier permeability

Table-5: Prediction of visual acuity in the case study group* by deep white matter lesions and diabetic retinopathy grade status at baseline.

	With any DWM Lesions	Without DWM Lesions	p-value
Visual Acuity at Baseline	0.84 (0.32)	0.86 (0.49)	N.S.
Visual Acuity at 12 Months	0.84 (0.31)	0.87 (0.52)	N.S.

Visual Acuity at 24 Months	0.84 (0.32)	0.88 (0.51)	0.036
	Diabetic Retinopathy Grades (C, D or F)	Early Diabetic Retinopathy	p-value
Visual Acuity at Baseline	0.85 (0.46)	0.86 (0.24)	N.S.
Visual Acuity at 12 Months	0.85 (0.49)	0.86 (0.35)	N.S.
Visual Acuity at 24 Months	0.86 (0.51)	0.87 (0.41)	N.S.

It seems that patients who have deep white matter lesions at baseline are more likely to have a lower visual acuity 24 months later. This same group, as depicted in Table-4, had a higher occipital blood-brain-barrier permeability. Variables are presented in the format: Mean (Standard Deviation).

* Case Study Group: Type 2 Diabetics with Established blood-retinal-barrier Leakage

DWM: Deep White Matter Lesions

DISCUSSION

The main purpose of this study was to assess the joint status of BRB and BBB in type 2 diabetics patients and whether the later could relate to visual performance. Pathophysiologic changes were assessed in the living human retina and brain using an extensive array of techniques to assess retinal (RLA), visual (best correct visual acuity) and brain (dynamic contrast enhanced MRI) barrier permeability and their respective functional impact.

BRB impairment in T2DM is well established and can be easily directly quantified by RLA or other techniques (23). Additionally, BRB increased permeability has been extensively studied in T2DM and several factors have been identified that are known to play a role in the pathology of diabetic retinopathy which include but

are not limited to the vascular endothelial growth factor and interleukin-6 (4,24–26). Because the same insulting factors for BRB such as hyperglycemia, hyperlipidemia and hypertension can influence the BBB, the development of novel techniques to study the status of the two barriers simultaneously is important to establish a correlation between these barriers, e.g. the estimation of BBB permeability by the quantification of BRB permeability in T2DM (27). The notion that the permeability of the two barriers are correlated has been also suggested in other conditions such as epilepsy (28). Moreover, a recent prospective study has reported an increase in the number of subclinical brain infarcts in patients with established BRB impairment further emphasizing that cortical small-vessel disease is more common in patients with diabetic retinopathy (29).

Therefore, a central issue in our study was whether a direct correlation can be established between BRB and BBB and their respective role in the emergence of complications of diabetes.

While there were no statistically significant differences in the demographics and clinical characteristics of the three studied groups, several trends were noted. It appears that the frequency of hypertension and hypercholesterolemia might be slightly higher in type 2 diabetics with established BRB leakage compared to type 2 diabetics without BRB leakage. The frequency of deep white matter lesions was also higher in the type 2 diabetics with established BRB leakage compared to type 2 diabetics without BRB leakage. Type 2 diabetics with established BRB leakage also had a slightly more advanced stage of retinopathy.

Surprisingly, despite the histologic and embryological similarities in addition to the previously discussed relationships between BRB and BBB impairment, our data suggests that the status of both barriers might be independent in type 2 diabetics. BBB permeability was not related to diabetic retinopathy grade, number of microaneurysms or macular leakage. This also point towards the possible independence of the two vascular systems and their respective barriers. V_p was higher in the type 2 diabetic groups compared to positive control group, which can be explained by the possibility of enhanced cerebral perfusion in type

2 diabetics (30). Further, the pro-angiogenic factor (vascular endothelial growth factor) levels were reported to be elevated in response to advanced glycation end-products (31). V_p has been shown in other disease conditions to be elevated in case of hypervascularity or enhanced angiogenesis (32–34).

In addition to exploring the relationship between occipital BBBp and visual performance, we also evaluated the correlation between BBBp and disease duration, BMI and HbA1C in the type 2 diabetics with and without established BRB leakage. K^{trans} , which is a BBBp parameter, showed a positive correlation with the HbA1C only in type 2 diabetic patients with established BRB leakage. Blood-brain barrier disruption in response to advanced glycation end-products has been previously reported in the literature, in animal models (31). Type 2 diabetics with established BRB leakage had a slightly higher K^{trans} and V_p within the occipital lobe in patients with deep white matter lesions which might be suggestive of silent ischemia. White matter hyperintensities in type 2 diabetic patients were previously reported to be associated with a higher signal from Gd-DTPA which agrees with our finding (14).

Although disease duration and HbA1C were not predictive of BCVA in type 2 diabetics with or without BRB leakage, baseline BMI was negatively correlated with BCVA at 12 and 24 months only in the type 2 diabetics with established BRB leakage group; another subtle difference that we noted between the two groups. A previous study in Central China showed that overweight children are more likely to have visual impairment compared to normal weight children (35). While this study agrees partially with our findings, we could not find any recent study in the literature that could explain why this relationship was only observed in type 2 diabetics with established BRB leakage.

Because of the subtle differences in BBB permeability predictors between type 2 diabetics with BRB leakage and without BRB leakage, we evaluated the relationship between BBB permeability and best corrected visual acuity in both groups.

Interestingly, occipital lobe V_p was predictive of BCVA at baseline, 12 months and 24 months later only in type 2 diabetics with established BRB leakage. This suggests that dysfunction of BBB in vascular sectors related to visual regions such as in the posterior circulation, do independently contribute to visual impairment at this stage. This finding suggests that cortical small vessel disease and BBB disruption are more evident in patients with BRB impairment (29), and BBB permeability in these patients can predict functional visual impairment in terms of BCVA but the permeability of the two barriers remains largely uncorrelated. Similarly, microbleeds, a sign of microangiopathy, was reportedly found to be more common in patients with established proliferative diabetic retinopathy in type 1 diabetes and not in the general type 1 diabetic population when compared to controls (36).

BBB disruption in the visual cortex has been shown previously in a rat model to alter the fMRI response to different visual stimuli (37). We hypothesize that increased BBB permeability, i.e. BBB disruption, in the occipital lobe might have a negative impact on visual acuity in type 2 diabetics with established BRB leakage.

In conclusion, we found that BBB permeability is predictive of visual impairment in T2DM in patients with established BRB disruption. We believe that patients with BRB disruption are at an increased risk of cerebral small vessel disease and BBB disruption, which can contribute to their visual functional phenotype.

ACKNOWLEDGMENTS

MCB is the guarantor of this work and, as such, had full access to all the data in the study and takes responsibility for the integrity of the data and the accuracy of the data analysis. This work was supported by the following grants: INFARMED-FIS-2015-01_DIA_20150630-173, within the scope of the strategic project FCT-UID/NEU/04539/2013– COMPETE, POCI-01-0145-FEDER-007440, BIGDATIMAGE, CENTRO-01-0145-FEDER-000016, Centro 2020 FEDER, COMPETE, PAC – MEDPERSYST, POCI-01-0145-FEDER-016428.

We thank the participants for their involvement in this study. We also thank João Marques, César Nunes and Ricardo Morais for help with patient informed consent in MRI studies.

REFERENCES

- 1 Whiting DR, Guariguata L, Weil C, Shaw J: IDF diabetes atlas: global estimates of the prevalence of diabetes for 2011 and 2030. *Diabetes Res Clin Pr* 2011;94:311–321.
- 2 Standards of Medical Care for Patients With Diabetes Mellitus. *Clin Diabetes* 2003;21:27–37.
- 3 Fong DS, Aiello L, Gardner TW, King GL, Blankenship G, Cavallerano JD, et al.: Diabetic Retinopathy. *Diabetes Care* 2003;26:s99–s102.
- 4 Ciulla TA, Amador AG, Zinman B: Diabetic retinopathy and diabetic macular edema: pathophysiology, screening, and novel therapies. *Diabetes Care* 2003;26:2653–2664.
- 5 Cunha-Vaz J, Ribeiro L, Lobo C: Phenotypes and biomarkers of diabetic retinopathy. *Prog Retin Eye Res* 2014;41:90–111.
- 6 Lobo CL, Bernardes RC, Figueira JP, de Abreu JR, Cunha-Vaz JG: Three-year follow-up study of blood-retinal barrier and retinal thickness alterations in patients with type 2 diabetes mellitus and mild nonproliferative diabetic retinopathy. *Arch Ophthalmol* 2004;122:211–217.
- 7 Sivaprasad S, Gupta B, Gulliford MC, Dodhia H, Mohamed M, Nagi D, et al.: Ethnic variations in the prevalence of diabetic retinopathy in people with diabetes attending screening in the United Kingdom (DRIVE UK). *PLoS One* 2012;7:e32182.
- 8 Kalmijn S, Feskens EJ, Launer LJ, Stijnen T, Kromhout D: Glucose intolerance, hyperinsulinaemia and cognitive function in a general population of elderly men. *Diabetologia* 1995;38:1096–1102.

- 9 Horani MH, Mooradian AD: Effect of diabetes on the blood brain barrier. *Curr Pharm Des* 2003;9:833–840.
- 10 Banks WA: The dam breaks: disruption of the blood-brain barrier in diabetes mellitus. *Am J Physiol Hear Circ Physiol* 2006;291:H2595-6.
- 11 Banks WA, Jaspan JB, Huang W, Kastin AJ: Transport of insulin across the blood-brain barrier: saturability at euglycemic doses of insulin. *Peptides* 1997;18:1423–1429.
- 12 Huber JD, VanGilder RL, Houser KA: Streptozotocin-induced diabetes progressively increases blood-brain barrier permeability in specific brain regions in rats. *Am J Physiol Hear Circ Physiol* 2006;291:H2660-8.
- 13 Prasad S, Sajja RK, Naik P, Cucullo L: Diabetes Mellitus and Blood-Brain Barrier Dysfunction: An Overview. *J Pharmacovigil* 2014;2:125.
- 14 Starr JM, Wardlaw J, Ferguson K, MacLulich A, Deary IJ, Marshall I: Increased blood-brain barrier permeability in type II diabetes demonstrated by gadolinium magnetic resonance imaging. *J Neurol Neurosurg Psychiatry* 2003 Jan [cited 2017 Jun 7];74:70–6.
- 15 Browning DJ: *Diabetic retinopathy: evidence-based management*. New York, Springer, 2010.
- 16 Bearnse MA, Han Y, Schneck ME, Barez S, Jacobsen C, Adams AJ: Local multifocal oscillatory potential abnormalities in diabetes and early diabetic retinopathy. *Invest Ophthalmol Vis Sci* 2004;45:3259–3265.
- 17 Bearnse MA, Adams AJ, Han Y, Schneck ME, Ng J, Bronson-Castain K, et al.: A multifocal electroretinogram model predicting the development of diabetic retinopathy. *Prog Retin Eye Res* 2006;25:425–48.
- 18 Reis A, Mateus C, Melo P, Figueira J, Cunha-Vaz J, Castelo-Branco M: Neuroretinal dysfunction with intact blood-retinal barrier and absent vasculopathy in type 1 diabetes. *Diabetes* 2014 Nov;63:3926–37.

- 19 Ingrisch M, Sourbron S, Morhard D, Ertl-Wagner B, Kümpfel T, Hohlfeld R, et al.: Quantification of Perfusion and Permeability in Multiple Sclerosis. *Invest Radiol* 2012;47:252–258.
- 20 Montagne A, Barnes SR, Sweeney MD, Halliday MR, Sagare AP, Zhao Z, et al.: Blood-Brain Barrier Breakdown in the Aging Human Hippocampus. *Neuron* 2015 Jan 21;85:296–302.
- 21 Barnes SR, Ng TSC, Montagne A, Law M, Zlokovic B V, Jacobs RE: Optimal acquisition and modeling parameters for accurate assessment of low Ktrans blood-brain barrier permeability using dynamic contrast-enhanced MRI. *Magn Reson Med* 2016 May;75:1967–77.
- 22 Parker GJM, Roberts C, Macdonald A, Buonaccorsi GA, Cheung S, Buckley DL, et al.: Experimentally-derived functional form for a population-averaged high-temporal-resolution arterial input function for dynamic contrast-enhanced MRI. *Magn Reson Med* 2006 Nov;56:993–1000.
- 23 Klein R, Klein BE, Moss SE, Davis MD, DeMets DL: The Wisconsin epidemiologic study of diabetic retinopathy. IV. Diabetic macular edema. *Ophthalmology* 1984 Dec [cited 2016 Nov 17];91:1464–74.
- 24 Paget C, Lecomte M, Ruggiero D, Wiernsperger N, Lagarde M: Modification of enzymatic antioxidants in retinal microvascular cells by glucose or advanced glycation end products. *Free Radic Biol Med* 1998 Jul 1 [cited 2016 Nov 17];25:121–9.
- 25 Aiello LP, Avery RL, Arrigg PG, Keyt BA, Jampel HD, Shah ST, et al.: Vascular endothelial growth factor in ocular fluid of patients with diabetic retinopathy and other retinal disorders. *N Engl J Med* 1994 Dec 1;331:1480–7.
- 26 Miller JW, Adamis AP, Aiello LP: Vascular endothelial growth factor in ocular neovascularization and proliferative diabetic retinopathy. *Diabetes Metab Rev* 1997 Mar [cited 2016 Nov 17];13:37–50.

- 27 Serlin Y, Levy J, Shalev H: Vascular pathology and blood-brain barrier disruption in cognitive and psychiatric complications of type 2 diabetes mellitus. *Cardiovasc Psychiatry Neurol* 2011;2011:609202.
- 28 Tomkins O, Shelef I, Kaizerman I, Eliushin A, Afawi Z, Misk A, et al.: Blood-brain barrier disruption in post-traumatic epilepsy. *J Neurol Neurosurg Psychiatry* 2008 Jul;79:774–7.
- 29 Cheung N, Mosley T, Islam A, Kawasaki R, Sharrett AR, Klein R, et al.: Retinal microvascular abnormalities and subclinical magnetic resonance imaging brain infarct: a prospective study. *Brain* 2010 Jul;133:1987–93.
- 30 Prakash R, Somanath PR, El-Remessy AB, Kelly-Cobbs A, Stern JE, Dore-Duffy P, et al.: Enhanced Cerebral but Not Peripheral Angiogenesis in the Goto-Kakizaki Model of Type 2 Diabetes Involves VEGF and Peroxynitrite Signaling. *Diabetes* 2012 Jun 1;61:1533–1542.
- 31 Shimizu F, Sano Y, Tominaga O, Maeda T, Abe M, Kanda T: Advanced glycation end-products disrupt the blood–brain barrier by stimulating the release of transforming growth factor- β by pericytes and vascular endothelial growth factor and matrix metalloproteinase-2 by endothelial cells in vitro. *Neurobiol Aging* 2013 Jul;34:1902–1912.
- 32 Cha S, Johnson G, Wadghiri YZ, Jin O, Babb J, Zagzag D, et al.: Dynamic, contrast-enhanced perfusion MRI in mouse gliomas: Correlation with histopathology. *Magn Reson Med* 2003 May;49:848–855.
- 33 Aronen HJ, Pardo FS, Kennedy DN, Belliveau JW, Packard SD, Hsu DW, et al.: High microvascular blood volume is associated with high glucose uptake and tumor angiogenesis in human gliomas. *Clin Cancer Res* 2000 Jun [cited 2017 Nov 3];6:2189–200.
- 34 Hatzoglou V, Tisnado J, Mehta A, Peck KK, Daras M, Omuro AM, et al.: Dynamic contrast-enhanced MRI perfusion for differentiating between melanoma and lung cancer brain metastases. *Cancer Med* 2017 Apr;6:761–767.

35 Yang F, Yang C, Liu Y, Peng S, Liu B, Gao X, et al.: Associations between Body Mass Index and Visual Impairment of School Students in Central China. *Int J Environ Res Public Health* 2016 Oct 18;13. DOI: 10.3390/ijerph13101024

36 Woerdeman J, van Duinkerken E, Wattjes MP, Barkhof F, Snoek FJ, Moll AC, et al.: Proliferative Retinopathy in Type 1 Diabetes Is Associated With Cerebral Microbleeds, Which Is Part of Generalized Microangiopathy. *Diabetes Care* 2014;37.

37 Fa Z, Zhang R, Li P, Zhang J, Zhang P, Zhu S, et al.: Effects of temporarily disrupting BBB on activity-induced manganese-dependent functional MRI. *Brain Imaging Behav* 2011 Sep 3;5:181–188.

SUPPLEMENTARY INFORMATION

Table-6: Prediction of visual acuity in the case study group and the negative control group by occipital and frontal blood-brain-barrier permeability parameters. (Supplementary Data)

Case Study			
Group*			
	Visual Acuity Baseline (r p-value)	Visual Acuity 12 Months (r p-value)	Visual Acuity 24 Months (r p-value)
Occipital			
K^{trans} [min ⁻¹]	-0.406 0.024	-0.324 0.061	-0.282 0.091
V_p	-0.683 0.0001	-0.605 0.001	-0.781 0.0001
Frontal			
K^{trans} [min ⁻¹]	0.110 0.304	0.240 0.129	0.164 0.221
V_p	-0.431 0.018	-0.128 0.276	-0.367 0.039
Type 2 Diabetics Without BRB			
Leakage			
	Visual Acuity Baseline (r p-value)	Visual Acuity 12 Months (r p-value)	Visual Acuity 24 Months (r p-value)

Occipital			
K^{trans} [min^{-1}]	-0.032 0.460	-0.133 0.340	0.407 0.095
V_p	-0.172 0.296	-0.171 0.297	0.332 0.146
Frontal			
K^{trans} [min^{-1}]	0.148 0.323	0.255 0.212	0.198 0.269
V_p	-0.032 0.460	-0.040 0.450	0.354 0.129

Visual acuity showed multiple statistically significant correlations with the blood-brain-barrier permeability parameter V_p from the occipital lobe. Bold and grey shadowed values survived correction for multiple comparisons.

K^{trans} : volume transfer coefficient reflecting vascular permeability.

V_p : fractional plasma volume

* Case Study Group: Type 2 Diabetics with Established blood-retinal-barrier Leakage

Chapter 3:

Occipital Cortex Disruption in Epilepsy:

Physiologic Gamma Oscillations:

Cortical functional topography of high frequency gamma activity relates to perceptual decision: an Intracranial study (Published original article)

Disruption of the GABAergic System in Drug-Resistant Epilepsy:

The impact of Cathodal tDCS on GABAergic-Inhibition Mediated Synchrony in epilepsy: a multimodal study on local epileptogenic and distant oscillatory patterns (Original article submitted to Brain)

Cortical functional topography of high frequency gamma activity relates to perceptual decision: an Intracranial study

João Castelhana^{1,2}, Isabel C. Duarte^{1,2}, Sulaiman I. Abuhaiba^{1,2}, Manuel Rito³, Francisco Sales³, Miguel Castelo-Branco^{1,2}^{✉*}

ABSTRACT

High-frequency activity (HFA) is believed to subserve a functional role in cognition, but these patterns are often not accessible to scalp EEG recordings. Intracranial studies provide a unique opportunity to link the all-encompassing range of high-frequency patterns with holistic perception. We tested whether the functional topography of HFAs (up to 250Hz) is related to perceptual decision-making. Human intracortical data were recorded (6 subjects; >250channels) during an ambiguous object-recognition task. We found a spatial topography of HFAs reflecting processing anterior dorsal and ventral streams, linked to decision independently of the type of processed object/stimulus category. Three distinct regional fingerprints could be identified, with lower gamma frequency patterns (<45Hz) dominating in the anterior semantic ventral object processing and dorsoventral integrating networks and evolving later, during perceptual decision phases, than early sensory posterior patterns (60 - 250Hz). This suggests that accurate object recognition/perceptual decision-making is related to distinct spatiotemporal signatures in the low gamma frequency range.

INTRODUCTION

Gamma-band oscillations have been proposed to play a functional role across a wide range of cognitive domains [1–4] but their physiological underpinnings remain unclear [5–8] because a significant range of oscillatory sub-bands are not accessible to scalp EEG recordings, and even when they are, the meaning of their functional topography is difficult to unravel. This is an important challenge, because the dependence on stimulus properties, general object recognition aspects and task demands [9–11] are difficult to investigate without analyzing their precise spatial correlates. Induced gamma (in a wide range of frequencies) reflects complex processing as required in perceptual decision-

making, and it is response to specific Mooney stimuli (two-tone abstract patterns depicting objects), comparing to the baseline. Hermes et al., 2014 reported a spatial distribution of increases in narrow and broadband oscillations with the broadband component being mainly located in early visual areas. Contrary to the frequently claimed stimulus specificity of the narrowband gamma oscillations, both suggested that all classes of visual stimuli induced responses in a broadband frequency range (80-200Hz) in a large portion of the fusiform gyrus and the visual cortex. Moreover, only part of the gamma activity (30 - 100Hz) is stimulus specific (and only in which concerns some types of stimuli: oriented gratings and only some natural images or Mooney objects). It is however possible, that in spite of the relative stimulus independence, such patterns may instead reflect general processing demands during perceptual decision-making and object recognition. Here we tested this hypothesis.

To test whether activity in the gamma-band represents particular signatures of specific processing modules, we investigated whether these patterns are organized in distinct spatial maps, as a function of the timing of perceptual decision-making. Although a specific functional role of distinct sub-bands has been suggested for different sources in the brain [23–26], this issue is complicated by the fact that these sub-bands are not always defined in the same manner in different studies. Our previous simultaneous EEG/fMRI study showed separate sources of distinct sub-bands but only for relatively low frequencies (30-45Hz; 60-75Hz) related either with perceptual processing or earlier visual processing [13]. Importantly, we found in this study that a gamma-band pattern around 40Hz emerged during successful perceptual decision making.

There is still a lot of controversy concerning the spatial organization of those patterns of activity and their functional relevance. While some authors reported that large increases in gamma power [27] dominate in early visual areas [10,28,29], others have suggested prominent propagation of high frequency activity (HFAs) in the visual pathway [22,24,30–32]. As reviewed by Sedley and Cunningham 2013, other studies showed that broadband gamma seems to occur in various cortical areas for incongruent stimuli while narrowband patterns only occur in visual cortex. These results seem contradictory and it is not clear which are their sources and what is their relation to task dependent information

processing [32–34] and in particular their link with perceptual decision-making. The relation to the timing of object recognition and decision is a critical aspect which was taken into account in our study design.

Invasive recordings are often used in the clinical context [30,35]. They provide a unique opportunity to measure brain signals at high temporal and spatial resolution [34,36–38]. This technique has been widely used to study high frequency activity [34,39,40] that cannot be uncovered by scalp EEG and their putative functional correlates have been widely debated [9,10,20,24,37]. Here we acquired intracranial data to test the following hypotheses: 1. high frequency activity is spatially organized across processing networks, i.e., their timing and functional topography reflect either early visual or late perceptual decision processes 2. their temporal patterning reflects specific object properties, or instead just a general recognition mechanism occurring during perceptual decision-making. These remain controversial hypotheses for which ECoG provides a unique opportunity to test, even with the limitations of available mathematical models for the analysis of high-density recordings at high spatio-temporal resolutions[41]. We acquired invasive data in six patients with refractory epilepsy and also extended the range of visual categories used in previous studies by including new ambiguous stimulus categories (faces, objects and scrambled stimuli that may also activate similar decision regions) [42], allowing to test general processes. Moreover, our setup involved a large sampling rate and explored the spatiotemporal dynamics of cortical activity up to 250Hz without the limitation of previously defined frequency sub-bands. Our results demonstrate a frequency dependent functional topography with lower frequencies dominating during perceptual decision-making and higher frequencies during early visual processing in more posterior regions. These maps show a strong and consistent region dependence during perceptual search and object recognition.

MATERIALS AND METHODS

Patients

We acquired invasive electrophysiology data from six epileptic patients (3 males and 3 females; see demographic and clinical details in [Table 1](#)) while they were performing a visual perceptual decision making task upon presentation of ambiguous stimuli (see details below). ECoG is a technique entailing data

acquisition from intracranial electrodes of surgically implanted patients with intractable epileptic seizures. The implantation of invasive electrodes is used for further localization of seizure foci and functional mapping that is not feasible when using scalp EEG. This approach enables the extraoperative functional mapping during several days. They underwent extraoperative subdural ECoG recordings as a part of pre-surgical evaluation (data acquired between 04-Feb-2015 and 20-Jan-2017) in the epilepsy unit of Coimbra University Hospital (UMES-CHUC). The study was approved by the Ethics board of the Faculty of Medicine of the University of Coimbra and has been conducted according to the principles expressed in the Declaration of Helsinki. The ethics approval covered the testing of children and written informed consent was obtained from the participants or their parents.

Electrode placement

For the invasive recordings, platinum electrodes were surgically implanted along the occipitotemporal and occipito-parietal areas (1-D strips of 8 electrodes and 2-D arrays (grids) of 2x8, 4x8 and 4x5 electrodes were used). The number and placement of the electrodes was determined by the clinical needs of the patients. To avoid movement of subdural electrodes after placement they were stitched to the edge of dura mater and digital photos were taken to confirm position of the electrodes on the 3D anatomical data acquired with MRI and CT.

Table 1. Demographic and clinical characteristics of the patients.

Case	Gender	Age	Seizure Type	Current Medication	Neuroanatomical Location of the intracranial EEG ^a
01	M	40	Focal Dyscognitive Seizures	Carbamazepine, Valproate, Zonisamide and Levetiracetam.	Left Parieto-Temporal (Subdural Grid: 48 to 60 contacts)
02	F	20		N.A.	
03	M	39		N.A.	
04	M	13		N.A.	
05	F	35		Zosimade, Levetiracetam	

06	F	30	Eslicarbazepine, Clobazam, Zonisamida	Right Parieto- Temporal (Subdural Grid: 56 contacts)
----	---	----	---	--

^a Note that five subjects have a left grid while the 6th had the grid on the right hemisphere.

Anatomical MRI, CT data and X-ray images (in which the electrodes were easily detected and localized in 3D) were acquired before and after subdural electrode placement, respectively. The individual data were then co-registered (using 3DSlicer software 4.3.0 r22408) to precisely localize the positions of the intracranial electrodes (a general registration algorithm with a linear transform was used with 6 degrees of freedom). Then, we applied a semi-automatic segmentation to extract electrode positions. The image data of the five subjects with left grids were co-registered to obtain a single map of all electrode locations (Fig 1). The data of the subject with a grid on the right hemisphere were analyzed separately.

Task description and invasive recordings

The subject was presented with four different categories of Mooney pictures. The categories included Mooney Faces, Mooney Guitars, Scrambled non-face stimuli and inverted Mooney Faces. To make the task easy to understand, for each stimulus, subjects were instructed to report if a face was present (response button 1, right hand) or not (response button 2, left hand), after stimulus offset (Fig 2). Stimuli were delivered using Presentation software (Neurobehavioral Systems). Stimulus duration was 250ms and inter-stimulus-interval varied randomly between 1900 and 2150ms. Stimulus order was randomized and the experiment was divided in three runs containing 100 stimuli per run (25 of each category). All subjects were submitted to at least 75 trials per category. Intracranial data were acquired from platinum grid electrodes at a high sampling rate (5kHz) using a 128 EEG system (SynAmps2, Compumedics, Neuroscan) used in parallel with the clinical video-EEG. No filters were applied during the recording. Data were analyzed offline.

Data analysis

Behavioral and **reaction time** data were calculated to assess the validity of the responses to the task. All subjects were able to understand and perform the task

above chance level. A Wilcoxon statistical test was applied to compare response rates per category ($p = 0.05$).

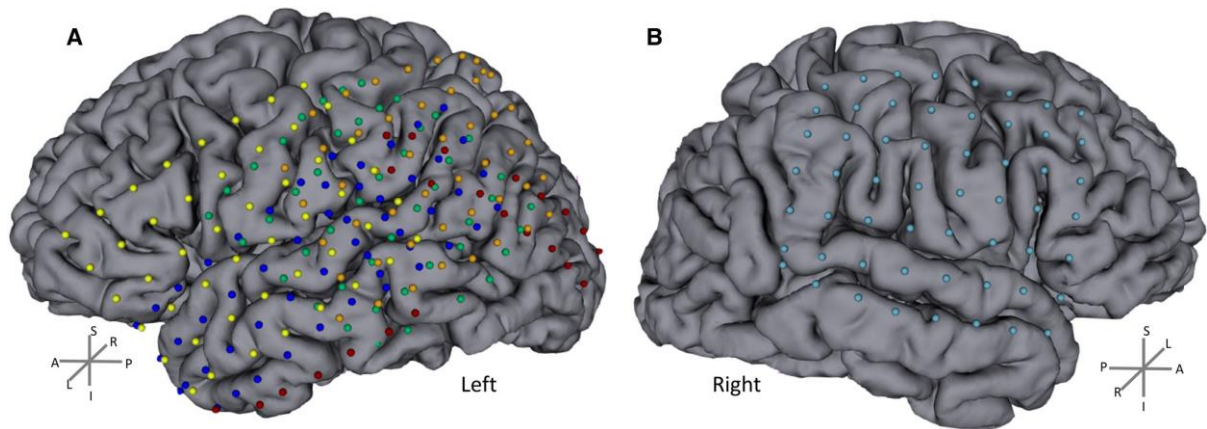


Fig 1. Electrode locations. A) 5 patients with left grids. B) 1 patient with grid on the right (subject 6). The individual anatomical (MRI and CT) data were co-registered to precisely localize the positions of the intracranial electrodes. Electrodes (represented as balls) were manually assigned after automatic electrode position segmentation. Each color represents one subject. Individual data were coregistered between the five subjects to obtain a single group map with the electrode locations. Note that there are matched electrode locations between subjects with an extensive coverage of both hemispheres. L/R, A/P and S/I stands for left/right, anterior/posterior and superior/inferior respectively.

Then, invasive data were visually assessed by an experienced epileptologist. Electrodes including epileptic spikes or artifacts were marked as bad (~20%). After artifact correction (using independent component analysis) a common average reference (excluding bad channels) was computed to avoid distributions that are biased by the location of the reference electrode [37]. Data were split into epochs locked to the beginning of the stimuli (-500 to 1500ms) and epochs with incorrect responses were discarded (on average >70% of trials remained for further analysis). The time-window before the stimulus onset was considered as baseline (-500 – 0ms) and the baseline correction was applied.

Event related spectral power (ERSP; time-frequency (TF) decomposition) analysis [43–45] was performed using the EEGLAB toolbox [46] and MATLAB v8.1 (The Mathworks, Inc.). The wavelet parameters were: 6 cycles, 250 frequency bins, 600 time points and the analysis frequency range was set to 15 to 500Hz. A notch filter was applied (45-55Hz) to avoid potential line current

artifacts. The change between post and pre-stimulus epochs was assessed. Timefrequency data per channel and subject were obtained and a semi-automatic iterative channel clustering procedure was applied based on the similarity of frequency-dependent responses to the stimuli. Briefly, we applied the k-means cluster analysis (MATLAB R2013a) to find the clusters of channels with a similar frequency dependent response (spectrum of the 0-600ms time window). The default squared Euclidean distance measure was used for clustering with input parameters $k = 3$ and 100 replicates. This clustering approach minimizes the sum, over all clusters, of the point-to-cluster centroid distances. Channels belonging to the same centroid (cluster) were concatenated per condition and analyzed together (see [Fig 3](#) and locations in “blue”, “orange” and “green” dots in results section figures).

Statistical comparisons were performed per cluster to compare the time–frequency results with the baseline and between stimulus conditions, with the alpha level set to 0.0125. A Wilcoxon rank sum test was carried out per time and frequency bin vs. baseline values.

Additionally, we computed the spectrum as given by the time-frequency transform to assess the changes during and after stimuli presentation. The group trimmed mean (10% threshold) of the activity spectrum per time-window (stimulus ON: 25-250ms; after the stimulus/decision period: 275-600ms) was computed [47] at the single trial level. The time-window was truncated at 600ms to avoid the concomitant motor response. A margin of 25ms was excluded at the beginning and end of each time-window to avoid possible edge effects of TF computation. Next, we computed the envelope (the absolute of the Hilbert transform) of the spectrum per condition and cluster of electrodes [48]. The data of the subject with a grid on the right hemisphere were analyzed separately. A statistical analysis was then performed to obtain the frequency bins where the envelope of the power was significantly different between timewindows (Stim On vs. After Stim). The `statcond()` function from EEGLAB was applied using paired t-tests with bootstrapping (2000).

The resultant P values from the `statcond` function and Wilcoxon tests were corrected for multiple comparisons using a false discovery rate (FDR) approach ($p = 0.0125$). Furthermore,



Fig 2. Task timeline: Mooney stimuli (ambiguous black and white shapes) of faces/inverted faces, guitars and scrambled pictures were presented for 250ms. Subjects had to detect a face (or not) and respond (button press) during the inter-stimulus interval (1900-2150ms). Stimulus order was randomized and the experiment was divided in three runs (100 trials per run) to avoid subject fatigue.

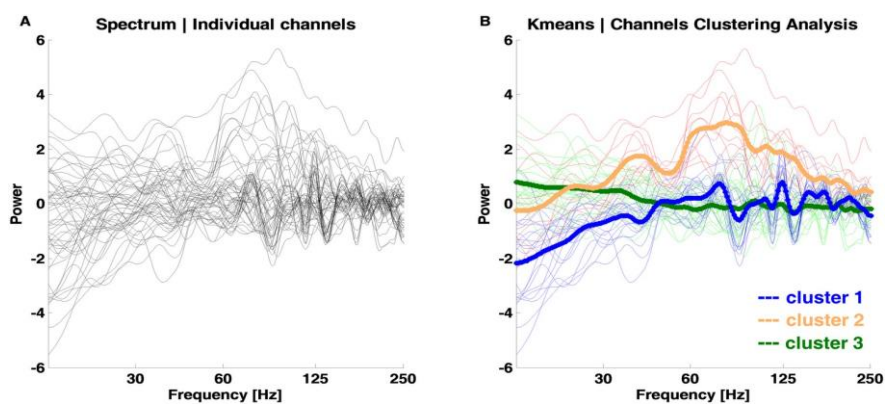


Fig 3. Channel clustering analysis of evoked frequency responses to faces.

A) Frequency response of the 0-600ms time window per channel. Black lines: individual channels over all five subjects from the left hemisphere. B) Channel clusters as computed by the semi-automatic iterative channel clustering procedure. The default Kmeans approach with squared Euclidean distance measure was computed (best sum of distances = 6796; cluster 1 blue = 2327; cluster 2 orange = 2274; cluster 3 green = 2195). Channels belonging to the same centroid (bold lines) are marked with the same line color. The locations of these channels are plotted in the results section.

to reduce the number of type-1 errors we follow the work by [49] and corrected the statistics at the cluster level based on the time-frequency adjacency (adjacent time-frequency points that all exhibit a similar difference). The time-frequency points that reached significance after FDR correction ($p < 0.0125$) and the cluster-based correction are marked in the TF and spectrum (envelop) plots (see [results](#) section). For the sake of clarity we call these significant TF clusters as 'blobs' and the similar channels are called clusters.

RESULTS

Behavioral data

We calculated the percentage of correct responses per category. All subjects were able to perform the task (discriminating between face and non-face objects) and could distinguish between face and non-face stimuli above the chance level. Behavioral data in Fig 4A show that ~80% of the faces/inverted faces were reported as 'faces' ($z = 2.201$, $p = 0.028$) while ~80% of the guitars were reported as 'not faces' ($z = 2.201$, $p = 0.028$). In the same line, scrambled stimuli (ambiguous) had reports of around 50% per response type ($z = 0.105$, $p = 0.917$) as was expected. Furthermore, response latencies (Fig 4B) were similar between stimulus categories and above 600ms after stimuli onset. In fact, concerning between category differences, only the Scrambled and Guitar categories differed in latency ($z = -2.417$, $p = 0.007$).

Evidence for a spatial map of frequency distribution during perceptual decision/object recognition

We investigated high frequency activity patterns as recorded with high spatiotemporal resolution using ECoG, during ambiguous perceptual decision making. Intracranial data analysis focused on visual processing regions covered by the occipito, parietal and temporal arrays of electrodes—corresponding to early visual and the dorsal/ventral pathways, which represent an important dichotomy in high level visual processing [50,51].

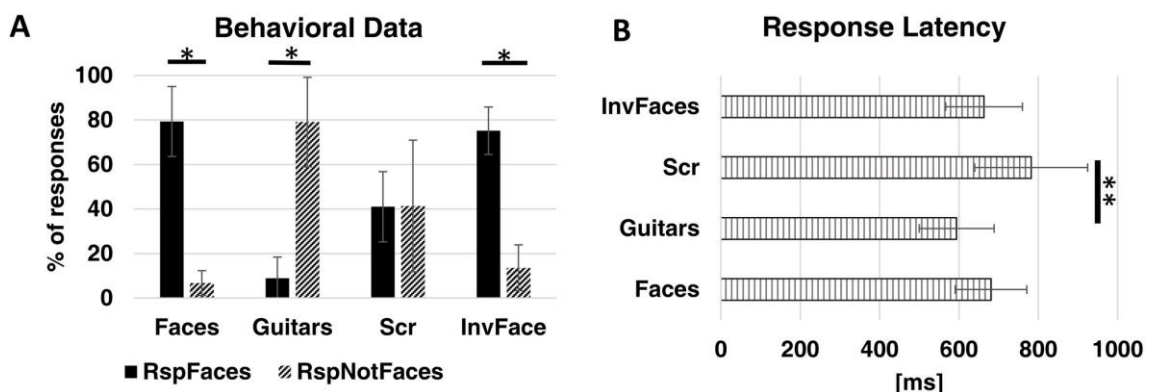


Fig 4. Behavioral results. A) Percentage of responses per stimuli category. *difference between responses per category with $p = 0.028$. B) Reaction time per stimuli condition. ** $p = 0.007$. Bars show the group average \pm SD (N = 6).

We found distinct activity patterns occurring with distinct timing during the ambiguous visual perception decision task across distinct regions in the brain. These patterns did indeed prove to be distinct in frequency and temporal onset of significantly increased activation. These effects occurred up to the upper 250Hz boundary. We performed a semi-automatic cluster analysis (see [Methods](#)) up to this frequency range. The electrodes that showed a similar type of activity between subjects were concatenated and the average TF analysis was computed. These clusters included electrodes with increased activity over 60Hz–to 250 Hz, electrodes with increased activity below 45Hz and electrodes with decreased activity in the beta band. The topography of these high-frequency activity is shown in [Fig 5A](#). We found a clear superior central region for the decreased beta activity as shown in electrodes labeled in blue. The early pattern of increase of higher frequencies (>60Hz–up to 250 Hz) is found in the posterior region electrodes related to early visual regions (labeled in “orange” dots). Moreover, the electrodes that represent the more anterior ventral visual processing pathways have increased later on (during perceptual decision) activation for the lower frequencies (“green” dots). These activity patterns are summarized in [Fig 5B](#) as a cluster average for the Mooney Faces category. A black line is shown to depict the TF blobs that activate significantly (FDR and cluster-based corrected for multiple comparisons) for each electrode cluster (‘blue’ $-5.39 < z < -3.12$, $6.8E-8 < p < 0.0017$; ‘orange’, $3.11 < z < 4.64$, $3.39E6 < p < 0.0018$; ‘green’, $3.09 < z < 5.40$, $6.8E-8 < p < 0.0019$). These results could be generalized for the other stimulus categories and subject 6 (who was recorded in the opposite hemisphere, see [Fig 1](#) and Figure B in [S1 File](#)). No significant differences were found between stimulus conditions after correction for multiple comparisons, suggesting that the observed topography is indeed related to general object processing mechanisms. It is important to note that lower frequencies emerge at anterior locations during late decision periods while higher frequencies are found for early visual stimulation periods at posterior sites (see next section). This is valid for all the six subjects and electrodes marked (individual graphs available upon request).

High and low-frequency patterns show a distinct spatiotemporal topographic map during perceptual decision making

To further clarify the relation of the distinct frequency band patterns with perceptual decision, the average envelope of ERS/ERSP per conditions was computed for two distinct time-windows. A statistical t-test with bootstrapping (2000) was performed (including FDR $p < 0.0125$ and cluster-based correction for multiple comparisons) to compare the activity during and after stimulus presentation (during decision) per frequency bin. The spectrum per time-window /conditions / cluster are shown in [Fig 6](#). We found a clear temporal pattern for the visual perception task, with power increasing at frequencies up to 250Hz in posterior electrodes (“orange”) for all stimulus conditions during the initial stimulus presentation period ($1.60 < t < 5.91$, $0.0005 < p < 0.0065$). For the time after stimulus offset (corresponding to the decision period), the activity at posterior electrodes (“orange”) is maintained while activity for lower frequencies ($< 45\text{Hz}$) is mainly increased at anterior electrodes (“green” and “blue”), corroborating the notion that lower frequencies are tightly linked with the decision phase at anterior ventral object recognition related regions. Note that “blue” electrodes show a decreased activity (in spite of high magnitude; $1.85 < t < 7.04$, $0.0005 < p < 0.0065$) while the “green” ones show increased activity (as well as high magnitude; $1.88 < t < 5.75$, $0.0005 < p < 0.0065$) at lower frequencies during the decision phase. The envelope of the spectrum is plotted in [Fig 6](#) for each category and time-window showing the distinct temporal pattern of the lower frequencies in the three electrode clusters (detailed statistical output is shown in Table A in [S1 File](#)). Notably, the small standard deviation demonstrates that this holds true for all the individual subjects. The results for the subject 6 (right subdural grid; summarized in Figure B in [S1 File](#)) show a similar pattern of high frequency topography and temporal mapping for the ‘blue’ and ‘green’ clusters.

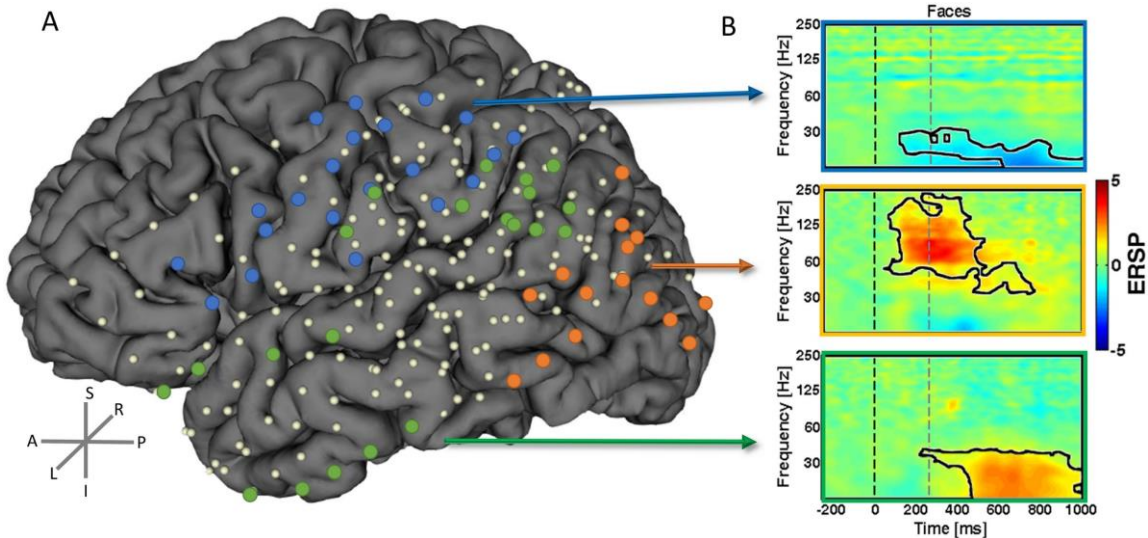


Fig 5. The topography of high frequency oscillations. We found distinct high frequency activity patterns during the ambiguous object recognition/perceptual decision task. The position of the electrodes per subject belonging to each of the clusters were marked as dots (in three distinct colors) in the coregistered brain. These patterns have distinct sources in the brain as represented by the correspondent dots. B) The example TF plots are a group average of all the *represented electrodes of that cluster* ($N = 3$ subjects for “blue” labels; $N = 4$ subjects for “orange” and “green” labels). Data (dB) are presented for the Mooney faces condition but these results could be generalized for the other conditions (see Figure A in [S1 File](#)). The black line segmented “blobs” in the plots depict the TF spectral–temporal patterns which are significant (blue $z = -3.12$, $p < 0.0017$; orange, $z = 3.11$, $p < 0.0018$; green, $z = 3.09$, $p < 0.0019$). The dashed lines mark the start and end of stimulus. White dots represent the contacts of the different grids co-registered in same space.

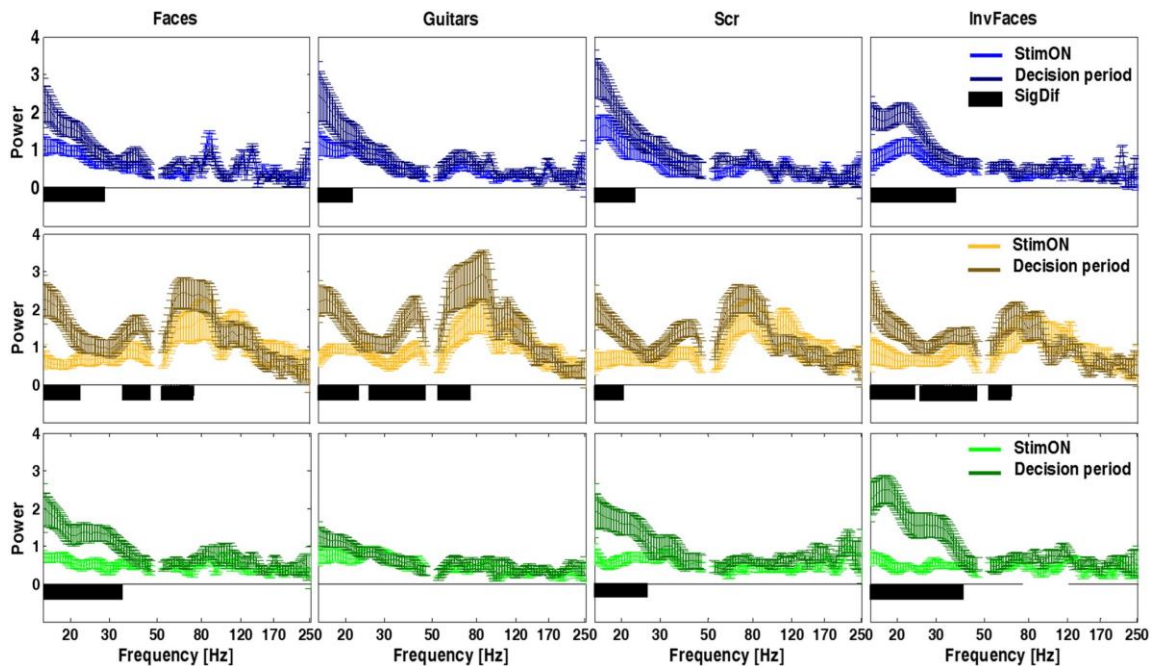


Fig 6. Analysis of Power per electrode cluster and condition reveals a temporal pattern of differences in power, with anterior object recognition regions showing increased decision related low frequency activity patterns. Cluster averaged power is plotted with standard deviation. Notably lower frequency band activation emerges after stimulus offset (decision period) for the more anterior *electrodes* (“green” and “blue”). *Color lines* (horizontal panels) represent the three clusters of electrodes. The more posterior channels (“orange” labels) have the main pattern increase at high gamma in contrast to the other locations. Black bars in the plots indicate the significant differences between time-windows ($p < 0.0065$; detailed statistical values are reported in Table A in S1 file). No difference was found across stimuli conditions, suggesting that the observed regional patterns reflect a general object recognition mechanism.

DISCUSSION

We were able to demonstrate a distinct topographic map of low (< 45 Hz) and high (up to 250 Hz) frequency activation patterns during a perceptual decision making task. The former were present in ventral anterior regions during the decision period and the later dominated early on during visual stimulation. These results are consistent with the notion distinct frequency bands have distinct sources and functional significance [13,27,37] and establish that they may be

organized in spatiotemporal maps [23] during perceptual decision-making and object recognition.

ECoG has been widely used to study high frequency oscillations [39,40]. Here we explicitly tested whether hierarchical visual processing streams relate differently to low and high temporal frequency patterns. To address this issue we took advantage of the opportunity to perform ECoG mapping in six patients with refractory epilepsy and explored the spatiotemporal dynamics of cortical high gamma-band activity during holistic visual perceptual decision-making. We used Mooney stimuli which are known to generate a state of perceptual ambiguity during object recognition [42].

Distinct spatial and temporal maps of high frequency activity

Previous reports suggested a functional dissociation between low and high gamma sub-bands [5,28,52,53] with distinct sources and cognitive functions [13,23,34]. Lachaux et al. 2005 showed an increase of gamma oscillations between 50 and 150Hz in response to particular Mooney stimuli, as compared to the baseline. All classes of stimuli activated a wide portion of the fusiform gyrus and the visual cortex. Castelhana et al., 2014 had suggested, using EEG/ fMRI, that frequency patterns < 45 Hz were related to perceptual decision-making, which could now explicitly test at the ECoG level.

We now provide evidence for topographic organization of visual sensory and perceptual processing and establish that these are related to a general object processing mechanism. We used a broad range of new ambiguous stimulus categories (faces, objects and scrambled stimuli that may also activate similar decision regions) [42] which allowed for generalization. Moreover, our setup comprised a higher sampling rate and explored the spatiotemporal dynamics of a broad range of cortical activity over an extensive part of the cortical mantle within whole hemispheres.

The frequency dependent spatial patterning can be summarized as follows: the low gamma and beta activity spatially involved mainly anterior regions (ventral and regions involved in dorsoventral integration) during perceptual-decision and object recognition while the higher frequencies (up to 250Hz) are increased at posterior areas [24] early on during sensory processing. Moreover, we show (Figure C in [S1 File](#)) that it is unlikely these patterns are due to epilepsy activity.

These patterns are very variable and our results are an average of many trials time-locked to a stimulus event, thus rendering that influence almost null. Additionally note no overlap between the SOZ electrodes and the ones we reported as a source of the different clusters (see Figure C in [S1 File](#)). Our previous studies, ranging from single EEG, simultaneous EEG/fMRI in normal subjects and neurodevelopmental disorders provided evidence along these lines [[7,8,26](#)], in particular the link of decision processes with lower frequencies (<45 Hz), but could neither provide evidence for topographic clustering nor for exact sources. Given that many cognitive processes elicit augmentation of gamma activity [[12,20,34,54](#)] involving occipital, occipito-temporal and other inferior-frontal regions [[9,37,47,55,56](#)] invasive studies are valuable in pinpointing their neural underpinnings in a more precise way [[34](#)]. This is also emphasized by the need to parse the different number of possible processing nodes that are activated by specific stimulus categories (including faces and other impoverished stimuli) and cognitive processes and which modulate over a wide range of frequencies (up to 100Hz) [[11,47](#)].

Some evidence is available pointing to a distinction between sub-bands or differences in broad vs. sharp band patterns across different types of paradigms [[13,23,27,37](#)]. They appear to be functionally distinct and previous studies have also suggested that information is transmitted across neural networks in a variety of frequencies in the high-gamma range [[10,37,57](#)]. These and other studies have expanded the scientific interest on the relevant biological rhythms to very high frequency bands (>500 Hz) [[19,22,58](#)]. However, high-gamma power changes were recognized to not modulate uniformly across a wide range of frequencies (60 - 500Hz) and locations [[22](#)]. Moreover, reliable evidence for gamma patterning has been proven only for some stimuli (gratings or natural pictures) [[10,55](#)]. In this line, there is still ongoing controversy about the sources of gamma oscillations and mechanisms that generate them as a function of the cognitive process in given cortical loci [[10,20,21,32](#)].

Here we found a perceptual-decision related graded posterior-anterior sharpening of frequency band response amplitudes and their respective sources at the cortical surface level. We provided evidence that this occurs at distinct frequencies and as a function of the cognitive moment (visual processing or

decision). In addition, we analyzed every frequency bin in an unbiased manner without any sort of selection. de Pestors et al. 2016 had suggested possible sources of distinct oscillatory patterns within the beta and gamma ranges and we now show a topographic dichotomy with defined functional significance. This is in line with previous EEG/fMRI evidence suggesting that lower frequency patterns are relevant during the decision period, irrespective of the object category. Additionally, we found a spatial map of decreased beta activity located at anterior motor areas. We thus suggest a posterior-anterior topographic pattern reflecting a processing hierarchy, from early visual procession to decision and object recognition.

This pattern of temporal and location precedence and dynamics of information processing is consistent with the known hierarchy of visual processing in the anterior dorsal/ventral streams. Given their close relationship to neuronal spiking, this ubiquity of high-frequency patterns, suggests that high-gamma may convey general mechanisms of cortical information transmission [16], namely object recognition. Our data, showing temporal dephasing of these patterns, are consistent with previous time-frequency analyses showing that high and low gamma power may be anti-correlated [27]. We postulate that this also holds true for each particular electrode location. Although these conclusions maybe limited by the limited sample size of invasive studies (six participants in our case), it suggests (with the added value of very high spatiotemporal resolution) that a distinct functional topographic map is present for different frequencies during visual perceptual decision-making. These results show that it is possible to parse the neural sources of high-gamma activity patterns during relatively complex tasks such as perceptual decision-making.

In sum, we have found a frequency dependent spatial patterning during object recognition, which is independent of the particular object category, suggesting a general processing mechanism. The perceptual search for an object and ensuing recognition seems to generate distinct spatio-temporal signatures during visual processing and decision. We thus found evidence in favor of the hypothesis that high frequency activity (up to 250 Hz) are spatially and temporally organized in three clusters (posterior and anterior ventral and dorsoventral) as a function of visual processing and perceptual demands.

To our knowledge, this is the first time that such a functional topographic map is shown in relation to accurate perceptual decision. Furthermore, we show also a time and space dependent (as a function of early visual processing vs. high level decision) patterning of high frequency gamma **activity**. The clear posterior-anterior pattern is consistent with hierarchical processing schemes from posterior to visual anterior dorsal/ventral streams and suggests that such object recognition related patterns are region and local connectivity dependent irrespective of the processed category.

ACKNOWLEDGMENTS

We would like to thank the patients for their willingness to participate in this study and all the team in the epilepsy unit for their help. We thank Michael Wibrál for providing the Mooney stimuli.

REFERENCES

1. Tallon-Baudry C. The roles of gamma-band oscillatory synchrony in human visual cognition. *Front Biosci.* 2009; 14: 321–32. Available: <http://www.ncbi.nlm.nih.gov/pubmed/19273069>
2. Güntekin B, Başar E. A review of brain oscillations in perception of faces and emotional pictures. *Neuropsychologia.* 2014; 58: 33–51. <https://doi.org/10.1016/j.neuropsychologia.2014.03.014> PMID: [24709570](https://pubmed.ncbi.nlm.nih.gov/24709570/)
3. Fries P, Nikolić D, Singer W. The gamma cycle. *Trends Neurosci.* 2007; 30: 309–16. <https://doi.org/10.1016/j.tins.2007.05.005> PMID: [17555828](https://pubmed.ncbi.nlm.nih.gov/17555828/)
4. Başar E. A review of gamma oscillations in healthy subjects and in cognitive impairment. *Int J Psychophysiol.* 2013; 90: 99–117. <https://doi.org/10.1016/j.ijpsycho.2013.07.005> PMID: [23892065](https://pubmed.ncbi.nlm.nih.gov/23892065/)
5. Uhlhaas PJ, Pipa G, Neuenschwander S, Wibrál M, Singer W. A new look at gamma? High- (>60 Hz) γ band activity in cortical networks: function, mechanisms and impairment. *Prog Biophys Mol Biol.* Elsevier Ltd; 2011; 105: 14–28. <https://doi.org/10.1016/j.pbiomolbio.2010.10.004> PMID: [21034768](https://pubmed.ncbi.nlm.nih.gov/21034768/)
6. Sun L, Gruetzner C, Bölte S, Wibrál M, Tozman T, Schlitt S, et al. Impaired gamma-band activity during perceptual organization in adults with autism spectrum disorders: evidence for dysfunctional network activity in frontal-

posterior cortices. *J Neurosci*. 2012; 32: 9563–73. <https://doi.org/10.1523/JNEUROSCI.1073-12.2012> PMID: [22787042](https://pubmed.ncbi.nlm.nih.gov/22787042/)

7. Castelhana J, Rebola J, Leitão B, Rodriguez E, Castelo-Branco M. To Perceive or Not Perceive: The Role of Gamma-band Activity in Signaling Object Percepts. Ward LM, editor. *PLoS One*. 2013; 8: e66363. <https://doi.org/10.1371/journal.pone.0066363> PMID: [23785494](https://pubmed.ncbi.nlm.nih.gov/23785494/)

8. Bernardino I, Castelhana J, Farivar R, Silva EDED, Castelo-Branco M. Neural correlates of visual integration in Williams syndrome: Gamma oscillation patterns in a model of impaired coherence. *Neuropsychologia*. Elsevier; 2013; 51: 1287–1295. <https://doi.org/10.1016/j.neuropsychologia.2013.03.020> PMID: [23587664](https://pubmed.ncbi.nlm.nih.gov/23587664/)

9. Cho-Hisamoto Y, Kojima K, Brown EC, Matsuzaki N, Asano E. Gamma activity modulated by naming of ambiguous and unambiguous images: Intracranial recording. *Clin Neurophysiol. International Federation of Clinical Neurophysiology*; 2015; 126: 17–26. <https://doi.org/10.1016/j.clinph.2014.03.034> PMID: [24815577](https://pubmed.ncbi.nlm.nih.gov/24815577/)

10. Hermes D, Miller KJ, Wandell BA, Winawer J. Stimulus Dependence of Gamma Oscillations in Human Visual Cortex. *Cereb Cortex*. 2015; 25: 2951–2959. <https://doi.org/10.1093/cercor/bhu091> PMID: [24855114](https://pubmed.ncbi.nlm.nih.gov/24855114/)

11. Jerbi K, Ossandón T, Hamame´ CMCM, Senova S, Dalal SSSS, Jung J, et al. Task-related gammaband dynamics from an intracerebral perspective: Review and implications for surface EEG and MEG. *Hum Brain Mapp. Wiley Online Library*; 2009; 30: 1758–1771. <https://doi.org/10.1002/hbm.20750> PMID: [19343801](https://pubmed.ncbi.nlm.nih.gov/19343801/)

12. Pelt S Van, Schoffelen J, Kennedy H, Fries P, Michalareas G, Vezoli J, et al. Alpha-Beta and Gamma Rhythms Subserve Feedback and Feedforward Influences among Human Visual Cortical Areas. *Neuron*. Elsevier; 2016; 89: 1–14. <https://doi.org/10.1016/j.neuron.2015.12.018> PMID: [26777277](https://pubmed.ncbi.nlm.nih.gov/26777277/)

13. Castelhana J, Duarte IC, Wibrál M, Rodriguez E, Castelo-Branco M. The dual facet of gamma oscillations: Separate visual and decision making circuits as

revealed by simultaneous EEG/fMRI. *Hum Brain Mapp.* 2014; 35: 5219–5235. <https://doi.org/10.1002/hbm.22545> PMID: 24839083

14. Gray CM, Singer W. Stimulus-specific neuronal oscillations in orientation columns of cat visual cortex. *Proc Natl Acad Sci U S A.* 1989; 86: 1698–702. Available: <http://www.pubmedcentral.nih.gov/articlerender.fcgi?artid=286768&tool=pmcentrez&rendertype=abstract> PMID: 2922407

15. Singer W. Neuronal Synchrony: A Versatile Code for the Definition of Relations? *Neuron.* 1999; 24: 49–65. PMID: 10677026

16. Ray S, Crone N, Niebur E, Franzaszczuk PJ, Hsiao SS. Neural correlates of high-gamma oscillations (60–200 Hz) in macaque local field potentials and their potential implications in electrocorticography. *J Neurosci.* 2008; 28: 11526–11536. <https://doi.org/10.1523/JNEUROSCI.2848-08.2008> PMID: 18987189

17. Crone NE, Hao L, Hart J, Boatman D, Lesser RP, Irizarry R, et al. Electrocorticographic gamma activity during word production in spoken and sign language. *Neurology.* 2001; 57: 2045–2053. PMID: 11739824

18. Crone NE, Boatman D, Gordon B, Hao L. Induced electrocorticographic gamma activity during auditory perception. *Clin Neurophysiol.* 2001; 112: 565–582. [https://doi.org/10.1016/S1388-2457\(00\)00545-9](https://doi.org/10.1016/S1388-2457(00)00545-9) PMID: 11275528

19. Edwards E, Soltani M, Deouell LYLY, Berger MSMS, Knight RTRT. High gamma activity in response to deviant auditory stimuli recorded directly from human cortex. *J Neurophysiol. Am Physiological Soc;* 2005; 94: 4269. <https://doi.org/10.1152/jn.00324.2005> PMID: 16093343

20. Lachaux J-P, George N, Tallon-Baudry C, Martinerie J, Hugueville L, Minotti L, et al. The many faces of the gamma band response to complex visual stimuli. *Neuroimage.* 2005; 25: 491–501. <https://doi.org/10.1016/j.neuroimage.2004.11.052> PMID: 15784428

21. Tallon-Baudry C, Bertrand O, Hénaff M-A, Isnard J, Fischer C. Attention modulates gamma-band oscillations differently in the human lateral occipital

cortex and fusiform gyrus. *Cereb Cortex*. 2005; 15: 654–62. <https://doi.org/10.1093/cercor/bhh167> PMID: 15371290

22. Gaona CM, Sharma M, Freudenburg Z V, Breshears JD, Bundy DT, Roland J, et al. Nonuniform highgamma (60–500 Hz) power changes dissociate cognitive task and anatomy in human cortex. *J Neurosci*. 2011; 31: 2091–2100. <https://doi.org/10.1523/JNEUROSCI.4722-10.2011> PMID: 21307246

23. Wyart V, Tallon-Baudry C. Neural dissociation between visual awareness and spatial attention. *J Neurosci*. 2008; 28: 2667–79. <https://doi.org/10.1523/JNEUROSCI.4748-07.2008> PMID: 18322110

24. Nagasawa T, Juha' sz C, Rothermel R, Hoechstetter K, Sood S, Asano E. Spontaneous and visually driven high-frequency oscillations in the occipital cortex: intracranial recording in epileptic patients. *Hum Brain Mapp*. 2012; 33: 569–83. <https://doi.org/10.1002/hbm.21233> PMID: 21432945

25. Harvey BM, Vansteensel MJ, Ferrier CH, Petridou N, Zuiderbaan W, Aarnoutse EJ, et al. Frequency specific spatial interactions in human electrocorticography: V1 alpha oscillations reflect surround suppression. *Neuroimage*. Elsevier Inc.; 2013; 65: 424–32. <https://doi.org/10.1016/j.neuroimage.2012.10.020> PMID: 23085107

26. Castelhana J, Bernardino I, Rebola J, Rodriguez E, Castelo-branco M. Oscillations or Synchrony? Disruption of Neural Synchrony despite Enhanced Gamma Oscillations in a Model of Disrupted Perceptual Coherence. *J Cogn Neurosci*. 2015; 27: 2416–2426. https://doi.org/10.1162/jocn_a_00863 PMID: 26284991

27. Ray S, Maunsell JHR. Different origins of gamma rhythm and high-gamma activity in macaque visual cortex. *PLoS Biol*. 2011; 9: e1000610. <https://doi.org/10.1371/journal.pbio.1000610> PMID: 21532743

28. Hoogenboom N, Schoffelen J-M, Oostenveld R, Parkes LM, Fries P. Localizing human visual gammaband activity in frequency, time and space. *Neuroimage*. 2006; 29: 764–73. <https://doi.org/10.1016/j.neuroimage.2005.08.043> PMID: 16216533

29. Matsuzaki N, Schwarzlose RF, Nishida M, Ofen N, Asano E. Upright face-preferential high-gamma responses in lower-order visual areas: Evidence from intracranial recordings in children. *Neuroimage*. Elsevier Inc.; 2015; 109: 249–259. <https://doi.org/10.1016/j.neuroimage.2015.01.015> PMID: 25579446
30. Nagasawa T, Matsuzaki N, Juha'sz C, Hanazawa A, Shah A, Mittal S, et al. Occipital gamma-oscillations modulated during eye movement tasks: Simultaneous eye tracking and electrocorticography recording in epileptic patients. *Neuroimage*. Elsevier B.V.; 2011; 58: 1101–9. <https://doi.org/10.1016/j.neuroimage.2011.07.043> PMID: 21816225
31. Dalal SS, Guggisberg AG, Edwards E, Sekihara K, Findlay AM, Canolty RT, et al. Spatial localization of cortical time-frequency dynamics. *Conf Proc IEEE Eng Med Biol Soc*. 2007; 2007: 4941–4. <https://doi.org/10.1109/IEMBS.2007.4353449> PMID: 18003115
32. Asano E, Nishida M, Fukuda M, Rothermel R, Juha'sz C, Sood S. Differential visually-induced gammaoscillations in human cerebral cortex. *Neuroimage*. 2009; 45: 477–489. <https://doi.org/10.1016/j.neuroimage.2008.12.003> PMID: 19135157
33. Sedley W, Cunningham MO. Do cortical gamma oscillations promote or suppress perception? An under-asked question with an over-assumed answer. *Front Hum Neurosci*. 2013; 7: 595. <https://doi.org/10.3389/fnhum.2013.00595> PMID: 24065913
34. de Pestors A, Coon WG, Brunner P, Gunduz A, Ritaccio AL, Brunet NM, et al. Alpha power indexes task-related networks on large and small scales: A multimodal ECoG study in humans and a nonhuman primate. *Neuroimage*. Elsevier B.V.; 2016; 134: 122–131. <https://doi.org/10.1016/j.neuroimage.2016.03.074> PMID: 27057960
35. Wyler A, Ojemann G a, Lettich E, Ward A. Subdural strip electrodes for localizing epileptogenic foci. *J Neurosurg*. 1984; 60: 1195–1200. <https://doi.org/10.3171/jns.1984.60.6.1195> PMID: 6726363

36. Lee HW, Youngblood MW, Farooque P, Han X, Jhun S, Chen WC, et al. Seizure localization using three-dimensional surface projections of intracranial EEG power. *Neuroimage*. Elsevier Inc.; 2013; 83:616–26. <https://doi.org/10.1016/j.neuroimage.2013.07.010> PMID: 23850575
37. Crone N, Sinai A, Korzeniewska A. High-frequency gamma oscillations and human brain mapping with electrocorticography. *Prog Brain Res*. 2006; 159: 275–295. [https://doi.org/10.1016/S0079-6123\(06\)59019-3](https://doi.org/10.1016/S0079-6123(06)59019-3) PMID: 17071238
38. Duarte IC, Castelhana J, Sales F, Castelo-Branco M. The anterior versus posterior hippocampal oscillations debate in human spatial navigation: Evidence from an electrocorticographic case study. *Brain and Behavior*. Sep 2016: e00507. <https://doi.org/10.1002/brb3.507> PMID: 27688937
39. Jacobs J, Staba R, Asano E, Otsubo H, Wu JY, Zijlmans M, et al. High-frequency oscillations (HFOs) in clinical epilepsy. *Prog Neurobiol*. 2012; 98: 302–15. <https://doi.org/10.1016/j.pneurobio.2012.03.001> PMID: 22480752
40. Kucewicz MT, Cimbalnik J, Matsumoto JY, Brinkmann BH, Bower MR, Vasoli V, et al. High frequency oscillations are associated with cognitive processing in human recognition memory. *Brain*. 2014; 2231–2244. <https://doi.org/10.1093/brain/awu149> PMID: 24919972
41. Navarrete M, Pyrzowski J, Corlier J, Valderrama M, Le Van Quyen M. Automated detection of high-frequency oscillations in electrophysiological signals: Methodological advances. *J Physiol Paris*. 2017; <https://doi.org/10.1016/j.jphysparis.2017.02.003> PMID: 28235667
42. Mooney CM. Age in the development of closure ability in children. *Can J Psychol*. 1957; 11: 219–26. Available: <http://www.ncbi.nlm.nih.gov/pubmed/13489559> PMID: 13489559
43. Lachaux JP, Rodriguez E, Martinerie J, Varela FJ. Measuring phase synchrony in brain signals. *Hum Brain Mapp*. 1999; 8: 194–208. Available: <http://www.ncbi.nlm.nih.gov/pubmed/10619414> PMID: 10619414

44. Rodriguez E, George N, Lachaux JP, Martinerie J, Renault B, Varela FJ. Perception's shadow: long-distance synchronization of human brain activity. *Nature*. 1999; 397: 430–3. <https://doi.org/10.1038/17120> PMID: 9989408
45. Uhlhaas PJ, Linden DEJ, Singer W, Haenschel C, Lindner M, Maurer K, et al. Dysfunctional long-range coordination of neural activity during Gestalt perception in schizophrenia. *J Neurosci*. 2006; 26: 8168–75. <https://doi.org/10.1523/JNEUROSCI.2002-06.2006> PMID: 16885230
46. Delorme A, Makeig S. EEGLAB: an open source toolbox for analysis of single-trial EEG dynamics including independent component analysis. *J Neurosci Methods*. 2004; 134: 9–21. <https://doi.org/10.1016/j.jneumeth.2003.10.009> PMID: 15102499
47. Engell AD, McCarthy G. The relationship of γ oscillations and face-specific ERPs recorded subdurally from occipitotemporal cortex. *Cereb Cortex*. 2011; 21: 1213–21. <https://doi.org/10.1093/cercor/bhq206> PMID: 20961973
48. Davis JJ, Kozma R. Sensitivity analysis of Hilbert transform with band-pass FIR filters for robust brain computer interface. 2014 IEEE Symp Comput Intell Brain Comput Interfaces. IEEE; 2014; 16–23. <https://doi.org/10.1109/CIBCI.2014.7007787>
49. Maris E, Oostenveld R. Nonparametric statistical testing of EEG- and MEG-data. *J Neurosci Methods*. 2007; 164: 177–190. <https://doi.org/10.1016/j.jneumeth.2007.03.024> PMID: 17517438
50. Farivar R. Dorsal-ventral integration in object recognition. *Brain Res Rev*. Elsevier B.V.; 2009; 61: 144–53. <https://doi.org/10.1016/j.brainresrev.2009.05.006> PMID: 19481571
51. Mishkin M, Ungerleider L, Macko K. Object vision and spatial vision: two cortical pathways. *Trends Neurosci*. 1983; 414–417. Available: <http://www.sciencedirect.com/science/article/pii/016622368390190X>
52. Lee B, Park KS, Kang D-H, Kang KW, Kim YY, Kwon JS. Generators of the gamma-band activities in response to rare and novel stimuli during the

auditory oddball paradigm. *Neurosci Lett.* 2007; 413: 210–5. <https://doi.org/10.1016/j.neulet.2006.11.066> PMID: 17208373

53. Gruber T, Maess B, Trujillo-Barreto NJ, Müller MM. Sources of synchronized induced gamma-band responses during a simple object recognition task: A replication study in human MEG. *Brain Res. Elsevier*; 2008; 1196: 74–84. <https://doi.org/10.1016/j.brainres.2007.12.037> PMID: 18234156

54. Uhlhaas PJ, Pipa G, Lima B, Melloni L, Neuenschwander S, Nikolić D, et al. Neural synchrony in cortical networks: history, concept and current status. *Front Integr Neurosci.* 2009; 3: 17. <https://doi.org/10.3389/neuro.07.017.2009> PMID: 19668703

55. Hermes D, Miller KJ, Wandell B a, Winawer J. Gamma oscillations in visual cortex: the stimulus matters. *Trends Cogn Sci.* 2014; <https://doi.org/10.1016/j.tics.2014.12.009> PMID: 25575448

56. Vansteensel MJ, Bleichner MG, Freudenburg Z V., Hermes D, Aarnoutse EJ, Leijten FSS, et al. Spatiotemporal characteristics of electrocortical brain activity during mental calculation. *Hum Brain Mapp.* 2014; 5920: 5903–5920. <https://doi.org/10.1002/hbm.22593> PMID: 25044370

57. Fries P, Scheeringa R, Oostenveld R. Finding gamma. *Neuron.* 2008; 58: 303–5. <https://doi.org/10.1016/j.neuron.2008.04.020> PMID: 18466741

58. Crone NE, Korzeniewska A, Franaszczuk PJ. Cortical γ responses: searching high and low. *Int J Psychophysiol. Elsevier B.V.*; 2011; 79: 9–15. <https://doi.org/10.1016/j.ijpsycho.2010.10.013> PMID: 21081143

SUPPORTING INFORMATION

Figure A in S1 File. Group Average Time-frequency activity per condition. Event-related spectral power (dB) were computed in EEGLAB per subject and condition. This figure summarizes the TF results per condition and cluster of electrodes (three horizontal panels with distinct colors). The black lines mark the time-frequency blobs that are significantly different from the baseline ($p < 0.0065$; Wincoxon Rank Sum test with FDR and cluster based correction for multiple comparisons). The detailed statistical values of the significant TF blobs are

reported in Table A in S1 File. The dashed lines mark the start and end of the stimulus presentation. Figure B in S1 File. Time-frequency results for the individual subject 6 (right subdural grid). A) Semi-automatic clustering of the spectrum per channel. 2 channel clusters are identified (best sumd = 454.58). B) Time-frequency plots and source locations for the two clusters of channels. Data (dB) are a cluster average for the Mooney faces condition (similar results are found for the other conditions). The dashed lines mark the start and end of stimulus and the black line signal the TF blobs significantly different from the baseline (blue cluster $p < 0.000621$; green cluster $p < 0.001165$). C) The power envelope of distinct time-windows and clusters of electrodes for the faces condition (mean \pm SD). Lower frequencies have higher power after stimulus offset. Horizontal black bar indicate the significant differences (blue cluster $2.455 < t < 8.5673$, $0.005 < p < 0.0065$; green cluster $1.594 < t < 6.5324$, $0.0035 < p < 0.0085$). Figure C in S1 File. Locations of the epilepsy related electrodes superimposed in the results image. The 'red labeled' electrodes represent the SOZ electrodes across all subjects while the others are the ones reported in our results. Note that there is no overlap because we did not include these 'bad electrodes' in the analysis. A normalized time-frequency activity (group average of these SOZ electrodes) locked to the Mooney faces stimuli is also shown. Table A in S1 File. Statistical results. The statistical test results are reported per condition and cluster of electrodes for the two main comparisons. Wilcoxon rank sum comparison of TF data with the baseline. T-test with bootstrap (2000) comparison of the spectrum per time-window (Stim On vs. Decision Period). The max and minimum values of significant blobs are reported (FDR and cluster-based corrected $p = 0.0125$).

Supplementary Material

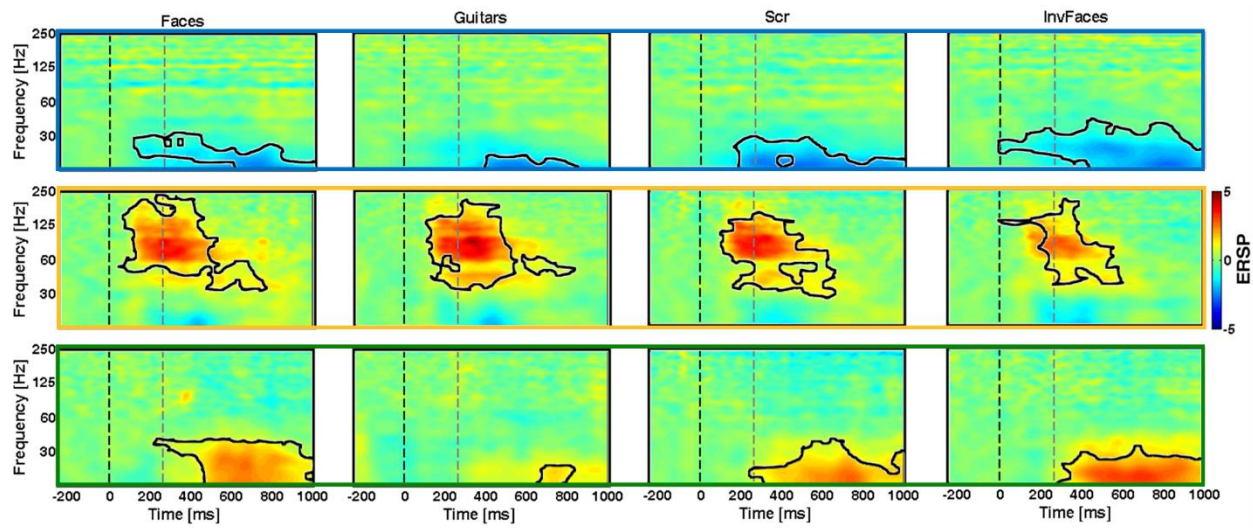


Figure A. Group Average Time-frequency activity per condition. Event-related spectral power (dB) were computed in EEGLAB per subject and condition. This figure summarizes the TF results per condition and cluster of electrodes (three horizontal panels with distinct colors). The black lines mark the time-frequency blobs that are significantly different from the baseline ($p < 0.0065$; Wincoxon Rank Sum test with FDR and cluster based correction for multiple comparisons). The detailed statistical values of the significant TF blobs are reported in S1 Table. The dashed lines mark the start and end of the stimulus presentation.

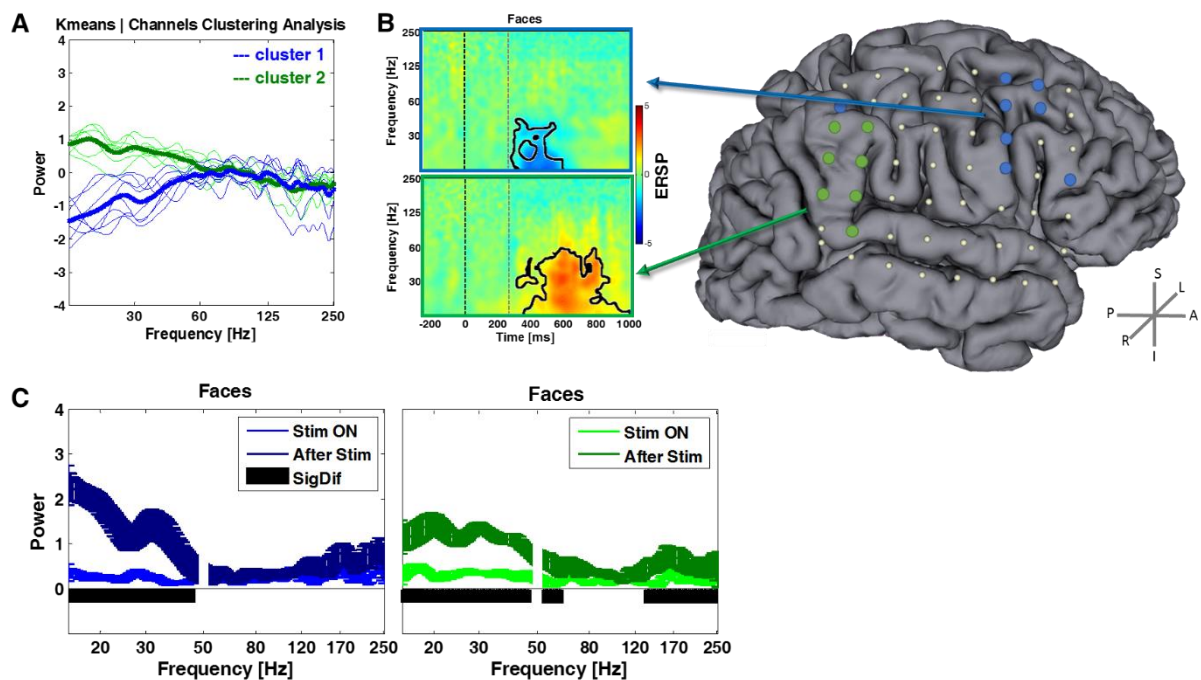


Figure B. Time-frequency results for the individual subject 6 (right subdural grid). A) Semi-automatic clustering of the spectrum per channel. 2 channel clusters are identified (best sumd = 454.58). B) Time-frequency plots and source locations for the two clusters of channels. Data (dB) are a cluster average for the Mooney faces condition (similar results are found for the other conditions). The dashed lines mark the start and end of stimulus and the black line signal the TF blobs significantly different from the baseline (blue cluster $p < 0.000621$; green cluster $p < 0.001165$). C) The power envelope of distinct time-windows and clusters of electrodes for the faces condition (mean \pm SD). Lower frequencies have higher power after stimulus offset. Horizontal black bar indicate the significant differences (blue cluster $2.455 < t < 8.5673$, $0.005 < p < 0.0065$; green cluster $1.594 < t < 6.5324$, $0.0035 < p < 0.0085$).

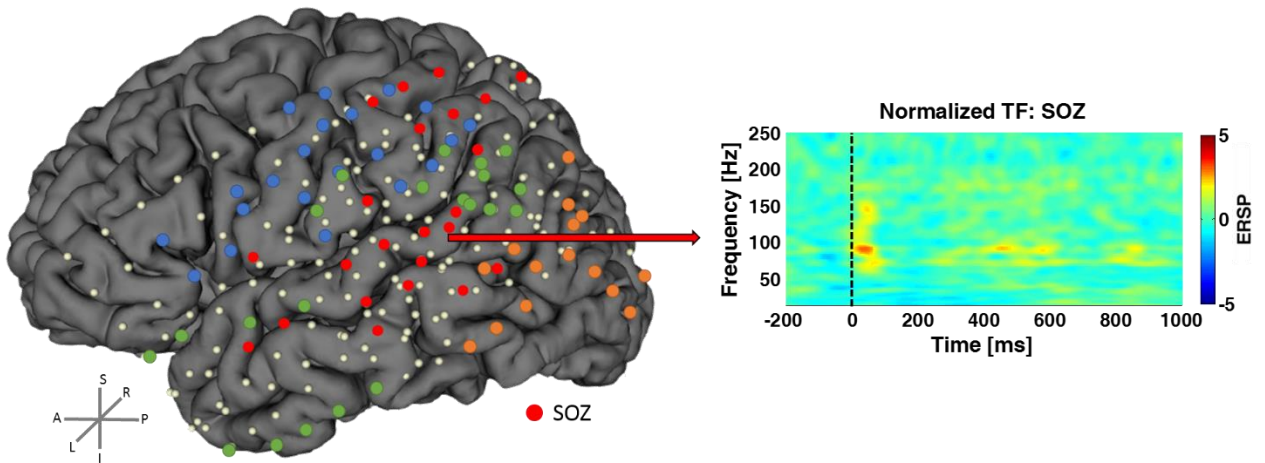


Figure C. Locations of the epilepsy related electrodes superimposed in the results image. The 'red labeled' electrodes represent the SOZ electrodes across all subjects while the others are the ones reported in our results. Note that there is no overlap because we did not include these 'bad electrodes' in the analysis. A normalized time-frequency activity (group average of these SOZ electrodes) locked to the Mooney faces stimuli is also shown.

Table A. Statistical results. The statistical test results are reported per condition and cluster of electrodes for the two main comparisons. * Wilcoxon rank sum comparison of TF data with the baseline. ** T-test with bootstrap (2000) comparison of the spectrum per time-window (Stim On vs. Decision Period). The max and minimum values of significant blobs are reported (FDR and cluster-based corrected $p=0.0125$).

Comparison of TF points with baseline	'Orange Cluster'				'Green Cluster'				'Blue Cluster'			
	P*		Z		P*		Z		P*		Z	
	Pmax	Pmin	Zmax	Zmin	Pmax	Pmin	Zmax	Zmin	Pmax	Pmin	Zmax	Zmin
Fac es	1,87 E-03	3,39 E-06	4,6 46	3, 11 1	1,95 E-03	6,80 E-08	5,3 96	3, 09 7	1,78 E-03	6,80 E-08	- 3,1 24	- 5,3 96
Guit ars	1,62 E-03	3,39 E-06	4,6 46	3, 15 2	3,05 E-04	3,94 E-07	5,0 72	3, 61 1	7,58 E-04	1,66 E-07	- 3,3 68	- 5,2 34
Scr	1,40 E-03	3,39 E-06	4,6 46	3, 19 4	2,14 E-03	6,80 E-08	5,3 96	3, 07 0	1,12 E-03	1,23 E-07	- 3,2 60	- 5,2 88
InvF aces	1,05 E-03	3,39 E-06	4,6 46	3, 27 7	1,63 E-03	6,80 E-08	5,3 96	3, 15 1	2,34 E-03	9,17 E-08	- 3,0 43	- 5,3 42
Comparison of Spectrum: StimOn vs Decision period	P**		T		P**		T		P**		T	
	Pmax	Pmin	Tmax	Tmin	Pmax	Pmin	Tmax	Tmin	Pmax	Pmin	Tmax	Tmin
Fac es	4,50 E-03	5,00 E-04	4,7 27	1, 60 9	2,50 E-03	5,00 E-04	4,6 65	2, 28 4	6,50 E-03	5,00 E-04	4,1 71	1,9 19
Guit ars	4,50 E-03	5,00 E-04	5,9 16	1, 69 4	n.s.	n.s.	n.s.	n. s.	2,50 E-03	5,00 E-04	4,4 81	1,8 58
Scr	2,50 E-03	5,00 E-04	3,9 90	2, 16 1	4,50 E-03	5,00 E-04	5,3 14	1, 92 3	2,50 E-03	5,00 E-04	5,5 58	2,1 53
InvF aces	6,50 E-03	5,00 E-04	3,9 10	1, 82 9	6,50 E-03	5,00 E-04	5,7 51	1, 88 5	3,50 E-03	5,00 E-04	7,0 41	1,9 33

The impact of Cathodal tDCS on GABAergic-Inhibition Mediated Synchrony in epilepsy: a multimodal study on local epileptogenic and distant oscillatory patterns

Abuhaiba SI, Castelhana J, Duarte IC, Rito M, Sales F, Castelo-Branco M.

Abstract

We aimed to investigate antiepileptic effects of cathodal trans direct-current stimulation and mechanisms of action based on its effects on the neurotransmitters responsible for the abnormal synchrony patterns seen in pharmacoresistant epilepsy. We hypothesized that non-invasive electrical stimulation exerts its antiepileptic activity by modulating GABAergic inhibitory circuits in the epileptogenic zone. This is a hypothesis-driven pilot prospective single-blinded repeated measure design study in patients diagnosed with pharmacoresistant epilepsy of temporal lobe onset. We included seven patients who underwent two sessions of cathodal stimulation (sham or real). After each session, we performed simultaneous electroencephalographic recording to count epileptic discharges and utilized two visual paradigms that are known to induce gamma oscillations (abstract “Mooney” faces and gratings). We also performed magnetic resonance spectroscopy to measure brain metabolite concentrations in the two areas of interest. This is the first study to test for the impact of neurostimulation on physiological and pathological brain oscillations, and to measure brain metabolites in the epileptogenic zone and control regions simultaneously in patients with pharmacoresistant epilepsy. We found that cathodal stimulation significantly decreased the number of interictal discharges per minute as well as GABA levels, in both areas of interest. Moreover, cathodal stimulation suppressed grating evoked gamma oscillations in the epileptogenic zone whereas it induced gamma oscillations in distant parieto-occipital regions. These results provide a window into the anti-epileptic mechanisms of action of tDCS, based on local and remote changes in GABA tonus and neural oscillatory patterning.

Introduction:

Epilepsy is a very common neurologic condition that has a prevalence of around 1% and an yearly incidence of 61/100.000[1]. A significant proportion (up to 40%) of patients remain intractable and are diagnosed with pharmacoresistant epilepsy[2]. Surgical intervention remains the mainstay of treatment in those

patients with focal onset, however this may be associated with significant neurologic deficits [3]. Moreover, symptomatic freedom after resection surgery is estimated to be around 70% [3] and to be less than that in patients with non-lesional MRI studies. Because of these, novel translational science approaches leading to less invasive treatments of drug-resistant epilepsy are needed. One of such possible new treatments is the utilization of focal noninvasive brain stimulation.

Epilepsy has historically been seen as a disorder of hypersynchronization/desynchronization. This places gamma-aminobutyric acid (GABA), the main inhibitory neurotransmitter as a putative main mechanistic player. GABAergic inhibition enables synchronization of activity in neuronal networks and underlies oscillations related to normal cognitive functions [4–6]. However, GABAergic inhibition might be responsible for the abnormal synchronization that leads to the generation of pathologic high frequency oscillations, seen in patients with epilepsy, especially temporal lobe epilepsy [6]. Seizures are the result of hypersynchronous neuronal discharges which result in the summation of the action potentials of multiple neurons in the epileptogenic zone, at least in the initiation phase. The summation of the postsynaptic currents results in large amplitude epileptic electroencephalographic (EEG) patterns. GABAergic inhibition is expected to play a critical role in the generation of this pathologic hypersynchronous state in the epileptogenic zone [7]. In vitro studies show that gamma frequency oscillations which are dependent on GABAergic synchronization are responsible for physiologic gamma oscillations and also pathologic oscillations seen in epilepsy [7]. However, in the case of epilepsy, the level of local and neuronal spike synchrony in the epileptogenic zone is much

higher than in normal tissues [8–10]. Physiological gamma frequency oscillations can be induced using visual stimuli as Mooney face and Grating stimuli [11–15]. Mooney faces are stimuli that challenge holistic perceptual processing, consisting of degraded pictures of human faces, where the shadows are rendered in black and the highlights in white. The task implies to group the fragmentary parts into coherent images to percept the Mooney face [16]. Gratings are periodic stimuli that are also well suited to study Gamma band oscillations. They consist of moving or static bars of variable spatial frequency and contrasts and are used to study induced synchronization of neural populations [15].

Synchrony in the context of epilepsy represents quite a complex matter. While there is evidence of local and neuronal spike hypersynchrony, there is also strong evidence of desynchrony at a larger scale [17]. GABAergic inhibition mediated synchrony is responsible mainly for local or neuronal spiking synchrony. GABAergic mediated synchrony is the generator of local high frequency oscillations in the gamma frequency range seen on EEG, whereas, the glutamatergic system is responsible for the maintenance of the power and amplitude of these gamma oscillations [18]. Beta range oscillations may also be dependent on GABAergic processes. Finally, it should be noted that there is evidence of a synchrony balance in the brain where, in disorders that are characterized by increased local synchrony in one area of the brain, one could expect to have less local synchrony in other brain regions [18]. This later observation could explain why patients with epilepsy might have less than optimal cognitive functioning in some domains.

A noninvasive stimulation method that has some form of antiepileptic effect should in theory modulate the neurotransmitters responsible for this abnormal

and complex synchrony patterns seen in epilepsy. Transcranial direct current stimulation (tDCS) is a safe method of focal brain stimulation [19]. Cathodal tDCS inhibits neuronal firing and decreases cortical excitability, which both are desirable effects in epilepsy patients. However, the exact mechanism of cathodal tDCS inhibitory effects in epilepsy are still unknown [20]. Cathodal tDCS has shown clear benefits in the control of seizures. In a preclinical study of tDCS in a rodent model of focal epilepsy, it was evident that the seizure threshold was elevated [21].

Cathodal tDCS has been previously used in adults and children in small clinical trials. In one study in children, after a single session of cathodal tDCS stimulation in patients with focal onset seizures, it was shown that the frequency of epileptiform discharges decreased by 45.3% immediately after the tDCS session, and the effect reached its maximum at 48 hours after treatment (57.6% reduction) [22]. Based on this, it became clear that cathodal tDCS is potentially useful noninvasive brain stimulation treatment technique for patients with drug resistant epilepsy.

In this study, we aimed to investigate the mechanistic role of cathodal tDCS in terms of inhibition and brain oscillations and to shed light on its role as an antiepileptic. We tested the hypothesis that cathodal tDCS modulates GABAergic inhibition and its mediated local synchrony in the epileptogenic zone as compared to a reference area in the occipital region. A multimodal imaging approach with MRS and EEG was used to measure the effects of ctDCS on brain metabolites and cortical epileptogenesis respectively after sham and real tDCS. Changes in metabolites are measured by magnetic resonance spectroscopy, whereas neurophysiologic effects are assessed with electroencephalography (EEG). This

is the first study to our knowledge that utilizes MRS to measure neurotransmitters in the epileptogenic zone and the occipital region post cathodal stimulation of the epileptogenic zone and correlate the modulated changes with EEG parameters. Our hypothesis was that c-tDCS would decrease cortical excitability and this could be measured by a reduction in the number of epileptiform discharges in the EEG. The results will provide direct evidence for the hypothesis of synchrony balance in epilepsy and for the efficacy of c-tDCS in focal non-lesional pharmacoresistant epilepsy. To our knowledge, this is the first study to test for the impact of neurostimulation on physiological and pathological brain oscillations, and to measure GABA, Glx, and Glutathione in the epileptogenic zone and occipital area simultaneously after real-c-tDCS in patients with pharmacoresistant temporal lobe epilepsy.

Methods:**Participants:**

This is a hypothesis-driven pilot prospective single-blinded repeated measure design study in patients diagnosed with pharmacoresistant epilepsy of temporal lobe onset. Seven participants with pharmacoresistant epilepsy were included. Inclusion criteria were the following: age above 18 years, diagnosis of pharmacoresistant epilepsy as defined by the International League Against Epilepsy, non-pregnant and non-lactating in women. Exclusion criteria were skin conditions such as eczema, metal inside head but outside the mouth, implanted devices such as cardiac pacemaker, cochlear implant, or vagal nerve stimulation device, history of recurrent or severe headaches, and presence of other comorbid neurologic conditions. All procedures used in this study conformed with the Declaration of Helsinki, and the protocol was approved by the Faculty of Medicine

of University of Coimbra Research Ethics Committee. A written informed consent was obtained from each participant and they accepted that their clinical information are to be used in the scope of this research project and for any publications that may result from this work.

Because it is common to have cognitive deficits in epilepsy patients, these seven participants were selected based on their ability to perform simple cognitive visual tasks such as detection of faces from non-faces, and maintaining focus in the center of the screen in the case of the gratings' visual task. Participants were recruited from the epilepsy monitoring unit at (Centro Hospitalar e Universitário de Coimbra). The decision to include patients only with left-side onset of seizures was based on the assumption that we want to uniform the stimulation protocol to be identical in all patients to allow for group-level analyses.

Participants were contacted two weeks after their discharge from the epilepsy monitoring unit and invited to participate in the study which was conducted at the Institute of Nuclear Sciences Applied to Health (ICNAS), University of Coimbra, Portugal. Patients were instructed to not make any changes to their medication while included in the study.

Participants visited ICNAS twice. The first visit was to explain the experiments, and to perform sham tDCS. The participants did not know that they will be starting with sham tDCS. One week later, the participants came for a second visit to ICNAS to perform real tDCS. After tDCS in each visit, EEG, EEG with visual tasks, and MRS were performed. Table 1 summarizes the demographic data of the included patients and their clinical information.

<i>ID</i>	<i>IED per minute⁺</i>	<i>Localization[*]</i>	<i>Age</i>	<i>Age at onset</i>	<i>Medications</i>	<i>Etiology^{&}</i>
1	5.6	Left frontotemporal	20	8	Levetiracetam Valproate Perampanel	FCD
2	31.3	Left temporal	32	22	CBZ	FCD
3	13.2	Left temporal	21	14	Valproate Oxcarbazepine Perampanel	FCD
4	9.6	Left temporal	33	22	CBZ Valproate	Tumor
5	5.5	Left temporal	35	17	CBZ Zonisamide	Tumor
6	7.3	Left temporal	46	40	Levetiracetam Valproate Zonisamide	FCD
7	8.2	Left temporal	37	23	Levetiracetam Valproate Perampanel Clobazam	FCD

⁺ During 25 minutes of acquisition (5 minutes resting state EEG and 5 minutes per visual task run for 4 runs).

^{*} Localization is based on the multidisciplinary team consensus based on multimodal imaging, interictal, ictal EEG, and ictal semiology supported by ESI (Electrical source imaging). FCD – focal cortical dysplasia.

[&] Based on epilepsy protocol structural MRI as interpreted by a neuroradiologist.

TDCS:

All participants underwent sham-tDCS in the first visit followed by real-tDCS. tDCS was performed in a quiet room at ICNAS using a Soterix Medical 1x1 tDCS Low-Intensity Stimulator (Soterix, New York, USA). Participants were blinded to the nature of the intervention.

Participants underwent a 20 min stimulation session at 1.5 mA continuous current delivered to the brain via two surface electrodes put in between saline-soaked sponges. Both electrodes had same dimensions of 3 by 4 cm. The cathode was placed at an area demonstrated in Fig. 1 whereas the anode was placed in the

occipital region. The stimulated area under the cathode electrode was chosen based on the lobar localization of the presumed epileptogenic zone.

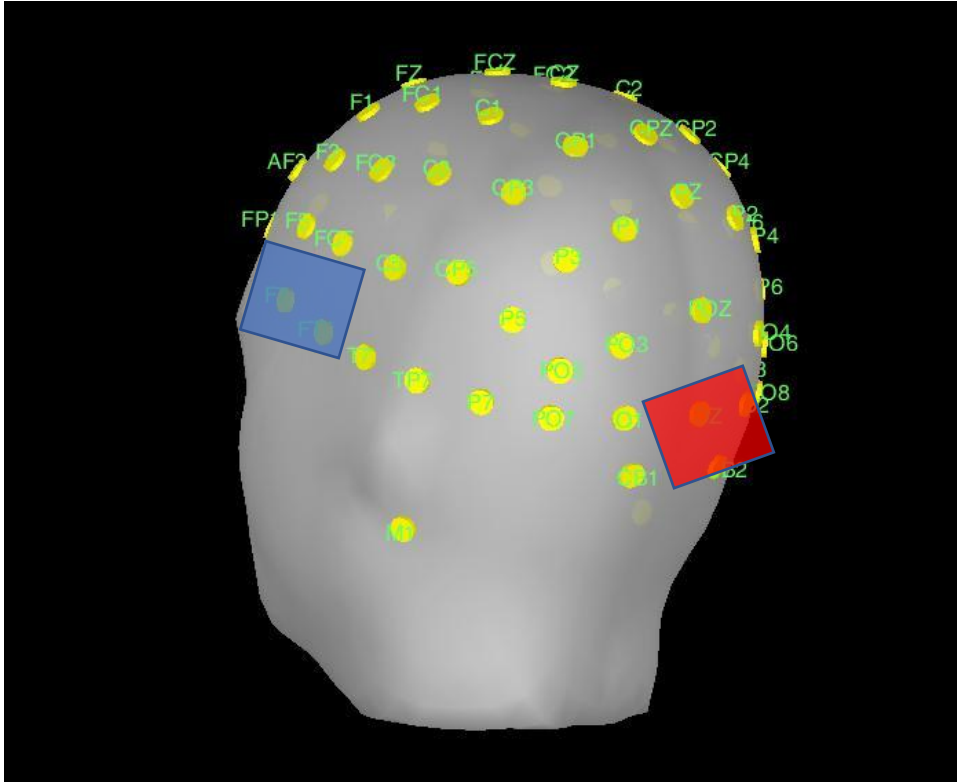


Fig. 1 *The cathode was placed on the left temporal region, whereas the anode on the occipital region with the center on Oz.*

Lobar Localization of the Presumed Epileptogenic Zone:

The presumed epileptogenic zone was determined based on multimodal imaging approach utilizing scalp EEG, MRI, FDG-PET and ictal-SPECT when available. A multidisciplinary meeting was held to discuss each participant before his/her enrolment in the study as part of their presurgical evaluation. Based on imaging findings and clinical semiology, lobar localization was determined in the multidisciplinary meeting. The lobar localization was confirmed using an in-house protocol of electrical source imaging which has been used as part of the routine presurgical evaluation.

Electrical Source Imaging to Identify the Presumed Epileptogenic Zone:

Long-term EEG data from the most recent admission to the epilepsy monitoring unit was exported for each patient. As expected, each patient could have more than one cluster of interictal discharges “spikes” and the most representative one was chosen by a neurologist. Template matching using Curry 7 was utilized to automatically detect spikes in the EEG recording and an average was obtained. Band pass filter (5 to 45 Hz) was used and the filtered average was exported in cnt format.

In Brainstorm the patient’s individual MRI was imported and a BEM model was generated [23,24]. Cortical-constrained sLORETA was used and the maximum point at the peak of the spike was identified in each patient [25]. The EEG electrode in closest proximity to the maximum point was determined in each patient and the center of the cathode electrode was placed over this point.

Tasks:

Scalp electroencephalography was performed after each tDCS session (sham or real). Visual tasks “Mooney faces” or “Gratings” were started 5 minutes after starting EEG recording. Resting state EEG was used to count the number of interictal discharges.

During Mooney faces we chose two runs in each session. Each run consisted of 80 stimuli (160 in total in both runs) of (40 faces; 40 non-faces per run) of 1 second duration of the stimulus and 1 to 1.5 second interval between stimuli. After each stimulus, the subject had to report by button press if it was a face or a non-face stimulus using two keyboard keys. The same protocol was repeated in the second session one week later after real c-tDCS.

For the gratings task subjects were instructed to fixate at a center circle in the screen and a press a button each time the circle color changed (red vs green). Two runs per session were used and each run consisted of 72 stimuli (24 per each grating's type and 144 in total per session) and of 1.5 second duration. The type of gratings was balanced and presented in random order. Contrast in the different gratings' stimuli was kept at 100%. Visual grating stimuli type A had a spatial frequency of 0.67 cpd, type B had a spatial frequency of 1.33 cpd and type C had a spatial frequency of 2.86 cpd. Visual angle velocity was 1.5 degrees per second. A central fixation cross of black color had a size of 0.25 visual degrees within a circle background where the color randomly changes to red or green during a 200 ms period. Afterwards, a question block was presented with a black background and a central fixation question mark of white color and 1.25 visual degrees size. The subject was instructed to report whether the fixation circle changed to red or green by pressing two different buttons at the time of the question block. The same protocol was repeated after real c-tDCS.

The duration of each run is 5 minutes, during which counting of interictal epileptic discharges (IEDs) was performed.

Patients had four runs each per their visit. The first two runs used Mooney task, whereas the second two runs used a gratings' visual task.

EEG recordings and analysis:

EEG was recorded using a 64 electrodes cap (QuickCap, NeuroScan, USA) with the electrodes placed according to the extended 10/20 system. The electrode impedances were kept below 20 k Ω . The signal was amplified and recorded at a sampling rate of 1 kHz, low pass filter at 200 Hz, using a SynAmps2/RT amplifier (NeuroScan, USA).

Electroencephalographic signal was recorded using Scan 4 (NeuroScan, USA), with the acquisition reference electrode placed at a half distance between CZ and FCZ.

Data analysis was performed with Brainstorm [26], which is documented and freely available for download online under the GNU general public license (<http://neuroimage.usc.edu/brainstorm>). The EEG signal was down sampled to 400 Hz and band filtered between 1 and 100 Hz.

For the task related signal, the epochs were defined from -1000 to 1000 ms, with the zero locked to the stimuli onset. The dataset was cleaned using an automatic rejection tool with a threshold of 120 μ V for all electrodes, and this was followed by a visual inspection to ensure the data was free from artifacts. Rejected channels due to abnormal noise activity were interpolated using spherical spline interpolation. The recordings were re-referenced to the average of all remaining channels.

Time-frequency decomposition was done in Brainstorm, with Morlet wavelet [27,28]. Electrode PO8 was chosen to perform time-frequency decomposition in Mooney task. In Gratings, oscillations were studied simultaneously in the EZ and a reference region at POZ. The EZ electrode in our cohort was FT7.

MRS acquisitions and analysis:

Patients underwent anatomical and spectroscopy imaging using a Siemens 3T Scanner (Siemens Magnetom 3 T TimTrio, Erlangen, Germany). T1-weighted structural images of the brain were acquired with a MPRAGE sequence with: 1 mm³ isotropic voxel, repetition time 2.53 s, echo time 3.42 ms, inversion time 1100 ms, flip angle 7°, field of view 256 × 256 mm², 256 × 256 matrix, 176 slices and GRAPPA acceleration factor = 2.

T1-weighted images were analyzed for structural abnormalities. Two MRS voxels were positioned one in the left anterior temporal lobe and another medially in the occipital cortex, see Fig. 2. The EZ voxel measured 15.625 cm³ whereas the occipital voxel had a volume of 27 cm³. We opted for a smaller volume in the temporal region because of the presence of bone and CSF in the selected area which rendered larger voxel volumes too noisy.

Data were acquired on a 3T Siemens Scanner (Siemens Magnetom 3T TimTrio, Erlangen, Germany). T1-weighted structural images were acquired with a MPRAGE sequence with: 1 mm³ isotropic voxel, repetition time 2.53 s, echo time 3.42 ms, inversion time 1100 ms, flip angle 7, field of view 256x256 mm², 256x256 matrix, 176 slices and GRAPPA acceleration factor = 2. We used the Hadamard Encoding and Reconstruction of MEGA-Edited Spectroscopy (HERMES) approach [29] to quantify GABA, Glx and Glutathione. Two voxels were chosen for each patient one in the left anterior temporal lobe and the second is bilateral occipital lobe. The volume of the EZ voxel in the temporal lobe is 15.625 cm³ whereas the occipital voxel had a volume of 27 cm³. The structural images were analyzed for structural abnormalities and bright objects detection. The HERMES data were processed with Gannet software [30]. GABA, Glx and Glutathione in addition creatine signals were obtained from the difference edited spectra. The peaks for each metabolite were fitted to a simple Gaussian model. Creatine signal was fitted to a double Lorentzian model. Results are expressed as levels of metabolite/Cr. Normalization to creatine is used to reduce intersubject variance from both different signal-to-noise levels and CSF fraction within the voxel [31]. An example output is shown in Fig. 3. GABA signal is known to be

contaminated by other macromolecules [32] therefore, we refer to GABA from now on as GABA+. Model fit errors for all spectra were set at $< 10\%$ to be accepted. Spectra with higher fit error for any of the metabolites were considered as missing values.

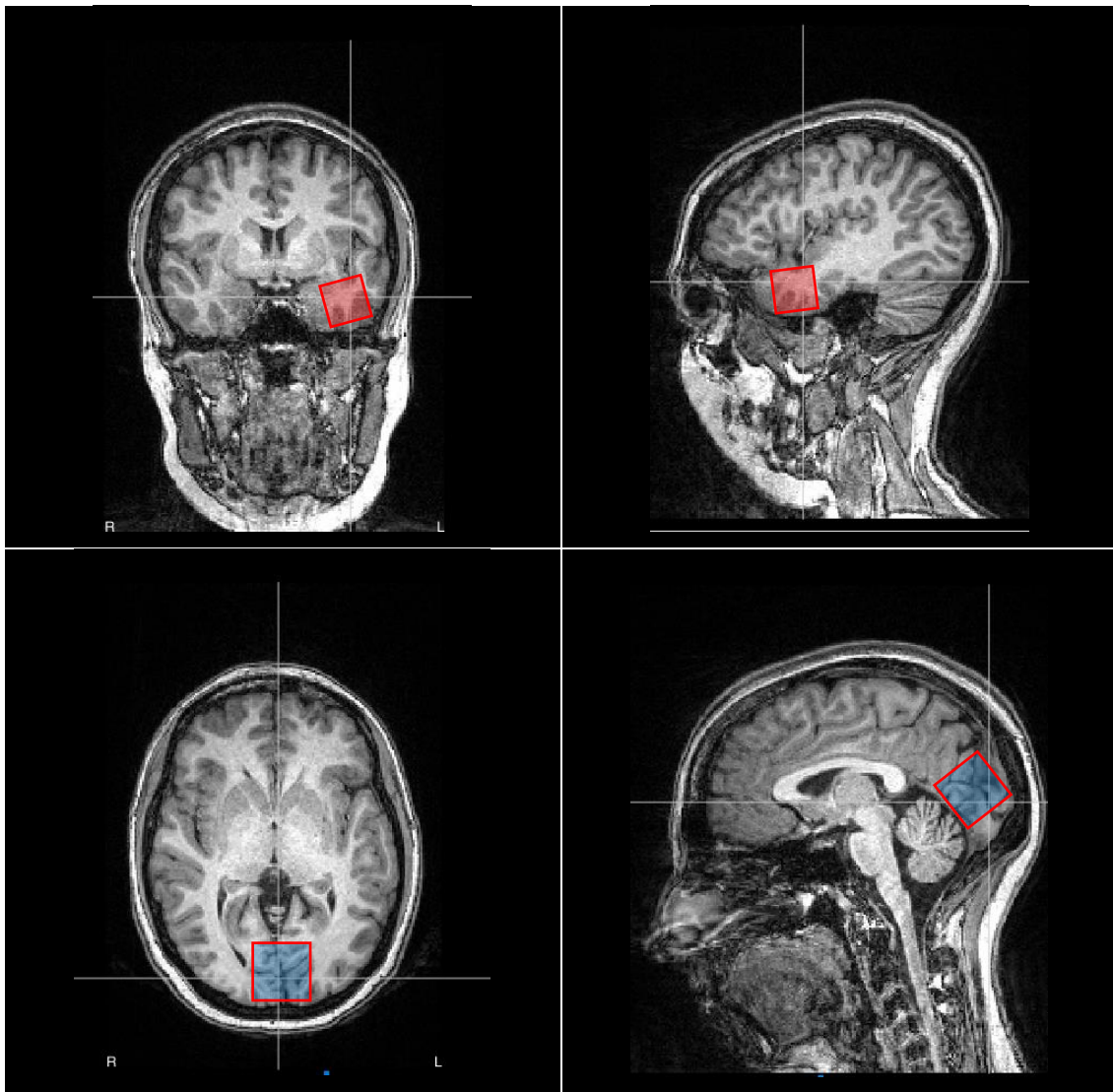


Fig. 2: Placement of the voxels for MRS. In red, we show the EZ voxel which is positioned in the left anterior temporal lobe whereas in blue we show the reference voxel which is positioned in the occipital zone medially. The EZ voxel measured $25 \times 25 \times 25$ mm whereas the occipital voxel measured $30 \times 30 \times 30$ mm.

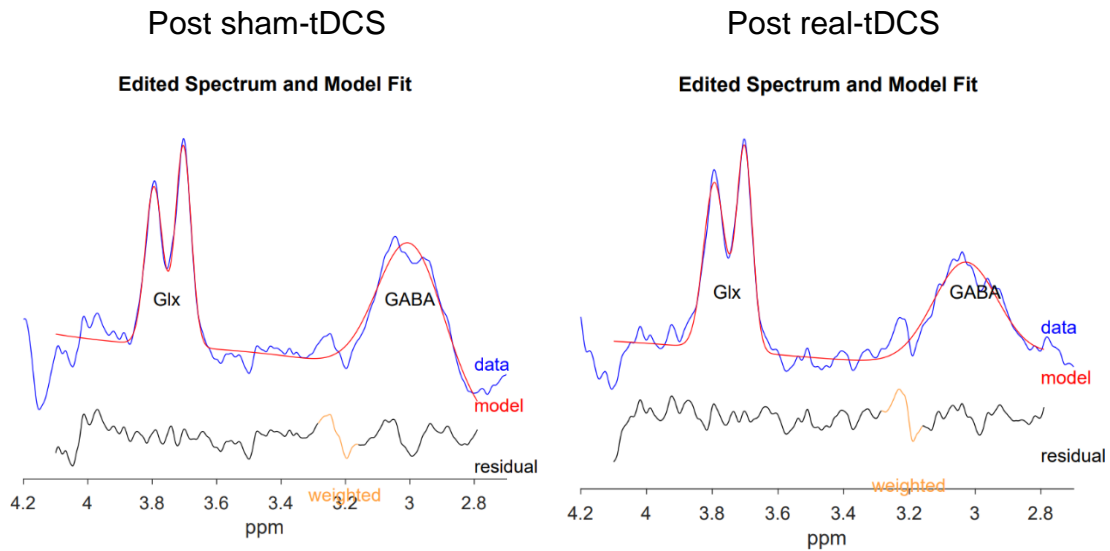


Fig. 3: Spectra obtained from the EZ. GABA+/Cr decreased from 120 to 100. Fit error for each metabolite is < 10%.

Statistical analysis:

Statistical analyses were performed with IBM SPSS Statistics version 20 software. Paired-sample t-student tests were used to investigate if there were differences between means of the main study variables, in this repeated measure design. Our statistical significance threshold was set at a p-value < 0.05.

Results:

Effects of tDCS on cortical excitability of the epileptogenic zone (presented as frequency of interictal discharges per minute):

c-tDCS did not induce any seizure activity in any of our patients. Moreover, the pattern and characteristics of the interictal discharges were not modified by c-tDCS.

Real c-tDCS decreased the number of interictal discharges per minute by 61%, $p = 0.013$ (paired t-test, Fig. 4, Table 2). The counting was performed during the

5-minute recording of resting-state EEG and during the visual tasks (total duration of 25 minutes).

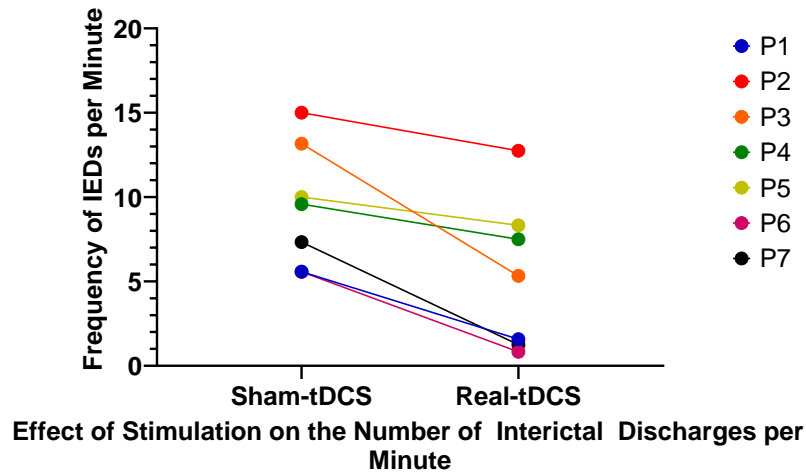


Fig. 4: Real c-tDCS decreased the number of interictal discharges per minute by 61%, $p = 0.013$.

Table 2: Frequency of Interictal Discharges Per Minute after Cathodal Stimulation

	Post sham-tDCS	Post real-tDCS	<i>p</i> -value
IEDs per minute	11.532 ± 3.432	4.464 ± 1.666	0.013
<i>N</i> (subjects)	7	7	

Effects of tDCS on neurotransmitters profile in the epileptogenic zone:

c-tDCS decreased GABA and GABA/Glx ratio in the EZ (see Suppl. Tables S1-S3). Moreover, glutathione in its reduced form is increased in the EZ after c-tDCS.

Fig. 5 shows that GABA in the epileptogenic zone is decreased, whereas glutathione is increased (p -value < 0.005 and 0.05 respectively). GABA/Glx ratio decreased from 1.611 ± 0.222 to 1.079 ± 0.195 , $p = 0.011$, after real c-tDCS stimulation of the epileptogenic zone.

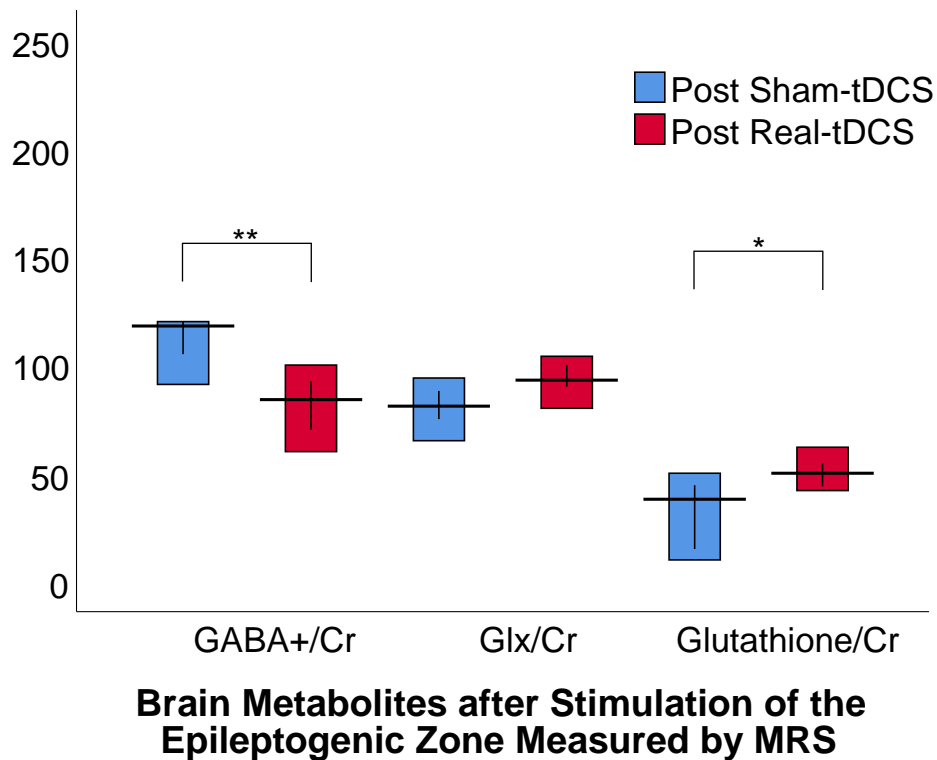


Fig. 5: GABA in the epileptogenic zone is decreased, whereas glutathione is increased. These effects were statistically significant with a p-value below 0.005 and 0.05 respectively. Glx was not statistically different after real c-tDCS as compared to sham c-TDCS.

Effects of tDCS on neurotransmitters profile in the occipital area:

GABA in the occipital zone which was under anodal stimulation is decreased, $p < 0.05$. The changes in the EZ and occipital GABA/Glx ratios are shown in Table S3.

Effects of tDCS on event-related potentials related to facial neural processing:

In this analysis, we chose to include only correct face-detection ERPs. Fig. S1 shows the averaged ERPs after sham versus real c-tDCS stimulation of the EZ.

Effects of tDCS on oscillations with Gratings task:

As visual gratings might induce beta or gamma oscillations in widespread areas, we wanted to compare post-sham-tDCS with real-tDCS in the epileptogenic zone (FT7) as compared to a distant brain region (POZ). Cathodal stimulation of the epileptogenic zone showed a trend for suppression of low gamma oscillations in the temporal region (epileptogenic zone)

whereas induced gamma oscillations in POZ which is distant from the epileptogenic zone Fig. S2.

Discussion:

In the present study, we investigated the mechanisms of action of cathodal tDCS in the treatment of pharmacoresistant epilepsy of temporal lobe origin. Cathodal tDCS was effective in suppressing interictal discharges by approximately 61% after a single session confirming that cathodal DC polarization indeed decreases cortical excitability in the epileptogenic zone in patients with left temporal lobe epilepsy. We found that cathodal stimulation of the epileptogenic zone decreased GABA concentration. This is the first study to report this effect in human subjects. These results provide the biological basis for the reported before efficacy of a single session of c-tDCS immediately after the session.

In our design, the anode was placed over the occipital region. Similar to [33] anodal stimulation of the occipital region in our patients did not increase cortical excitability or increased epileptic activity.

At baseline, we show that GABA levels were significantly higher in the epileptogenic zone as compared to the reference area in the occipital region. One of the possible hypotheses for the development of pharmacoresistant epilepsy is reduced sensitivity to GABA_A receptors to agents binding to the benzodiazepine receptor site 1 and other changes in GABA_A receptors were reported in brain tissues resected from patients with pharmacoresistant temporal lobe epilepsy (TLE) [34]. In common etiologies of drug resistant epilepsy such as cortical tubers in tuberous sclerosis or in patients with focal cortical dysplasia it has been previously shown that extracellular GABA is markedly elevated in the epileptogenic zone [35–38]. It should be noted that the etiology of pharmacoresistant epilepsy in two of our patients is tuberous sclerosis. Taki and colleagues reported that epileptic tuberi in tuberous sclerosis have an elevated level of GABA as compared to non-epileptic tuberi [38]. On the other hand, it has been reported that GABA levels were low in patients with drug-sensitive epilepsy syndromes

and the use of antiepileptics in that subgroup of patients was associated with an elevation in GABA which was associated with response to treatment [35]. Therefore, one can conclude that GABAergic dysfunction in epilepsy is multifaceted and in patients with drug-resistant epilepsy as in our cohort one expects to find an elevated GABA in the epileptogenic zone which agrees with our findings.

Cathodal stimulation of the epileptogenic zone resulted in a decrease in GABA concentration which has relevant clinical significance. We hypothesize that this decrease in GABA could be due to improved transportation of GABA, increased degradation of GABA, or other unexplored mechanisms. Surprisingly, the decrease in GABA in our study was associated with a decrease in cortical excitability in the epileptogenic zone as evidenced by a decrease in the frequency of epileptic discharges post real-tDCS. A recent modeling study suggested that cathodal stimulation of the EZ in a drug resistant epilepsy model would mainly suppress GABAergic interneurons which was associated with less epileptic spiking (Denoyer et al. 2020). Cathodal stimulation has been previously reported to decrease GABA by approximately 11% [39]. In our study, GABA in the EZ decreased by approximately 25%. Froc et al also reported that cathodal stimulation decreases glutamate significantly however we did not see any change in glutamate in our study. Bilateral stimulation with the cathode placed at M1 has been reported to result in a decrease in GABA concentration in the cathode-stimulated area [40].

GABA degradation is dependent on the TCA cycle and glutathione in its reduced form is needed for proper trafficking of GABA in the TCA cycle. In this study, we show that glutathione in its reduced form is decreased in the epileptogenic zone as compared to the reference area. Glutathione has been previously reported to be decreased in the epileptogenic zone in patients with drug resistant epilepsy measured by in vivo (1)H-MRS [41]. Moreover, cathodal tDCS stimulation of the epileptogenic zone has increased the concentration of glutathione which is a potent antioxidant in the brain. This could be the explanation of

improved degradation of GABA and could explain why GABA is decreased in the epileptogenic zone after tDCS.

These findings suggest that a decrease in GABA in the epileptogenic zone is associated with a decrease in epileptogenicity as measured by number of interictal discharges per minute. GABAergic inhibitory interneurons are known to play a role in local synchrony in the gamma frequency range [18]. Because of that we chose two visual tasks that are known to be dependent on the inhibition/excitation balance in the occipital region, and which induce clear gamma oscillations, namely the Mooney faces task and Gratings [11–14].

Visual processing of faces and no-faces has been previously shown to be dependent on the function of inhibitory GABAergic interneurons. In our study, we show that GABA is decreased in the occipital region, under anodal stimulation. Moreover, we show a decrease in the P100 (and marginally N170) components of the event-related potentials of faces. This could be explained by a decrease in the summation of the action potentials of neurons in the occipital region due to decreased GABAergic-mediated synchrony. It has been previously reported that the P100 and N170 components have higher amplitudes with inverted or scrambled faces as opposed to upright faces [42] which is consistent with the notion that the perception of the task as less challenging could be associated with a decrease in the amplitudes of these two components. If this is true, then one might argue that cathodal stimulation of the epileptogenic zone has influenced the occipital region which resulted in an improvement in facial processing. It has been reported that the epileptogenic zone has abnormal functional and structural connectivity to distant cortical regions and increased local synchrony in the epileptogenic zone could have a deleterious effect on cognitive functioning [18].

Anodal stimulation of the occipital region resulted in a decrease in GABA. Visual gratings are known to induce temporal-parietal-occipital gamma oscillations [43] which make them a good candidate to study the modulation of gamma oscillations simultaneously in the

epileptogenic zone and the reference occipital area post sham and real tDCS. We show that real tDCS has suppressed gamma oscillations in the epileptogenic zone and evoked gamma oscillations in the occipital region which further establishes the hypothesis that increased local synchrony in one area (i.e. the EZ), one would expect to have less local synchrony in normal functioning brain regions (i.e. occipital region).

In conclusion, our findings suggest that c-tDCS provides potent antiepileptic mechanisms in patients with pharmaco-resistant epilepsy as it has been associated with a significant decrease in the frequency of interictal discharges. The possible mechanism of action of c-tDCS according to our findings is the modulation of the GABAergic inhibition mediated synchrony in the epileptogenic zone, with a reduction of GABAergic inhibition in the cathodal-stimulated region.

References:

- [1] Fiest KM, Sauro KM, Wiebe S, et al. Prevalence and incidence of epilepsy: A systematic review and meta-analysis of international studies. *Neurology*. 2017;88:296.
- [2] Sharma AK, Rani E, Waheed A, et al. Pharmaco-resistant Epilepsy: A Current Update on Non-Conventional Pharmacological and Non-Pharmacological Interventions. *Journal of Epilepsy Research*. 2015;5:1.
- [3] Spencer S, Huh L. Outcomes of epilepsy surgery in adults and children. *The Lancet Neurology*. 2008;7:525–537.
- [4] Freund TF, Buzsáki G. Interneurons of the hippocampus. *Hippocampus*. 1998;6:347–470.
- [5] Buzsaki G. *Rhythms of the Brain*. 2006.
- [6] Klausberger T, Somogyi P. Neuronal Diversity and Temporal Dynamics: The Unity of Hippocampal Circuit Operations. *Science*. 2008;321:53–57.
- [7] Khazipov R, Holmes GL. Synchronization of kainate-induced epileptic activity via GABAergic inhibition in the superfused rat hippocampus in vivo. *The Journal of neuroscience : the official journal of the Society for Neuroscience*. 2003;23:5337–5341.
- [8] Mann EO, Paulsen O. Role of GABAergic inhibition in hippocampal network oscillations. *Trends in Neurosciences*. 2007;30:343–349.
- [9] Gulyas AI, Szabo GG, Ulbert I, et al. Parvalbumin-Containing Fast-Spiking Basket Cells Generate the Field Potential Oscillations Induced by Cholinergic Receptor Activation in the Hippocampus. *Journal of Neuroscience*. 2010;30:15134–15145.
- [10] Whittington MA, Cunningham MO, LeBeau FEN, et al. Multiple origins of the cortical gamma rhythm. *Developmental Neurobiology*. 2011;71:92–106.

- [11] Castelhana J, Rebola J, Rodriguez E, et al. Neural synchronization in the gamma frequency range is tightly associated with detection of ambiguous face stimuli. *NeuroImage*. 2009;47:S155.
- [12] Castelhana J, Rebola J, Leitão B, et al. To Perceive or Not Perceive: The Role of Gamma-band Activity in Signaling Object Percepts. *PLoS ONE*. 2013;8.
- [13] Castelhana J, Tavares P, Mouga S, et al. Stimulus dependent neural oscillatory patterns show reliable statistical identification of autism spectrum disorder in a face perceptual decision task. *Clinical Neurophysiology*. 2018;129:981–989.
- [14] Bernardino I, Castelhana J, Farivar R, et al. Neural correlates of visual integration in Williams syndrome: Gamma oscillation patterns in a model of impaired coherence. *Neuropsychologia*. 2013;51:1287–1295.
- [15] Muthukumaraswamy SD, Singh KD. Visual gamma oscillations: The effects of stimulus type, visual field coverage and stimulus motion on MEG and EEG recordings. *NeuroImage*. 2013;69:223–230.
- [16] Mooney CM, Ferguson GA. A new closure test. *Canadian Journal of Psychology/Revue canadienne de psychologie*. 1951;5:129–133.
- [17] Jiruska P, de Curtis M, Jefferys JGR, et al. Synchronization and desynchronization in epilepsy: controversies and hypotheses. *The Journal of physiology*. 2013;591:787–797.
- [18] Uhlhaas PJ, Singer W. Neural synchrony in brain disorders: relevance for cognitive dysfunctions and pathophysiology. *Neuron*. 2006;52:155–168.
- [19] Poreisz C, Boros K, Antal A, et al. Safety aspects of transcranial direct current stimulation concerning healthy subjects and patients. *Brain Research Bulletin*. 2007;72:208–214.
- [20] Kabakov AY, Muller PA, Pascual-Leone A, et al. Contribution of axonal orientation to pathway-dependent modulation of excitatory transmission by direct current stimulation in isolated rat hippocampus. *Journal of Neurophysiology*. 2012;107:1881–1889.
- [21] Liebetanz D, Klinker F, Hering D, et al. Anticonvulsant Effects of Transcranial Direct-current Stimulation (tDCS) in the Rat Cortical Ramp Model of Focal Epilepsy. *Epilepsia*. 2006;47:1216–1224.
- [22] Auvichayapat N, Rotenberg A, Gersner R, et al. Transcranial Direct Current Stimulation for Treatment of Refractory Childhood Focal Epilepsy. *Brain Stimulation*. 2013;6:696–700.
- [23] Gramfort A, Papadopoulos T, Olivi E, et al. OpenMEEG: opensource software for quasistatic bioelectromagnetics. *BioMedical Engineering OnLine*. 2010;9:45.
- [24] Kybic J, Clerc M, Abboud T, et al. A common formalism for the Integral formulations of the forward EEG problem. *IEEE Transactions on Medical Imaging*. 2005;24:12–28.
- [25] Pascual-Marqui RD. Standardized low-resolution brain electromagnetic tomography (sLORETA): technical details. undefined. 2002;
- [26] Tadel F, Baillet S, Mosher JC, et al. Brainstorm: A User-Friendly Application for MEG/EEG Analysis. *Computational Intelligence and Neuroscience*. 2011;2011:1–13.
- [27] O B, C T-B. Oscillatory Gamma Activity in Humans: A Possible Role for Object Representation. *International journal of psychophysiology : official journal of the International Organization of Psychophysiology*. 2000;38.

- [28] Pantazis D, Nichols TE, Baillet S, et al. A comparison of random field theory and permutation methods for the statistical analysis of MEG data. *NeuroImage*. 2005;25:383–394.
- [29] Chan KL, Puts NAJ, Schär M, et al. HERMES: Hadamard encoding and reconstruction of MEGA-edited spectroscopy. *Magnetic Resonance in Medicine*. 2016;76:11–19.
- [30] Edden RAE, Puts NAJ, Harris AD, et al. Gannet: A batch-processing tool for the quantitative analysis of gamma-aminobutyric acid–edited MR spectroscopy spectra. *Journal of Magnetic Resonance Imaging*. 2014;40:1445–1452.
- [31] Bogner W, Gruber S, Doelken M, et al. In vivo quantification of intracerebral GABA by single-voxel (1)H-MRS-How reproducible are the results? *Eur J Radiol*. 2009/02/10. 2010;73:526–531.
- [32] Aufhaus E, Weber-Fahr W, Sack M, et al. Absence of changes in GABA concentrations with age and gender in the human anterior cingulate cortex: A MEGA-PRESS study with symmetric editing pulse frequencies for macromolecule suppression. *Magnetic Resonance in Medicine*. 2013;69:317–320.
- [33] Fregni F, Thome-Souza S, Nitsche MA, et al. A Controlled Clinical Trial of Cathodal DC Polarization in Patients with Refractory Epilepsy. *Epilepsia*. 2006;47:335–342.
- [34] Remy S, Beck H. Molecular and cellular mechanisms of pharmacoresistance in epilepsy. *Brain*. 2006;129:18–35.
- [35] Levy LM, Degnan AJ. GABA-based evaluation of neurologic conditions: MR spectroscopy. *AJNR American journal of neuroradiology*. 2013;34:259–265.
- [36] Petroff OAC, Rothman DL, Behar KL, et al. Initial Observations on Effect of Vigabatrin on In Vivo 1H Spectroscopic Measurements of gamma-Aminobutyric Acid, Glutamate, and Glutamine in Human Brain. *Epilepsia*. 1995;36:457–464.
- [37] Aasly J, Silfvenius H, Aas TC, et al. Proton magnetic resonance spectroscopy of brain biopsies from patients with intractable epilepsy. *Epilepsy research*. 1999;35:211–217.
- [38] Taki MM, Harada M, Mori K, et al. High gamma-aminobutyric acid level in cortical tubers in epileptic infants with tuberous sclerosis complex measured with the MEGA-editing J-difference method and a three-Tesla clinical MRI Instrument. *NeuroImage*. 2009;47:1207–1214.
- [39] Froc DJ, Chapman CA, Trepel C, et al. Long-term depression and depotentiation in the sensorimotor cortex of the freely moving rat. *The Journal of neuroscience : the official journal of the Society for Neuroscience*. 2000;20:438–445.
- [40] Bachtiar V, Johnstone A, Berrington A, et al. Modulating Regional Motor Cortical Excitability with Noninvasive Brain Stimulation Results in Neurochemical Changes in Bilateral Motor Cortices. *Journal of Neuroscience*. 2018;38:7327–7336.
- [41] Mueller SG, Trabesinger AH, Boesiger P, et al. Brain glutathione levels in patients with epilepsy measured by in vivo (1)H-MRS. *Neurology*. 2001;57:1422–1427.
- [42] Rossion B, Gauthier I, Tarr MJ, et al. The N170 occipito-temporal component is delayed and enhanced to inverted faces but not to inverted objects. *NeuroReport*. 2000;11:69–72.
- [43] Castelhana J, Duarte IC, Wibral M, et al. The dual facet of gamma oscillations: Separate visual and decision making circuits as revealed by simultaneous EEG/fMRI. *Human Brain Mapping*. 2014;35:5219–5235.

Supplementary Tables:**Supplementary Table 1: Effects of Cathodal Stimulation on Brain Metabolites in the Epileptogenic Zone.**

	<i>Post sham-tDCS</i>	<i>Post real-tDCS</i>	<i>p-value</i>
<i>GABA</i>	0.129 + 0.019	0.096 + 0.018	0.002
<i>Glx</i>	0.08 ± 0.004	0.093 ± 0.003	NS
<i>Glutathione</i>	0.031 + 0.007	0.048 + 0.004	0.049
<i>GABA/Glx ratio</i>	1.611 + 0.222	1.079 + 0.195	0.011
<i>N (subjects)</i>	7	7	

Supplementary Table 2: Effects of Cathodal Stimulation on Brain Metabolites in the Occipital Zone.

	<i>Post sham-tDCS</i>	<i>Post real-tDCS</i>	<i>p-value</i>
<i>GABA</i>	0.098 + 0.004	0.086 ± 0.004	0.02
<i>Glx</i>	0.087 + 0.003	0.088 + 0.002	NS
<i>Glutathione</i>	0.051 + 0.005	0.046 + 0.003	NS
<i>GABA/Glx ratio</i>	1.129 + 0.053	0.994 + 0.081	0.025
<i>N (subjects)</i>	7	7	

Supplementary Table 3: Inhibition/Excitation Balance in the Epileptogenic Zone versus the Occipital Region after Cathodal Stimulation.

	<i>EZ GABA/Glx</i>	<i>Occipital GABA/Glx</i>	<i>p-value</i>
<i>Post sham-tDCS</i>	1.61 ± 0.23	1.09 ± 0.05	0.042
<i>Post real-tDCS</i>	1.08 ± 0.19	0.98 ± 0.07	NS 0.555
<i>N</i>	7	7	

The EZ GABA/Glx ratio was significantly higher than the occipital ratio after sham-tDCS. Cathodal stimulation of the epileptogenic zone abolished this difference between the EZ and occipital region.

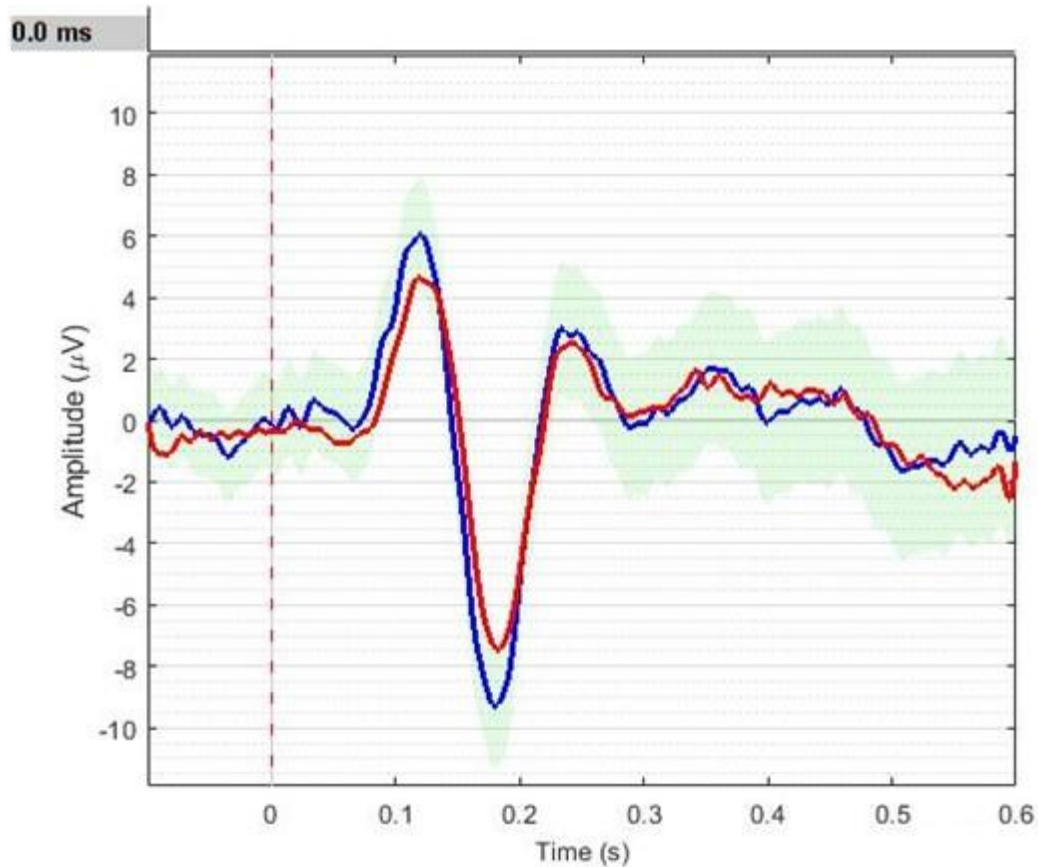


Figure S1: ERP of faces and non-faces from Mooney tasks. Blue is post sham-tDCS (based on 515 trials) whereas, red is post real-tDCS (based on 651 trials). Green-shade represents SEM.

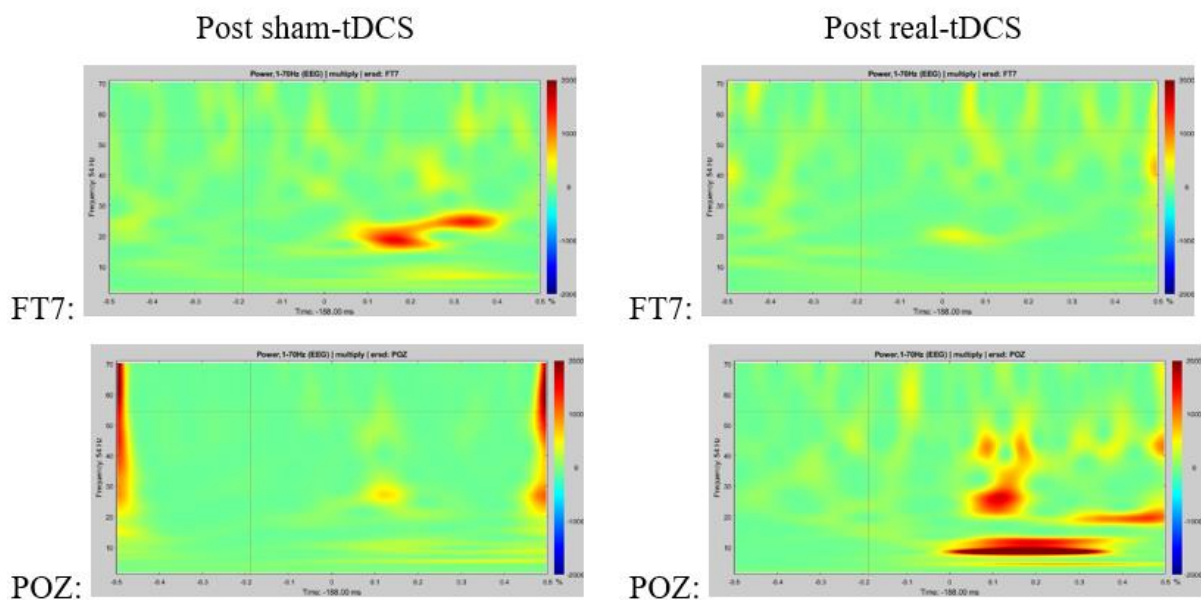


Figure S2: Cathodal stimulation of the epileptogenic zone has suppressed low gamma oscillations in the temporal region (epileptogenic zone) whereas induced gamma oscillations in POZ which is distant from the epileptogenic zone.

Chapter 4:

Cortical Metabolites Disruption in Epilepsy: Future Work

Lovastatin as an Antiepileptic

AMT-PET for the Localization of the EZ in TSC-associated Epilepsy and Drug Resistant Epilepsy

Lovastatin as an antiepileptic: Effect of lovastatin as a physiologic challenge on the GABAergic system in drug-resistant epilepsy and TSC-Associated Epilepsy

INTRODUCTION:

Epilepsy is a common neurologic disorder that presents with recurrent seizures in about 1% of the general population with one third of the patients having poor control with multiple antiepileptic medication despite recent novel AEDs (1,2). Recently, increasing evidence has emerged pointing towards possible involvement of astrocytes, other immune cells, and blood-brain-barrier breakdown in epileptogenesis (3). Inflammation has also been shown to be related to epileptogenesis in several animal models of epilepsy (4–6).

With this new understanding of pathology in epilepsy, studies have been done to assess the role of specific anti-inflammatories in epilepsy (6–8). Statins, in addition to their cholesterol lowering effects, have been shown to have anti-inflammatory effects as they reduce expression of interleukin-1b and interferon-c (9,10). Additionally, they were found to have a protective effect for the endothelium and the blood-brain barrier (11). Because of these properties and the safety profile, several studies in vivo and in vitro have tried to evaluate if they have any anticonvulsant effect.

Atorvastatin, lovastatin and simvastatin have been studied in different animal models of epilepsy to investigate their effects on quinolone acid (KA) or pilocarpine induced seizures as well as audiogenic induced seizures (12–17). Atorvastatin is the most studied statin in epilepsy with possible anticonvulsant effects in KA-induced seizures, absence seizures, and audiogenic seizures (18,19). This effect can be mainly appreciated early in the disease process and with repeated doses suggesting a possible neuroprotective role. The mechanism of action as an anticonvulsant was explained by an increase in NO synthesis, and a possible direct negative modulation of NMDA glutamate receptor activity but not to HMG-CoA reductase inhibition (12,20,21).

Simvastatin was less evaluated as an antiepileptic, but the few studies done are very promising. In vitro studies showed an excitoprotective effect of simvastatin against NMDA-induced neuronal damage (22). Simvastatin was tested in KA-induced animal models of epilepsy with a significant reduction of seizures frequency and hippocampal cell death (17,23). Moreover, simvastatin was

showed to abolish status epilepticus induced by KA (24). Finally, simvastatin was also found to be effective in animal models of audiogenic seizures (18).

Lovastatin on the other hand was extensively studied in neurofibromatosis type 1 and been found to improve cognitive function due to an inhibitory cortical effect (25). Lovastatin has been found to have a similar anti-epileptic profile to atorvastatin with the only exception of exacerbating absence seizures induced by AY-9944 (15,16,26). Lovastatin has also been found to be effective antiepileptic in fragile X syndrome by preventing excess hippocampal protein synthesis in an animal model (27).

In humans, statins were found to reduce epilepsy risk in the elderly, and mortality related to status epilepticus (28,29). Despite the amount of evidence in favor of a possible antiepileptic effect to statins, they were not studied in randomized clinical trials in humans.

Next, we will study high frequency oscillations and use statins in this group of patients to evaluate gamma oscillations as a possible biomarker for epileptogenesis in patients with tuberous sclerosis.

Due to the previously discussed relationship between HFOs and epileptogenesis, we hypothesize that they could be modulated by statins. Their spatial distribution or occurrence could be reduced which could explain in part how statins potentiate the effect of most commonly used antiepileptics. Additionally, we hypothesize that these direct effects on the epileptogenic network could be related to changes in brain metabolites such as glutamate, GABA or NAA which will be evaluated using MRS.

STUDY OBJECTIVES:

1. To study the effects of a pharmacological challenge, lovastatin 180 mg over three days, on brain oscillations and inhibition/excitation balance.

AIMS:

1. High frequency oscillations characterization in drug resistant patients
2. Mechanism of anticonvulsant effect of statins. Statins have been found to have neuroprotective, antiepileptic and anticonvulsant effects in animal models and human observational studies.

3. Relationship between dynamic GABA and HFOs in epilepsy
Our approach should allow us to study how dynamic GABA changes in the seizure onset zone evaluated by MRS correlate with similar changes in HFOs and possibly elucidating a link between brain metabolites and high frequency oscillations in epilepsy.

REFERENCES:

1. Sasa M. A new frontier in epilepsy: novel antiepileptogenic drugs. *J Pharmacol Sci* [Internet]. 2006 [cited 2016 Aug 30];100(5):487–94. Available from: <http://www.ncbi.nlm.nih.gov/pubmed/16799261>
2. Canevini MP, De Sarro G, Galimberti CA, Gatti G, Licchetta L, Malerba A, et al. Relationship between adverse effects of antiepileptic drugs, number of coprescribed drugs, and drug load in a large cohort of consecutive patients with drug-refractory epilepsy. *Epilepsia* [Internet]. 2010 May [cited 2016 Aug 30];51(5):797–804. Available from: <http://www.ncbi.nlm.nih.gov/pubmed/20545754>
3. Friedman A, Dingledine R. Molecular cascades that mediate the influence of inflammation on epilepsy. *Epilepsia* [Internet]. 2011 May [cited 2016 Aug 30];52(Suppl 3):33–9. Available from: <http://doi.wiley.com/10.1111/j.1528-1167.2011.03034.x>
4. Turrin NP, Rivest S. Innate immune reaction in response to seizures: implications for the neuropathology associated with epilepsy. *Neurobiol Dis* [Internet]. 2004 Jul [cited 2016 Aug 30];16(2):321–34. Available from: <http://www.ncbi.nlm.nih.gov/pubmed/15193289>
5. Gorter JA, van Vliet EA, Aronica E, Breit T, Rauwerda H, Lopes da Silva FH, et al. Potential new antiepileptogenic targets indicated by microarray analysis in a rat model for temporal lobe epilepsy. *J Neurosci* [Internet]. 2006 Oct 25 [cited 2016 Aug 30];26(43):11083–110. Available from: <http://www.ncbi.nlm.nih.gov/pubmed/17065450>
6. Dedeurwaerdere S, Friedman A, Fabene PF, Mazarati A, Murashima YL, Vezzani A, et al. Finding a better drug for epilepsy: antiinflammatory targets. *Epilepsia* [Internet]. 2012 Jul [cited 2016 Aug 30];53(7):1113–8. Available from: <http://www.ncbi.nlm.nih.gov/pubmed/22691043>

7. Vezzani A, Aronica E, Mazarati A, Pittman QJ. Epilepsy and brain inflammation. *Exp Neurol* [Internet]. 2013 Jun [cited 2016 Aug 30];244:11–21. Available from: <http://www.ncbi.nlm.nih.gov/pubmed/21985866>
8. D'Ambrosio R, Eastman CL, Fattore C, Perucca E. Novel frontiers in epilepsy treatments: preventing epileptogenesis by targeting inflammation. *Expert Rev Neurother* [Internet]. 2013 Jun [cited 2016 Aug 30];13(6):615–25. Available from: <http://www.ncbi.nlm.nih.gov/pubmed/23738999>
9. Weber MS, Youssef S, Dunn SE, Prod'homme T, Neuhaus O, Stuve O, et al. Statins in the treatment of central nervous system autoimmune disease. *J Neuroimmunol* [Internet]. 2006 Sep [cited 2016 Aug 30];178(1–2):140–8. Available from: <http://linkinghub.elsevier.com/retrieve/pii/S0165572806002128>
10. Clarke RM, Lyons A, O'Connell F, Deighan BF, Barry CE, Anyakoha NG, et al. A pivotal role for interleukin-4 in atorvastatin-associated neuroprotection in rat brain. *J Biol Chem* [Internet]. 2008 Jan 25 [cited 2016 Aug 30];283(4):1808–17. Available from: <http://www.ncbi.nlm.nih.gov/pubmed/17981803>
11. Pannu R, Christie DK, Barbosa E, Singh I, Singh AK. Post-trauma Lipitor treatment prevents endothelial dysfunction, facilitates neuroprotection, and promotes locomotor recovery following spinal cord injury. *J Neurochem* [Internet]. 2006 Nov 17 [cited 2016 Aug 30];101(1):182–200. Available from: <http://doi.wiley.com/10.1111/j.1471-4159.2006.04354.x>
12. Bösel J, Gandor F, Harms C, Synowitz M, Harms U, Djoufack PC, et al. Neuroprotective effects of atorvastatin against glutamate-induced excitotoxicity in primary cortical neurones. *J Neurochem* [Internet]. 2005 Mar [cited 2016 Aug 30];92(6):1386–98. Available from: <http://www.ncbi.nlm.nih.gov/pubmed/15748157>
13. Piermartiri TCB, Figueiredo CP, Rial D, Duarte FS, Bezerra SC, Mancini G, et al. Atorvastatin prevents hippocampal cell death, neuroinflammation and oxidative stress following amyloid- β (1-40) administration in mice: evidence for dissociation between cognitive deficits and neuronal damage. *Exp Neurol* [Internet]. 2010 Dec [cited 2016 Aug 30];226(2):274–84. Available from: <http://www.ncbi.nlm.nih.gov/pubmed/20816828>
14. Lee J-K, Won J-S, Singh AK, Singh I. Statin inhibits kainic acid-induced seizure and associated inflammation and hippocampal cell death. *Neurosci Lett*

[Internet]. 2008 Aug 8 [cited 2016 Aug 30];440(3):260–4. Available from: <http://www.ncbi.nlm.nih.gov/pubmed/18583044>

15. Funck VR, de Oliveira CV, Pereira LM, Rambo LM, Ribeiro LR, Royes LFF, et al. Differential effects of atorvastatin treatment and withdrawal on pentylentetrazol-induced seizures. *Epilepsia* [Internet]. 2011 Nov [cited 2016 Aug 30];52(11):2094–104. Available from: <http://www.ncbi.nlm.nih.gov/pubmed/21906051>

16. Uzüm G, Akgün-Dar K, Aksu U. The effects of atorvastatin on memory deficit and seizure susceptibility in pentylentetrazole-kindled rats. *Epilepsy Behav* [Internet]. 2010 Nov [cited 2016 Aug 30];19(3):284–9. Available from: <http://www.ncbi.nlm.nih.gov/pubmed/20888302>

17. Xie C, Sun J, Qiao W, Lu D, Wei L, Na M, et al. Administration of Simvastatin after Kainic Acid-Induced Status Epilepticus Restrains Chronic Temporal Lobe Epilepsy. Mouillet-Richard S, editor. *PLoS One* [Internet]. 2011 Sep 19 [cited 2016 Aug 30];6(9):e24966. Available from: <http://dx.plos.org/10.1371/journal.pone.0024966>

18. Russo E, Donato di Paola E, Gareri P, Siniscalchi A, Labate A, Gallelli L, et al. Pharmacodynamic potentiation of antiepileptic drugs' effects by some HMG-CoA reductase inhibitors against audiogenic seizures in DBA/2 mice. *Pharmacol Res* [Internet]. 2013 Apr [cited 2016 Aug 30];70(1):1–12. Available from: <http://www.ncbi.nlm.nih.gov/pubmed/23253428>

19. Citraro R, Chimirri S, Aiello R, Gallelli L, Trimboli F, Britti D, et al. Protective effects of some statins on epileptogenesis and depressive-like behavior in WAG/Rij rats, a genetic animal model of absence epilepsy. *Epilepsia* [Internet]. 2014 Aug [cited 2016 Aug 30];55(8):1284–91. Available from: <http://doi.wiley.com/10.1111/epi.12686>

20. Moezi L, Shafaroodi H, Hassanipour M, Fakhrzad A, Hassanpour S, Dehpour AR. Chronic administration of atorvastatin induced anti-convulsant effects in mice: the role of nitric oxide. *Epilepsy Behav* [Internet]. 2012 Apr [cited 2016 Aug 30];23(4):399–404. Available from: <http://www.ncbi.nlm.nih.gov/pubmed/22405864>

21. Shafaroodi H, Moezi L, Fakhrzad A, Hassanipour M, Rezayat M, Dehpour AR. The involvement of nitric oxide in the anti-seizure effect of acute atorvastatin

treatment in mice. *Neurol Res* [Internet]. 2012 Nov [cited 2016 Aug 30];34(9):847–53. Available from:

<http://www.ncbi.nlm.nih.gov/pubmed/22909758>

22. Ponce J, de la Ossa NP, Hurtado O, Millan M, Arenillas JF, Dávalos A, et al. Simvastatin reduces the association of NMDA receptors to lipid rafts: a cholesterol-mediated effect in neuroprotection. *Stroke* [Internet]. 2008 Apr [cited 2016 Aug 30];39(4):1269–75. Available from:

<http://www.ncbi.nlm.nih.gov/pubmed/18323503>

23. Ramirez C, Tercero I, Pineda A, Burgos JS. Simvastatin is the statin that most efficiently protects against kainate-induced excitotoxicity and memory impairment. *J Alzheimers Dis* [Internet]. 2011 [cited 2016 Aug 30];24(1):161–74.

Available from: <http://www.ncbi.nlm.nih.gov/pubmed/21224519>

24. Sun J, Xie C, Liu W, Lu D, Qiao W, Huang Q, et al. The effects of simvastatin on hippocampal caspase-3 and Bcl-2 expression following kainate-induced seizures in rats. *Int J Mol Med*. 2012;30(4):739–46.

25. Mainberger F, Jung NH, Zenker M, Wahlländer U, Freudenberg L, Langer S, et al. Lovastatin improves impaired synaptic plasticity and phasic alertness in patients with neurofibromatosis type 1. *BMC Neurol* [Internet]. 2013 [cited 2016 Aug 30];13:131. Available from: <http://www.ncbi.nlm.nih.gov/pubmed/24088225>

26. Serbanescu I, Ryan MA, Shukla R, Cortez MA, Snead OC, Cunnane SC. Lovastatin exacerbates atypical absence seizures with only minimal effects on brain sterols. *J Lipid Res* [Internet]. 2004 Nov [cited 2016 Aug 30];45(11):2038–43. Available from: <http://www.ncbi.nlm.nih.gov/pubmed/15314096>

27. Osterweil EK, Chuang S-C, Chubykin AA, Sidorov M, Bianchi R, Wong RKS, et al. Lovastatin corrects excess protein synthesis and prevents epileptogenesis in a mouse model of fragile X syndrome. *Neuron* [Internet]. 2013 Jan 23 [cited 2016 Aug 30];77(2):243–50. Available from: <http://www.ncbi.nlm.nih.gov/pubmed/23352161>

28. Sierra-Marcos A, Alvarez V, Faouzi M, Burnand B, Rossetti AO. Statins are associated with decreased mortality risk after status epilepticus. *Eur J Neurol* [Internet]. 2015 Feb [cited 2016 Aug 30];22(2):402–5. Available from: <http://www.ncbi.nlm.nih.gov/pubmed/24684345>

29. Nejm MB, Gouveia TL, da Graça Naffah-Mazacoratti M, Scorza CA, Cavalheiro EA, Scorza FA. Lovastatin and sudden unexpected death in epilepsy: a matter for debate. *Epilepsy Behav* [Internet]. 2013 Jul [cited 2016 Aug 30];28(1):10–1. Available from: <http://www.ncbi.nlm.nih.gov/pubmed/23648273>

30. Chu-Shore CJ, Major P, Camposano S, Muzykewicz D, Thiele EA. The natural history of epilepsy in tuberous sclerosis complex. *Epilepsia* [Internet]. 2010 Jul [cited 2017 Jan 31];51(7):1236–41. Available from: <http://www.ncbi.nlm.nih.gov/pubmed/20041940>

Supplementary Materials:

METHODOLOGICAL ASPECTS

Population definition:

Patients with focal-onset drug-resistant epilepsy (50% TSC-associated and 50% due to other etiologies), males and females (non-pregnant), who are competent enough to sign an informed consent. Patients should not have any metallic implants such as cardiac pacemakers, medication pumps, VNS, or history of active heart disease or stroke. Use of tricyclic antidepressants, bupropion, and neuroleptic medications is an exclusion criterion. Patients should not have any ictal autonomic features and should have no history of neurodegenerative disease.

Participants:

- Patients with non-invasive EEG and epilepsy: up to 12 epilepsy due to any cause

Visit 1:

- Obtain informed consent and explain the study protocol
- Give a box of the drug which could be either placebo or lovastatin:
 - o The box contains 9 pills of 20 grams “either placebo or lovastatin”
 - o The patient is instructed to take three pills per night for three consecutive nights
 - o The possible side effects of lovastatin were explained to the patient

- The patient is instructed to not make any changes to their antiepileptics

Visit 2:

- Perform EEG with Mooney and Gratings tasks (see Chapter 3: Mechanisms of action of tDCS neurostimulation on neurochemistry, neurophysiological responses, and oscillatory patterning in refractory epilepsy) for explanation of the tasks
- Perform MRS with one voxel in the EZ and another in the occipital region
- Give another box of the drug which will be the opposite of what was given in visit 1
 - The patient is instructed to start taking the pills three weeks after the date of visit 2
 - A reminder as a text message is sent to the patient one day before the supposed date to start taking the pills
 - The patient will come for the third visit after taking the third dose of the pills

Visit 3:

- Repeat EEG with tasks and MRS

Follow-up:

- All patients are to be contacted 30 days after concluding their participation in the study Repeat MRS

AMT-PET for the Localization of the EZ in TSC-Associated Epilepsy and Drug Resistant Epilepsy

INTRODUCTION:

Several molecular probes are being used in PET, however only alpha-[¹¹C]-methyl-L-Tryptophan (AMT) is the only biomarker that has been shown to be able to pinpoint the epileptic focus itself in the interictal state (Kumar et al., 2011). It has been estimated that one quarter of people with epilepsy will develop drug-resistant epilepsy (Kwan & Brodie, 2000) and such patients may benefit from surgery if accurate presurgical localization of the epileptogenic zone is possible. Unfortunately, most patients with drug resistant epilepsy have a discordance between their clinical, electrophysiological and imaging data that would make accurate localization of the EZ to be problematic. Several tracers of PET have been used in epilepsy and of these tracers is AMT. AMT traces tryptophan metabolism via the serotonin and/or kynurenine pathways. AMT can identify the EZ by showing a localized area of increased AMT uptake. One of the advantages of AMT over FDG-PET is that the signal of AMT is easier to interpret visually and because the tracer uptake is increased in the EZ unlike that of FDG, atrophy of the region of interest will not adversely affect the results. Another advantage of AMT-PET is that the results are not affected by the frequency of seizure activity or interictal discharges on scalp EEG (C. Juhász et al., 2003; Wakamoto et al., 2008) making it convenient to perform without the need of continuous EEG monitoring such as is the case with EEG-fMRI, Ictal-SPECT or Interictal-SPECT. Increased uptake of AMT in the EZ has been previously documented and explored by (Chugani, 2011).

Tuberous sclerosis complex (TSC) is an autosomal dominant disorder characterized by hamartomas in various body organs including the brain. Epilepsy is the most common neurologic presentation and is reported in up to 90% of patients with TSC (Chu-Shore et al., 2010; Józwiak et al., 2000). Most likely, the brain tubers and the associated cortical dysplasia are the main key players in epileptogenesis in TSC (Crino, 2004; Uhlmann et al., 2002). It has been suggested that up to two thirds of TSC-associated epilepsy cases will eventually develop drug-resistant epilepsy (Chu-Shore et al., 2010). TSC-associated drug resistant epilepsy patients who do not undergo aggressive treatment will develop

epileptic encephalopathy and poor cognitive outcome. The issue with TSC is that there is a large number of multifocal tubers throughout the brain, however not all of them are epileptogenic (Jansen et al., 2007; Kagawa et al., 2005; Teutonico et al., 2008; Weiner et al., 2006; Wu et al., 2010). Therefore, it is reasonable to look for methods of identifying the epileptogenic tubers from non-epileptogenic ones. FDG-PET shows hypometabolism in all kinds of tubers, making it unsuitable to identify truly epileptogenic tubers from non-epileptogenic tubers (Rintahaka & Chugani, 1997; Szelies et al., 1983). On the other hand, seizures in TSC patients tend to be very brief making them unsuitable for ictal SPECT. AMT-PET is a potentially helpful and promising tracer in such patients with drug-resistant epilepsy including TSC-associated and those with focal cortical dysplasias (Asano et al., 2000; Chugani et al., 1998; Marco Fedi et al., 2003). AMT-PET is helpful because it has been shown that its uptake is increased only in epileptogenic tubers (Asano et al., 2000; Chugani et al., 1998). In many TSC-associated epilepsy patients, the EEG point towards a bilateral source or EEG changes are diffuse because the location of the tubers is deep.

Cortical developmental malformations also show increased AMT uptake (M. Fedi et al., 2001). This is helpful as in a significant number of patients with drug resistant epilepsy the etiology is a focal cortical dysplasia that cannot be easily identified by MRI (Jeha et al., n.d.). It is estimated that 10 to 40% of people with a cortical developmental malformation will have a normal MRI (Jeha et al., n.d.).

Study Objectives

To evaluate tryptophan metabolism via serotonin and/or kynurenine pathways in an attempt to identify the epileptogenic zone in TSC-associated epilepsy and drug resistant epilepsy of other etiologies.

Aims:

- Epileptogenic tuber localization in patients with TSC-associated drug resistant epilepsy
- Epileptogenic zone localization in patients with drug resistant epilepsy due to cortical developmental malformations (focal cortical dysplasia, periventricular heterotopia, congenital perisylvian syndrome and polymicrogyria)

- Characterization of AMT uptake by other brain tumors
- To assess cortical plasticity after cortical resection in surgical epilepsy patients

References:

- Asano, E., Chugani, D. C., Muzik, O., Shen, C., Juhász, C., Janisse, J., Ager, J., Canady, A., Shah, J. R., Shah, A. K., Watson, C., & Chugani, H. T. (2000). Multimodality imaging for improved detection of epileptogenic foci in tuberous sclerosis complex. *Neurology*, 54(10), 1976–1984. <https://doi.org/10.1212/WNL.54.10.1976>
- Chugani, D. C. (2011). α -methyl-L-tryptophan: Mechanisms for tracer localization of epileptogenic brain regions. In *Biomarkers in Medicine* (Vol. 5, Issue 5, pp. 567–575). *Biomark Med.* <https://doi.org/10.2217/bmm.11.73>
- Chugani, D. C., Chugani, H. T., Muzik, O., Shah, J. R., Shah, A. K., Canady, A., Mangner, T. J., & Chakraborty, P. K. (1998). Imaging epileptogenic tubers in children with tuberous sclerosis complex using α -[11C]methyl-L-tryptophan positron emission tomography. *Annals of Neurology*, 44(6), 858–866. <https://doi.org/10.1002/ana.410440603>
- Chu-Shore, C. J., Major, P., Camposano, S., Muzykewicz, D., & Thiele, E. A. (2010). The natural history of epilepsy in tuberous sclerosis complex. *Epilepsia*, 51(7), 1236–1241. <https://doi.org/10.1111/j.1528-1167.2009.02474.x>
- Crino, P. B. (2004). Molecular pathogenesis of tuber formation in tuberous sclerosis complex. In *Journal of Child Neurology* (Vol. 19, Issue 9, pp. 716–725). BC Decker Inc. <https://doi.org/10.1177/08830738040190091301>
- Fedi, M., Reutens, D., Okazawa, H., Andermann, F., Boling, W., Dubeau, F., White, C., Nakai, A., Gross, D. W., Andermann, E., & Diksic, M. (2001). Localizing value of α -methyl-L-tryptophan PET in intractable epilepsy of neocortical origin. *Neurology*, 57(9), 1629–1636. <https://doi.org/10.1212/WNL.57.9.1629>
- Fedi, Marco, Reutens, D. C., Andermann, F., Okazawa, H., Boling, W., White, C., Dubeau, F., Nakai, A., Gross, D. W., Andermann, E., & Diksic, M. (2003). α -[11C]-methyl-L-tryptophan PET identifies the epileptogenic tuber and correlates with interictal spike frequency. *Epilepsy Research*, 52(3), 203–213. [https://doi.org/10.1016/S0920-1211\(02\)00216-4](https://doi.org/10.1016/S0920-1211(02)00216-4)
- Jansen, F. E., van Huffelen, A. C., Algra, A., & van Nieuwenhuizen, O. (2007). Epilepsy surgery in tuberous sclerosis: A systematic review. In *Epilepsia* (Vol. 48, Issue 8, pp. 1477–1484). *Epilepsia.* <https://doi.org/10.1111/j.1528-1167.2007.01117.x>
- Jeha, L., Najm, I., Bingaman, W., Brain, D. D., & 2007, undefined. (n.d.). Surgical outcome and prognostic factors of frontal lobe epilepsy surgery. *Academic.Oup.Com.* Retrieved October 25, 2020, from <https://academic.oup.com/brain/article-abstract/130/2/574/287391>
- Józwiak, S., Schwartz, R. A., Janniger, C. K., & Bielicka-Cymerman, J. (2000). Usefulness of diagnostic criteria of tuberous sclerosis complex in pediatric patients. *Journal of Child Neurology*, 15(10), 652–659. <https://doi.org/10.1177/088307380001501003>
- Juhász, C., Chugani, D. C., Muzik, O., Shah, A., Asano, E., Mangner, T. J., Chakraborty, P. K., Sood, S., & Chugani, H. T. (2003). Alpha-methyl-L-tryptophan

- PET detects epileptogenic cortex in children with intractable epilepsy. *Neurology*, 60(6), 960–968. <https://doi.org/10.1212/01.WNL.0000049468.05050.F2>
- Juhász, Csaba, Chugani, D. C., Muzik, O., Wu, D., Sloan, A. E., Barger, G., Watson, C., Shah, A. K., Sood, S., Ergun, E. L., Mangner, T. J., Chakraborty, P. K., Kupsky, W. J., & Chugani, H. T. (2006). In vivo uptake and metabolism of α -[11C]methyl-L-tryptophan in human brain tumors. *Journal of Cerebral Blood Flow and Metabolism*, 26(3), 345–357. <https://doi.org/10.1038/sj.jcbfm.9600199>
- Juhász, Csaba, Muzik, O., Chugani, D. C., Chugani, H. T., Sood, S., Chakraborty, P. K., Barger, G. R., & Mittal, S. (2011). Differential kinetics of α -[11C]methyl-L-tryptophan on PET in low-grade brain tumors. *Journal of Neuro-Oncology*, 102(3), 409–415. <https://doi.org/10.1007/s11060-010-0327-1>
- Kagawa, K., Chugani, D. C., Asano, E., Juhász, C., Muzik, O., Shah, A., Shah, J., Sood, S., Kupsky, W. J., Mangner, T. J., Chakraborty, P. K., & Chugani, H. T. (2005). Epilepsy surgery outcome in children with tuberous sclerosis complex evaluated with α -[11C]methyl-L-tryptophan positron emission tomography (PET). *Journal of Child Neurology*, 20(5), 429–438. <https://doi.org/10.1177/08830738050200050701>
- Kumar, A., Asano, E., & Chugani, H. T. (2011). α -[11C]-methyl-L-tryptophan PET for tracer localization of epileptogenic brain regions: Clinical studies. In *Biomarkers in Medicine* (Vol. 5, Issue 5, pp. 577–584). NIH Public Access. <https://doi.org/10.2217/bmm.11.68>
- Kwan, P., & Brodie, M. J. (2000). Early identification of refractory epilepsy. *New England Journal of Medicine*, 342(5), 314–319. <https://doi.org/10.1056/NEJM200002033420503>
- Rintahaka, P. J., & Chugani, H. T. (1997). Clinical role of positron emission tomography in children with tuberous sclerosis complex. *Journal of Child Neurology*, 12(1), 42–52. <https://doi.org/10.1177/088307389701200107>
- Szelies, B., Herholz, K., Heiss, W. D., Rackl, A., Pawlik, G., Wagner, R., Ilsen, H. W., & Wienhard, K. (1983). Hypometabolic cortical lesions in tuberous sclerosis with epilepsy: Demonstration by positron emission tomography. *Journal of Computer Assisted Tomography*, 7(6), 946–953. <https://doi.org/10.1097/00004728-198312000-00002>
- Teutonico, F., Mai, R., Devinsky, O., Io Russo, G., Weiner, H. L., Borrelli, P., Balottin, U., & Veggiotti, P. (2008). Epilepsy surgery in tuberous sclerosis complex: Early predictive elements and outcome. *Child's Nervous System*, 24(12), 1437–1445. <https://doi.org/10.1007/s00381-008-0679-4>
- Uhlmann, E. J., Wong, M., Baldwin, R. L., Bajenaru, M. L., Onda, H., Kwiatkowski, D. J., Yamada, K., & Gutmann, D. H. (2002). Astrocyte-specific TSC1 conditional knockout mice exhibit abnormal neuronal organization and seizures. *Annals of Neurology*, 52(3), 285–296. <https://doi.org/10.1002/ana.10283>
- Wakamoto, H., Chugani, D. C., Juhász, C., Muzik, O., Kupsky, W. J., & Chugani, H. T. (2008). Alpha-Methyl-L-Tryptophan Positron Emission Tomography in Epilepsy With Cortical Developmental Malformations. *Pediatric Neurology*, 39(3), 181–188. <https://doi.org/10.1016/j.pediatrneurol.2008.05.014>
- Weiner, H. L., Carlson, C., Ridgway, E. B., Zaroff, C. M., Miles, D., LaJoie, J., & Devinsky, O. (2006). Epilepsy surgery in young children with tuberous sclerosis: Results of a novel approach. *Pediatrics*, 117(5), 1494–1502. <https://doi.org/10.1542/peds.2005-1206>

Wu, J. Y., Salamon, N., Kirsch, H. E., Mantle, M. M., Nagarajan, S. S., Kurelowech, L., Aung, M. H., Sankar, R., Shields, W. D., & Mathern, G. W. (2010). Noninvasive testing, early surgery, and seizure freedom in tuberous sclerosis complex. *Neurology*, 74(5), 392–398. <https://doi.org/10.1212/WNL.0b013e3181ce5d9e>

Supplementary Materials:

Methods:

Subjects:

- Adult and children will be included
- The patient must have focal onset drug-resistant epilepsy
- A presumed epileptic focus is needed for each patient based on seizure's semiology, and scalp or intracranial EEG
- No evidence of other psychiatric disease
- No evidence of isolated mesial temporal sclerosis or focal cerebral atrophy because of a previous cerebrovascular event

Technique:

- Duration of the PET study is 60 minutes
- A PET/CT GEMINI GXL Philips scanner is used
- The patient is instructed to fast for six hours and to consume a low-protein diet on the previous day of the scan
- Children may be sedated by an anesthetist or a pediatrician. Pentobarbital, fentanyl or midazolam may be used based on the child's age
- Patients will be closely monitored during the scan time to detect any seizures
- Adequate hydration will be provided to allow for good radiopharmaceutical excretion
- A venous line will be placed for tracer administration. A second venous line will be placed for the collection of timed blood samples to be collected at 0, 20, 30, 40, 50, and 60 minutes after AMT injection
- The arms will be placed below head in supine position during the acquisition

Radiopharmaceutical:

- AMT will be administered
- Slow IV administration over 2 minutes period
- Children's dose: 0.1 mCi/Kg
- Adults dose: 370 MBq in average

Image Acquisition:

- Acquisition starts after tracer administration and post-voiding
- Qualitative and semiquantitative image analysis by nuclear medicine physician

Blood sample protocol:

- A 0.5 mL sample will be collected at the previously mentioned time points after AMT injection similar to Juasz approach (Csaba Juhász et al., 2006, 2011).
- After 20 minute of AMT injection, a 20-minute dynamic PET scan of the heart will be performed in a 2D model to obtain the left ventricular input function
- At 25 minute of AMT injection, a dynamic emission scan of the brain will be acquired in a high-sensitivity 3D mode
- Measured attenuation correction obtained from transmission scans is applied to the AMT-PET images
- Summed activity images of AMT concentration in the brain and tumors are created to visualize the results

Outcome measures:

- Was the EZ localized by the AMT-PET scan
- Concordance with multimodal imaging approach in the presurgical evaluation
- Impact of AMT-PET result on surgical decision

CONCLUDING REMARKS:

The excitation-inhibition balance hypothesis is an exciting topic that is intriguing to neuroscientists and neurologists. Understanding the impact of different diseases on the E-I balance not only serve our comprehension of the pathogenesis of such complex disorders, but can also shed light onto the fine line between physiologic adaptations of the GABAergic system and pathologic states. In this work we studied the different effects of two common disorders that are clearly linked to an abnormal E-I balance and showed how the integrity of the GABAergic system is important at the local and distant neural circuit level. This chapter summarizes the findings of our work and their relevance for further studies.

Type 2 Diabetes Mellitus Affects the Occipital Cortex

One of the most feared complications of T2DM is visual and cognitive impairment. In the first study related to T2DM we reported three main novel findings related to T2DM visual performance in early diabetic retinopathy. We used novel chromatic, achromatic and speed discrimination visual tasks in this study, for which T2DM patients scored worse than healthy controls. We also found that they had a lower best corrected visual acuity (BCVA) and that their BCVA correlated with metabolic and retinal biomarkers. However, their poor performance on speed and achromatic luminance discrimination tasks could only be explained by impaired cortical processing.

The visual psychophysical tasks used in this study were partially dependent on contrast detection of moving dots. We chose this paradigm because of the growing evidence of impaired contrast-dependent visual processing in T2DM (Reis et al., 2014). Occipital cortical GABA concentration is reported to be elevated in T2DM (van Bussel et al., 2016) especially in patients with evidence of cognitive impairment. The visual tasks used in our study can be considered a special type of combination of contrast and motion detection which have been previously related to cortical processing and occipital inhibitory circuits (Edden et al., 2009). We showed that speed and achromatic luminance discrimination thresholds were correlated with occipital GABA at baseline and also predicted one year later. We showed that patients who had a higher occipital GABA

concentration had worse performance on these visual tasks. Accordingly, we concluded that higher GABA concentration in the occipital cortex in T2DM has a deleterious effect on visual performance, similar to the previously reported adverse effects on cognitive integrity (van Bussel et al., 2016).

In the second study in this disease model we investigated the relationship between BRB and BBB disruption in T2DM and BBB permeability could relate to visual performance. There is growing evidence of BBB disruption in T2DM. First, it has been previously reported that BBB integrity is compromised in T2DM by in vitro and in vivo experimental models (Pasquier et al., 2006). BBB permeability is increased in aging rhesus monkeys with T2DM (Xu et al., 2017). These disruptions of the BBB in T2DM have been previously linked to impaired cognition even before the onset of microvascular or macrovascular disease in T2DM (Bogush et al., 2017).

BRB leakage in T2DM is well established (Klein et al., 1984) and is linked to hyperglycemia, hyperlipidemia and hypertension which are possible complications of T2DM. As these same insulting factors are also associated with BBB disruption in other diseases, it was reasonable to assume that the BBB in T2DM is also somehow disrupted. There is growing evidence of BBB disruption in patients with BRB leakage in addition to an increased risk of cortical small-vessel disease (Cheung et al., 2010). Our findings however point to the independence of the two barriers in the early stages of T2DM. We found that BBB permeability is not linked to the grade of diabetic retinopathy, number of microaneurysms or the presence/absence of macular leakage. Interestingly, BBB permeability was positively correlated with HbA1C only in type 2 diabetics with established BRB leakage. Such patients with poor metabolic control have been reported to have an elevated E-I ratio suggesting a link between metabolic control, neurotransmission in T2DM (d'Almeida et al., 2020). Moreover, in T1DM, poor metabolic control was associated with increased markers of neuroinflammation, further linking neuroinflammation, neurotransmission and metabolic control together (d'Almeida et al., 2020). As HbA1C is related to advanced glycation processes, we conclude that BBB disruption occurs in response to advanced glycation end-products which is in agreement with animal model studies (Shimizu et al., 2013). Finally, we looked for a correlation between

BBB permeability and best corrected visual acuity. BBB permeability in the occipital lobe was predictive of BCVA at baseline, 12 and 24 months later only in type 2 diabetics with established BRB leakage. Clearly, BBB disruption in the occipital lobe contributes to visual impairment in this group of patients, adding to the identified contribution of GABA

An association between T2DM and BBB disruption has been previously reported (Hawkins et al., 2007). We hypothesize that the main mechanism of BBB disruption in T2DM is endothelial and small vessel pathology induced by chronic inflammation, oxidative stress and poor metabolic control which is in agreement with the literature (Janelidze et al., 2017; Tousoulis et al., 2013). Our results are unique in that they show BBB disruption in the visual cortex is linked to visual impairment in T2DM which is similar to the results of a previously published study on a rat model which showed altered fMRI response to visual stimuli if the BBB is disrupted (Fa et al., 2011).

In conclusion, BBB permeability is predictive of visual impairment in T2DM especially in patients with established BRB leakage. We hypothesize that this is the case because of the evidence of increased risk of cortical small vessel disease and BBB disruption in patients with BRB disruption. These findings will need in the future to be integrated with the neurotransmission changes in E/I balance in T2DM,

Physiological relevance of High Frequency Activity: a role in Perceptual Decision Making

Gamma activity and high frequency activity are both linked to physiologic and pathologic GABAergic mediated mechanisms (Gulyas et al., 2010; Lewis et al., 2005; Mann & Paulsen, 2007; Uhlhaas et al., 2009; Whittington et al., 2011). We first studied physiologic gamma oscillations in a cohort of drug resistant epilepsy patients and how their spatiotemporal maps are related to perceptual decision-making and object recognition.

Our results showed that there is evidence of topographic organization of visual sensory and perceptual processing. First, we found that low gamma and beta activity spatially involved the anterior regions (ventral and regions involved in dorsoventral integration) during perceptual decision and objective recognition. Higher frequency activity up to 250 Hz was confined to the posterior areas

(Nagasawa et al., 2012) early during sensory processing. It has been previously reported that many cognitive processes may induce gamma activity in the occipital, occipito-temporal and inferior frontal regions (Cho-Hisamoto et al., 2015; Crone et al., 2006; de Pestors et al., 2016; Engell & McCarthy, 2011; Hermes et al., 2015; Lachaux et al., 2005; Michalareas et al., 2016). However, this is the first study to show how high frequency activity is clustered among different regions in relation to time and type of process. Our findings also showed that spatial organization of high gamma activity is related to object recognition regardless of the nature of the presented object, suggesting a general processing mechanism.

As this high frequency activity is generated by inhibitory circuits in the neocortex, we consider them in the scope of this thesis, by identifying a physiological basis for high frequency oscillations.

GABAergic System Dysfunction in Drug Resistant Epilepsy

Epilepsy is a very common neurological disorder and approximately 30% of those with epilepsy will not respond to antiepileptic drugs in maximum dose (Berg, 2009; Berg et al., 2010). The main question in such patients is whether localization of seizure's onset is possible which would render them possible candidates for resection surgery (Chandra et al., 2010).

GABA is the main inhibitory neurotransmitter in the brain. It is easy to understand how a decreased inhibitory tone in the cortex might be related to epileptogenesis which is the case in patients with drug-responsive epilepsies. However, several studies pointed to the possibility of a dual action of GABA in the epileptogenic zone where they reported elevated GABA concentration in focal cortical dysplasia, tuberous sclerosis associated epilepsy, and in patients with drug-resistant epilepsy in general (Cepeda et al., 2007; Cherubini et al., 1991). Several studies from intracranial EEG showed that patients with drug resistant epilepsy typically have areas that generate pathologic interictal HFOs and the generation of HFOs is also dependent on spontaneous inhibitory postsynaptic currents (Cepeda et al., 2006).

In our second study related to epilepsy as a disease model, we investigated the possible mechanism of action of cathodal tDCS as an antiepileptic in patients with drug resistant epilepsy of temporal lobe origin. We showed that at baseline,

GABA levels were significantly higher in the epileptogenic zone as compared to the occipital region. Increased GABA tone measured by infrared videomicroscopy and whole-cell patch clamp recordings on biopsied samples of the epileptogenic zone in patients with drug resistant epilepsy has been reported before in the literature (Cepeda et al., 2006, 2020, 2007), however this was the first study to compare GABA concentration in the EZ to that in a reference area (the occipital lobe).

Cathodal stimulation of the EZ resulted in a significant decrease in GABA concentration which is a novel finding and to our knowledge this is the first study to report this in human subjects. In addition to decreasing GABA in the EZ, cathodal stimulation also reduced interictal discharges by 61%, which could be translated as a decrease in cortical epileptogenesis. A recent modeling study showed that cathodal stimulation in drug resistant epilepsy will mainly suppress GABAergic interneurons in a computer model which is associated with decreased number of epileptic spikes (Denoyer et al., 2020).

Moreover, a recent study showed that pathological HFOs are associated with increased GABAergic synaptic activity in the epileptic focus (Cepeda et al., 2020). We chose to study the effects of cathodal stimulation on evoked gamma oscillations in the EZ as compared to the occipital region. In summary, we found that low gamma oscillations were evoked by certain visual tasks in the temporal region (epileptogenic zone) and were absent in the occipital region at baseline. After cathodal stimulation of the epileptogenic zone, we showed that evoked gamma oscillations were suppressed in the epileptogenic zone and rescued in the occipital region. This is one of the most relevant findings of our work, because it suggests a long-range delicate balance of the control of neural oscillations. We therefore suggest that GABAergic inhibition tone in distant networks need to be in balance. When GABA concentration was markedly elevated in the EZ as compared to the occipital region, optimum processing of visual information was defective in the occipital region. After a balance was restored between EZ and occipital GABA (EZ/Occipital GABA ratio reduced from 1.31 to 1.08 $p = 0.031$), gamma oscillations were evoked in the occipital region as one would normally expect with the used visual tasks in our study. These findings can be seen as generalization to a more global framework of the hypothesis of local synchrony

balance (Uhlhaas et al., 2009; Uhlhaas & Singer, 2006) given that local synchrony is mediated by GABAergic tone.

Conclusion

In summary, we showed that the GABAergic system is disrupted in T2DM and epilepsy. In both of these conditions, an elevated GABA concentration was associated with an adverse outcome.

In the case of T2DM, higher occipital GABA was associated with poor visual performance and metabolic control. Additionally, we showed that BBB is disrupted in the occipital region of patients with T2DM, and this can predict BCVA and visual performance up to one year later.

Finally, we show that higher frequency oscillations are mediated by the GABAergic system and a balance is needed for optimum functioning. In line with this tenet, we showed that c-tDCS works as an antiepileptic by decreasing GABA concentration in the epileptogenic zone, suppressing abnormal gamma oscillations, and restoring a balance of local synchrony in the brain.

References:

- Berg, A. T. (2009). Identification of Pharmacoresistant Epilepsy. In *Neurologic Clinics* (Vol. 27, Issue 4, pp. 1003–1013). Elsevier. <https://doi.org/10.1016/j.ncl.2009.06.001>
- Berg, A. T., Berkovic, S. F., Brodie, M. J., Buchhalter, J., Cross, J. H., van Emde Boas, W., Engel, J., French, J., Glauser, T. A., Mathern, G. W., Moshé, S. L., Nordli, D., Plouin, P., & Scheffer, I. E. (2010). Revised terminology and concepts for organization of seizures and epilepsies: Report of the ILAE Commission on Classification and Terminology, 2005-2009. *Epilepsia*, 51(4), 676–685. <https://doi.org/10.1111/j.1528-1167.2010.02522.x>
- Bogush, M., Heldt, N. A., & Persidsky, Y. (2017). Blood Brain Barrier Injury in Diabetes: Unrecognized Effects on Brain and Cognition. In *Journal of Neuroimmune Pharmacology* (Vol. 12, Issue 4, pp. 593–601). Springer New York LLC. <https://doi.org/10.1007/s11481-017-9752-7>
- Cepeda, C., André, V. M., Levine, M. S., Salamon, N., Miyata, H., Vinters, H. v., & Mathern, G. W. (2006). Epileptogenesis in pediatric cortical dysplasia: The dysmature cerebral developmental hypothesis. In *Epilepsy and Behavior* (Vol. 9, Issue 2, pp. 219–235). Academic Press. <https://doi.org/10.1016/j.yebeh.2006.05.012>
- Cepeda, C., André, V. M., Wu, N., Yamazaki, I., Uzgil, B., Vinters, H. v., Levine, M. S., & Mathern, G. W. (2007). Immature neurons and GABA networks may contribute to epileptogenesis in pediatric cortical dysplasia. *Epilepsia*, 48(SUPPL. 5), 79–85. <https://doi.org/10.1111/j.1528-1167.2007.01293.x>
- Cepeda, C., Levinson, S., Nariai, H., Yazon, V. W., Tran, C., Barry, J., Oikonomou, K. D., Vinters, H. v., Fallah, A., Mathern, G. W., & Wu, J. Y. (2020). Pathological high frequency oscillations associate with increased GABA synaptic activity in

- pediatric epilepsy surgery patients. *Neurobiology of Disease*, 134, 104618.
<https://doi.org/10.1016/j.nbd.2019.104618>
- Chandra, P., Neurology, M. T.-A. of I. A. of, & 2010, undefined. (n.d.). Epilepsy surgery: recommendations for India. Ncbi.Nlm.Nih.Gov. Retrieved October 24, 2020, from <https://www.ncbi.nlm.nih.gov/pmc/articles/pmc2924525/>
- Cherubini, E., Gaiarsa, J. L., & Ben-Ari, Y. (1991). GABA: an excitatory transmitter in early postnatal life. *Trends in Neurosciences*, 14(12), 515–519.
[https://doi.org/10.1016/0166-2236\(91\)90003-D](https://doi.org/10.1016/0166-2236(91)90003-D)
- Cheung, N., Mosley, T., Islam, A., Kawasaki, R., Sharrett, A. R., Klein, R., Coker, L. H., Knopman, D. S., Shibata, D. K., Catellier, D., & Wong, T. Y. (2010). Retinal microvascular abnormalities and subclinical magnetic resonance imaging brain infarct: A prospective study. *Brain*, 133(7), 1987–1993.
<https://doi.org/10.1093/brain/awq127>
- Cho-Hisamoto, Y., Kojima, K., Brown, E. C., Matsuzaki, N., & Asano, E. (2015). Gamma activity modulated by naming of ambiguous and unambiguous images: Intracranial recording. *Clinical Neurophysiology*, 126(1), 17–26.
<https://doi.org/10.1016/j.clinph.2014.03.034>
- Crone, N. E., Sinai, A., & Korzeniewska, A. (2006). Chapter 19 High-frequency gamma oscillations and human brain mapping with electrocorticography. In *Progress in Brain Research* (Vol. 159, pp. 275–295). Prog Brain Res.
[https://doi.org/10.1016/S0079-6123\(06\)59019-3](https://doi.org/10.1016/S0079-6123(06)59019-3)
- d’Almeida, O. C., Violante, I. R., Quendera, B., Moreno, C., Gomes, L., & Castelo-Branco, M. (2020). The neurometabolic profiles of GABA and Glutamate as revealed by proton magnetic resonance spectroscopy in type 1 and type 2 diabetes. *PLOS ONE*, 15(10), e0240907.
<https://doi.org/10.1371/journal.pone.0240907>
- de Pestors, A., Coon, W. G., Brunner, P., Gunduz, A., Ritaccio, A. L., Brunet, N. M., de Weerd, P., Roberts, M. J., Oostenveld, R., Fries, P., & Schalk, G. (2016). Alpha power indexes task-related networks on large and small scales: A multimodal ECoG study in humans and a non-human primate. *NeuroImage*, 134, 122–131. <https://doi.org/10.1016/j.neuroimage.2016.03.074>
- Denoyer, Y., Merlet, I., Wendling, F., & Benquet, P. (2020). Modelling acute and lasting effects of tDCS on epileptic activity. *Journal of Computational Neuroscience*, 48(2), 161–176. <https://doi.org/10.1007/s10827-020-00745-6>
- Edden, R. A. E., Muthukumaraswamy, S. D., Freeman, T. C. A., & Singh, K. D. (2009). Orientation discrimination performance is predicted by GABA concentration and gamma oscillation frequency in human primary visual cortex. *Journal of Neuroscience*, 29(50), 15721–15726.
<https://doi.org/10.1523/JNEUROSCI.4426-09.2009>
- Engell, A. D., & McCarthy, G. (2011). The relationship of gamma oscillations and face-specific ERPs recorded subdurally from occipitotemporal cortex. *Cerebral Cortex*, 21(5), 1213–1221. <https://doi.org/10.1093/cercor/bhq206>
- Fa, Z., Zhang, R., Li, P., Zhang, J., Zhang, P., Zhu, S., Wu, Q., Huang, F., Liu, Y., Yang, L., Chang, H., Wen, Z., Gao, D., Zeng, Y., & Jiang, X. (2011). Effects of temporarily disrupting BBB on activity-induced manganese-dependent functional MRI. *Brain Imaging and Behavior*, 5(3), 181–188.
<https://doi.org/10.1007/s11682-011-9122-7>
- Gulyas, A. I., Szabo, G. G., Ulbert, I., Holderith, N., Monyer, H., Erdelyi, F., Szabo, G., Freund, T. F., & Hajos, N. (2010). Parvalbumin-Containing Fast-Spiking

- Basket Cells Generate the Field Potential Oscillations Induced by Cholinergic Receptor Activation in the Hippocampus. *Journal of Neuroscience*, 30(45), 15134–15145. <https://doi.org/10.1523/JNEUROSCI.4104-10.2010>
- Hawkins, B. T., Lundeen, T. F., Norwood, K. M., Brooks, H. L., & Egleton, R. D. (2007). Increased blood-brain barrier permeability and altered tight junctions in experimental diabetes in the rat: Contribution of hyperglycaemia and matrix metalloproteinases. *Diabetologia*, 50(1), 202–211. <https://doi.org/10.1007/s00125-006-0485-z>
- Hermes, D., Miller, K. J., Wandell, B. A., & Winawer, J. (2015). Gamma oscillations in visual cortex: The stimulus matters. In *Trends in Cognitive Sciences* (Vol. 19, Issue 2, pp. 57–58). Elsevier Ltd. <https://doi.org/10.1016/j.tics.2014.12.009>
- Janelidze, S., Hertze, J., Nägga, K., Nilsson, K., Nilsson, C., Wennström, M., van Westen, D., Blennow, K., Zetterberg, H., & Hansson, O. (2017). Increased blood-brain barrier permeability is associated with dementia and diabetes but not amyloid pathology or APOE genotype. *Neurobiology of Aging*, 51, 104–112. <https://doi.org/10.1016/j.neurobiolaging.2016.11.017>
- Klein, R., Klein, B. E. K., Moss, S. E., Davis, M. D., & DeMets, D. L. (1984). The Wisconsin Epidemiologic Study of Diabetic Retinopathy: IV. Diabetic Macular Edema. *Ophthalmology*, 91(12), 1464–1474. [https://doi.org/10.1016/S0161-6420\(84\)34102-1](https://doi.org/10.1016/S0161-6420(84)34102-1)
- Lachaux, J. P., George, N., Tallon-Baudry, C., Martinerie, J., Hugueville, L., Minotti, L., Kahane, P., & Renault, B. (2005). The many faces of the gamma band response to complex visual stimuli. *NeuroImage*, 25(2), 491–501. <https://doi.org/10.1016/j.neuroimage.2004.11.052>
- Lewis, D. A., Hashimoto, T., & Volk, D. W. (2005). Cortical inhibitory neurons and schizophrenia. In *Nature Reviews Neuroscience* (Vol. 6, Issue 4, pp. 312–324). Nature Publishing Group. <https://doi.org/10.1038/nrn1648>
- Mann, E. O., & Paulsen, O. (2007). Role of GABAergic inhibition in hippocampal network oscillations. In *Trends in Neurosciences* (Vol. 30, Issue 7, pp. 343–349). *Trends Neurosci.* <https://doi.org/10.1016/j.tins.2007.05.003>
- Michalareas, G., Vezoli, J., van Pelt, S., Schoffelen, J. M., Kennedy, H., & Fries, P. (2016). Alpha-Beta and Gamma Rhythms Subserve Feedback and Feedforward Influences among Human Visual Cortical Areas. *Neuron*, 89(2), 384–397. <https://doi.org/10.1016/j.neuron.2015.12.018>
- Nagasawa, T., Juhász, C., Rothermel, R., Hoehstetter, K., Sood, S., & Asano, E. (2012). Spontaneous and visually driven high-frequency oscillations in the occipital cortex: Intracranial recording in epileptic patients. *Human Brain Mapping*, 33(3), 569–583. <https://doi.org/10.1002/hbm.21233>
- Pasquier, F., Boulogne, A., Leys, D., & Fontaine, P. (2006). Diabetes mellitus and dementia. In *Diabetes and Metabolism* (Vol. 32, Issue 5, pp. 403–414). Elsevier Masson SAS. [https://doi.org/10.1016/S1262-3636\(07\)70298-7](https://doi.org/10.1016/S1262-3636(07)70298-7)
- Reis, A., Mateus, C., Melo, P., Figueira, J., Cunha-Vaz, J., & Castelo-Branco, M. (2014). Neuroretinal dysfunction with intact blood-retinal barrier and absent vasculopathy in type 1 diabetes. *Diabetes*, 63(11), 3926–3937. <https://doi.org/10.2337/db13-1673>
- Shimizu, F., Sano, Y., Tominaga, O., Maeda, T., Abe, M. aki, & Kanda, T. (2013). Advanced glycation end-products disrupt the blood-brain barrier by stimulating the release of transforming growth factor- β by pericytes and vascular endothelial growth factor and matrix metalloproteinase-2 by endothelial cells in

- vitro. *Neurobiology of Aging*, 34(7), 1902–1912.
<https://doi.org/10.1016/j.neurobiolaging.2013.01.012>
- Tousoulis, D., Papageorgiou, N., Androulakis, E., Siasos, G., Latsios, G., Tentolouris, K., & Stefanadis, C. (2013). Diabetes mellitus-associated vascular impairment: Novel circulating biomarkers and therapeutic approaches. In *Journal of the American College of Cardiology* (Vol. 62, Issue 8, pp. 667–676). Elsevier USA. <https://doi.org/10.1016/j.jacc.2013.03.089>
- Uhlhaas, P. J., Pipa, G., Lima, B., Melloni, L., Neuenschwander, S., Nikolić, D., & Singer, W. (2009). Neural synchrony in cortical networks: History, concept and current status. *Frontiers in Integrative Neuroscience*, 3(JUL), 17.
<https://doi.org/10.3389/neuro.07.017.2009>
- Uhlhaas, P. J., & Singer, W. (2006). Neural synchrony in brain disorders: relevance for cognitive dysfunctions and pathophysiology. *Neuron*, 52(1), 155–168.
<https://doi.org/10.1016/j.neuron.2006.09.020>
- van Bussel, F. C. G., Backes, W. H., Hofman, P. A. M., Puts, N. A. J., Edden, R. A. E., van Boxtel, M. P. J., Schram, M. T., Stehouwer, C. D. A., Wildberger, J. E., & Jansen, J. F. A. (2016). Increased GABA concentrations in type 2 diabetes mellitus are related to lower cognitive functioning. *Medicine (United States)*, 95(36). <https://doi.org/10.1097/MD.0000000000004803>
- Whittington, M. A., Cunningham, M. O., LeBeau, F. E. N., Racca, C., & Traub, R. D. (2011). Multiple origins of the cortical gamma rhythm. *Developmental Neurobiology*, 71(1), 92–106. <https://doi.org/10.1002/dneu.20814>
- Xu, Z., Zeng, W., Sun, J., Chen, W., Zhang, R., Yang, Z., Yao, Z., Wang, L., Song, L., Chen, Y., Zhang, Y., Wang, C., Gong, L., Wu, B., Wang, T., Zheng, J., & Gao, F. (2017). The quantification of blood-brain barrier disruption using dynamic contrast-enhanced magnetic resonance imaging in aging rhesus monkeys with spontaneous type 2 diabetes mellitus. *NeuroImage*, 158, 480–487. <https://doi.org/10.1016/j.neuroimage.2016.07.017>

Acknowledgements:

Back in 2015, I made one of the most important decisions in my life when I decided that I am looking forward to becoming a medical researcher. I started a new chapter in my life with unwavering determination and moved to Portugal to chase after my dreams. At the end of my road I am finally getting to the end of a PhD and for that I feel the obligation to thank everyone who has been supporting and who helped me achieve this milestone in my life.

I am deeply thankful for my mentor and supervisor Prof. Dr. Miguel Castelo-Branco for his support, guidance, and precious advice during the practical phase and for his patience and perfectionism for the correction of this dissertation. I still remember his first words to me when I started working under his supervision whether I am going to stay until the end and be responsible or I do not have the required discipline to finish my PhD. I hope by this stage I have proven myself to him in every possible way that I got what it needs to get the job done! From the start of my PhD, he gave me the opportunity to pursue my own ideas and to think out of the box. Indeed, I still needed his guidance and wisdom to polish my raw ideas, but I am glad that I finished my PhD doing what I like the way I like but most importantly with the correct methodology and approach thanks to his mentorship. I do believe that I was lucky to have him as my supervisor as he really cared about my work and always listened to my concerns and addressed them promptly. I am glad to call Prof. Dr. Miguel Castelo-Branco my mentor and my friend.

I will always be thankful to Dr Francisco Sales, my co-supervisor. He was always kind to me, supportive, passionate about my work and became a close friend to me. His guidance and professionalism were unheard of and I am grateful for his input regarding my work especially on the second disease model in this thesis “Drug Resistant Epilepsy”. I am also grateful for the opportunity to link my experimental and research work with individual clinical benefit to patients in his care at the epilepsy monitoring unit.

I am very grateful for Catarina Duarte for her warmth and kindness. She was always encouraging to me during the difficult times of my PhD and she really cared about me professionally and as a very close friend.

I also express my gratitude to my friend Joao Castelhana. He helped me with the transition from pure clinical sciences to transitional sciences and provided great guidance for the development of the different experiments used in this thesis.

Completing this work would have been impossible without the support and friendship of everyone at ICNAS and the epilepsy monitoring unit at CHUC. I am very thankful for Gabriel, Ana Dionisio, Mafalda, Andre, Pedro, Beatriz and everyone else who helped me accomplish this. I am very thankful for their friendship and support. I am really glad to know all of you and it was a pleasure working with you.

I would also like to thank everyone from the MRI laboratory at ICNAS, especially Sonia and her team who were kind and helpful to me. Despite some of the difficulty of some of my experiments with MRS in patients with epilepsy, they were understanding and patient.

I would like to thank my wonderful and supportive father, Prof. Ibrahim, for his support and understanding during this period of my life. He has always helped me to stay on the right path, guided me to make the right choices and encouraged me to finally achieve this. I am also thankful to my dear mother, Suhad, who always gave me strength and morale support whenever needed. I am glad that you will see your oldest son finish this phase with success. I hope I made you proud.

Finally, I would like to thank my dearest wife, Walaa, who has always stood by me like a pillar in times of need. I am always going to be grateful for your understanding and support in this phase of my life. You always showed me unconditional love, encouragement and supported me every step of the way.

At the end, I am grateful to God for all the blessings he bestowed on me scientifically, academically, and personally.

CURRICULUM VITAE

Sulaiman I S Abuhaiba, was born on 17th of December 1989 in Riyadh, Saudi Arabia. His primary education was done in Riyadh, and his basic and secondary education were completed in Palestine. In 2007, he went to the Islamic University of Gaza to study Medicine. He completed his Doctor of Medicine (M.D.) degree in 2013. He has always been interested in clinical research and his first conference publication was in 2012 in a neurosurgery conference in Izmir, Turkey.

From 2013 to 2015, he has been working in epilepsy research in Royal Melbourne Hospital, Royal Children's Hospital in Melbourne and then Toronto Western Hospital. He also worked as an emergency medicine doctor at Mount Sinai Hospital in Toronto Canada in 2014.

In February 2015, he moved to Portugal to start his PhD at the University of Coimbra. He is a PhD student in the PHD Program in Experimental Biology and Biomedicine (PDBEB). His PhD research is being held at the Institute of Nuclear Sciences Applied to Health (ICNAS) and focuses on the "integrity of the GABAergic system and its role in health and disease". His research is mainly done in cooperation with the Central Hospital of the University of Coimbra (CHUC) where he is involved with data acquisition and analysis of multimodal imaging data in epilepsy patients (EEG, fMRI, MRS, ECoG, PET and tDCS).

List of Publications

- **Abuhaiba SI**, Duarte IC, Castelhana J, Rito M, Sales F, Castelo-Branco M. Mechanisms of action of tDCS neurostimulation on neurochemistry, neurophysiological responses, and oscillatory patterning in refractory epilepsy. Submitted to Brain.
- **Abuhaiba SI**, Cordeiro M, Amorim A, Cruz Â, Quendera B, Ferreira C, Ribeiro L, Bernardes R, Castelo-Branco M. Occipital blood-brain barrier permeability is an independent predictor of visual outcome in type 2 diabetes, irrespective of the retinal barrier: A longitudinal study. *J Neuroendocrinol.* 2018 Jan;30(1). doi: 10.1111/jne.12566. PMID: 29247551.
- Sanches M*, **Abuhaiba SI***, d'Almeida OC, Quendera B, Gomes L, Moreno C, Guelho D, Castelo-Branco M. Diabetic brain or retina? Visual psychophysical performance in diabetic patients in relation to GABA levels in occipital cortex. *Metab Brain Dis.* 2017 Jun;32(3):913-921. doi:

10.1007/s11011-017-9986-3. Epub 2017 Mar 30. PMID: 28361261. * contributed equally to the work.

- Castelhana J, Duarte IC, **Abuhaiba SI**, Rito M, Sales F, Castelo-Branco M. Cortical functional topography of high-frequency gamma activity relates to perceptual decision: an Intracranial study. PLoS One. 2017 Oct 26;12(10):e0186428. doi: 10.1371/journal.pone.0186428. PMID: 29073154; PMCID: PMC5657999.

Selected Conference Presentations:

- **Abuhaiba SI**, Castelhana J, Duarte IC, Rito M, Sales F, Castelo-Branco M. Interictal versus Ictal High Frequency Oscillations in Temporal Lobe Epilepsy: A Time-Frequency Analysis Study Oral Presentation. 3rd Congress of European Academy of Neurology. 2017 June. doi: 10.13140/RG.2.2.26971.05925.
- **Abuhaiba SI**, Castelhana J, Duarte IC, Rito M, Sales F, Castelo-Branco M. Ictal High Frequency Oscillations in Drug Resistant Epilepsy. 51st Annual Scientific Meeting of the European Society for Clinical Investigation. 2017 May. doi: 10.13140/RG.2.2.11032.70408.
- **Abuhaiba SI**, Castelhana J, Duarte IC, Rito M, Sales F, Castelo-Branco M. Prediction of the Seizure's Onset Zone from Interictal HFOs: An Intracranial EEG Study. 29 Encontro Nacional de Epileptologia. 2017 March. doi: 10.13140/RG.2.2.15227.00801.
- **Abuhaiba SI**, Castelhana J, Duarte IC, Rito M, Sales F, Castelo-Branco M. Lateralization and Localization of Bilateral Mesial Frontal Lobe Epilepsy with sEEG: A Case Report. 28 Encontro Nacional de Epileptologia. 2017 March. doi: 10.13140/RG.2.2.32004.22409.
- **Abuhaiba SI**, Mahdi MY, Abuhadrous N. Comparative Study between Standard Open Lumbar Discectomy at EGH "European Gaza Hospital" and Egypt National Hospitals "Ain Shams Hospital". The 3rd International Levantine Forum "Advances in Neurological Surgery". 2012 November. doi: 10.13140/RG.2.2.12697.31845.

Book Publications:

- **Sulaiman Abuhaiba**, Adeleke Adesina, Mohamed Edfawy Hussien (2019). USMLE Step 1 Biochemistry Masterclass: The Complete Review for Medical Biochemistry for the USMLE Exam. (Kindle Edition). ASIN: B07ZBJG335
- **Sulaiman Abuhaiba**, Adeleke Adesina, Mohamed Edfawy Hussien (2020). SMASH USMLE STEP 1 High Yield Review (Kindle Edition). ASIN: B08FC437PD